TURKISH JOURNAL OF
INTENSIVE CARE

Online ISSN: 2602-2974

VOLUME 24 ISSUE 1 March 2026

TYBD
Türk Yoğun Bakım Derneği
Turkish Society of Intensive Care

Online ISSN: 2602-2974

TURKISH JOURNAL OF INTENSIVE CARE

Volume **24** | *Issue* **1** | *March* **2026**

TYBD
Türk Yoğun Bakım Derneği
Turkish Society of Intensive Care

Online ISSN: 2602-2974
www.turkishjic.org

Turkish Journal of Intensive Care

Official abbreviation: Turk J Intensive Care

ISSN (Online): 2602-2974

DOI Prefix: 10.63729

Owner
On behalf of Turkish Society of Intensive Care
Prof. Fethi Gül (President)

Publication Type
International peer-reviewed journal

Publication Frequency and Language
Quarterly (March, June, September, December), English

Editor-in-Chief
Prof. Dr. Perihan Ergin Özcan
Department of Anesthesiology and Reanimation, İstanbul Faculty of Medicine, İstanbul University, İstanbul, Türkiye
pergin@istanbul.edu.tr - https://orcid.org/0000-0001-7986-4984

Publisher
Turkish Society of Intensive Care

Publisher Address
Gümüşsuyu Mah. İnönü Cad. No:53 Kat:4, 34437 Beyoğlu, İstanbul, Türkiye
Email: info@yogunbakim.org.tr
Web: www.yogunbakim.org.tr

Publishing Services
Akdema Informatics and Publishing
Address: Kızılay Mah. Gazi Mustafa Kemal Bulvarı No: 23/8 06420 Çankaya, Ankara, Türkiye
Certificate number: 52576
Email: bilgi@akdema.com
Tel: +90 533 166 80 80
Web: www.akdema.com

Turkish Journal of Intensive Care is indexed in Emerging Sources Citation Index (ESCI), ProQuest Health & Medical Complete, EBSCO Database, Gale, CINAHL, TR Index, Turkiye Citation Index, Hinari, GOALI, ARDI, OARE, AGORA, J-Gate, IdealOnline, Embase and Turk Medline.

You can reach all publication policies and author guidelines from www.turkishjic.org.

EDITORIAL BOARD

İÇİNDEKİLER / CONTENTS

Turk J Intensive Care 2026;24(1):1-10
DOI: 10.63729/TJIC.2026.683

INVITED REVIEW

Artificial intelligence in preoperative assessment and optimization: a narrative review

Yoann Elmaleh[1], Yassine Moussali[1,2], Richard Boyer[2]

[1]Quincy Anaesthesia, Ramsay Santé, Claude Galien Private Hospital, Quincy-sous-Sénart, France
[2]HoopCare US

ABSTRACT

Background: Preoperative assessment and optimization are pivotal for complex surgical patients, yet traditional scores and clinician-driven workflows may miss subtle risk interactions and modifiable factors. Artificial intelligence (AI), especially machine learning (ML), can leverage large-scale electronic health record (EHR) data to improve risk stratification and support targeted optimization strategies.

Methods: We conducted a narrative review focusing on practical, clinically actionable AI applications in preoperative assessment and optimization, emphasizing recent advances and implementation considerations for high-risk surgical patients.

Results: ML-based preoperative risk models can outperform conventional calculators, exemplified by a gradient-boosted decision-tree model trained on >1.4 million surgical cases that achieved an AUROC of 0.95 for 30-day mortality and exceeded NSQIP performance, with prospective real-world deployment. Automated frailty phenotyping from structured preoperative EHR data (demographics, ASA/acuity, ICD-10/CCS diagnoses, and routine labs) has also been externally validated in older adults and shows strong stepwise associations with adverse outcomes. AI additionally supports preoperative optimization by identifying actionable targets such as anemia risk (supporting early iron/EPO pathways), penicillin allergy delabeling opportunities, and improved detection of risky alcohol use via natural language processing of clinical notes. Successful clinical impact depends on workflow integration, interpretability, and attention to privacy, bias, regulation, and prospective evidence.

Conclusions: AI-enabled preoperative assessment can enhance identification of high-risk patients and systematically surface modifiable factors for optimization, with early evidence of improved predictive performance and feasible integration into point-of-care workflows. Future work should prioritize robust external validation across diverse populations, implementation studies demonstrating patient-centered benefit, and governance frameworks ensuring safety, fairness, and clinician trust.

Keywords: Artificial intelligence, management, optimization, preoperative assessment, prediction

Introduction

Preoperative assessment is a critical step in managing patients before major surgery, especially for complex surgical patients with multiple comorbidities or high-risk factors. Such complicated patients often face elevated risks of postoperative complications, prolonged hospital stays, or intensive care unit (ICU) admissions. Traditional preoperative evaluation relies on clinical judgment, risk scores (like ASA classification or NSQIP calculators), and multidisciplinary optimization (e.g., controlling chronic diseases, nutritional support, prehabilitation). In recent years, artificial intelligence (AI), particularly machine learning (ML) algorithms, has emerged as a promising tool to enhance preoperative risk stratification and patient optimization. By analyzing large volumes of health data, AI can uncover complex patterns not easily accessible to clinicians, potentially improving prediction of adverse outcomes and guiding tailored interventions.

This narrative review examines the role of AI in the preoperative assessment and optimization

✉ Yoann Elmaleh • y.elmaleh@quincyanesthesie.com

Received: 01.03.2026 **Accepted:** 09.03.2026 **Published:** 26.03.2026

of high-risk surgical patients, aimes to highlight recent advances within the last 7 years, practical applications, and future directions. We focus on how AI-driven approaches may augment the preoperative clinic functions in identifying patient risk profiles, recommending optimization strategies, and ultimately improving surgical and operational outcomes.

Traditional challenges in identifying high-risk preoperative assessment

Complex surgical patients (such as elderly, frail and individuals with significant comorbid conditions) pose challenges in preoperative evaluation. These patients are more likely to suffer from complications like cardiac, respiratory events, delirium, or infections after surgery. Conventional risk assessment tools exist, for example, the ASA score, American College of Surgeons NSQIP risk calculator and various organ-specific risk indices, but they have limitations in accuracy for individual patients. They often use a limited number of variables and may not capture subtle interactions between patient factors. Moreover, identifying all modifiable risk factors (including unoptimized medical conditions and factors like substance use) can be time-consuming.

Preoperative optimization clinics have been established in many centers to address these issues, providing comprehensive assessment and interventions before surgery (e.g., anemia correction, smoking cessation, medication adjustments). These clinics have shown improved surgical outcomes by optimizing patients' conditions, reducing unnecessary tests, and minimizing last-minute cancellations (1). However, they require significant resources and rely on clinicians to accurately identify high-risk patients and intervention targets. This is where AI can contribute, by automating and refining risk detection and ensuring that no important detail is overlooked in complex patients.

AI for preoperative risk stratification

One of the more advanced applications of AI in perioperative medicine is predictive modeling for surgical risk. Machine learning algorithms can analyze extensive electronic health record (EHR) data to predict which patients are at high risk for adverse postoperative outcomes. These models may often outperform traditional risk prediction tools in accuracy. For example, Mahajan et al. (2) developed a preoperative ML model using gradient-boosted decision trees on data from over 1.4 million surgical cases. This model achieved an area under the ROC curve (AUROC) of 0.95 for 30-day mortality prediction and significantly outperformed the standard NSQIP surgical risk calculator (AUROC margin of 0.048) in identifying high-risk patients (2,3) using exclusively preoperative data. Notably, the ML model used only preoperative variables readily available in the EHR and was validated prospectively in clinical practice, suggesting it could integrate into real-world preoperative workflows to flag patients at risk. The authors concluded that such an AI tool may allow targeted perioperative interventions and resource allocation (e.g., ICU bed planning) to those who need it most (2). Similarly, an earlier study by Corey et al. (4) termed "Pythia" demonstrated that ML models could automatically curate EHR data and identify high-risk surgical patients, laying groundwork for subsequent AI risk predictors (4,5).

Cardiac & respiratory risk prediction

Specific risk predictions have also been enhanced through AI. Cardiac complications and pulmonary complications are two major concerns in high-risk patients. Modern ML models can incorporate granular patient data to predict these events more precisely than older scoring systems. For instance, researchers have applied ML to forecast postoperative major cardiac events (e.g. myocardial infarction) or cerebrovascular events, as part of composite risk modeling (2). For postoperative pulmonary complications (PPCs), numerous AI-driven models have been developed in recent years. These include models for general surgery patients and specialty-specific ones (such as for lung surgery) that use features like patient demographics, lung function, imaging results, and even intraoperative

data to predict risks of pneumonia, respiratory failure, or need for ventilation. Many show high accuracy in identifying patients likely to develop PPCs, although some still require external validation.

Shelley et al. (6) note that while machine learning can produce powerful risk prediction models, it is crucial to choose appropriate endpoints and timing, predicting the right complication at a time when an intervention is possible, to make these models clinically useful (6). In practice, an AI model that flags a patient as high-risk for, say, respiratory failure could prompt preoperative pulmonary optimization (like inspiratory muscle training, bronchodilator therapy) or a decision to postoperatively monitor in ICU, thereby preventing or better managing the complication.

Frailty assessment

Another particularly important domain for risk stratification in complex patients is frailty. Frailty, often defined as an age-related decline in physiological reserves, is a strong predictor of poor surgical outcomes (e.g., mortality, delirium, loss of independence) in older adults. Traditional frailty assessments (like questionnaires or walking tests) can be subjective or time-consuming. AI offers a way to quantify frailty from routine data. Bai et al. (7) externally validated an AI-based preoperative frailty index derived from EHR data on over 150,000 surgical patients ≥65 years old. They used structured preoperative EHR data from the months before surgery, including demographics (e.g., age/sex), clinical acuity/history variables (e.g., ASA class, cancer history), and diagnosis information from ICD-10 codes grouped into CCS categories. They also included commonly available pre-op laboratory measurements (e.g., hemoglobin/hematocrit and related routine biochemistry). Patients classified in the highest frailty tier by the AI had dramatically higher odds of 30-day mortality (over 4-fold increase), longer hospital stays, and greater chances of discharge to nursing facilities compared to the least frail, confirming a strong, stepwise association between the AI frailty score and outcomes (7). Interestingly, this AI frailty index, which compiles dozens of deficit variables from the health record, performed as well as or better than procedure-specific frailty models, suggesting a generalizable tool. This kind of automated frailty assessment could alert clinicians to an at-risk elderly patient during preoperative clinic visits, prompting geriatric co-management or prehabilitation referrals. Incorporating frailty via AI thus refines risk stratification beyond what age and comorbidities alone convey.

Overall, machine-learning risk models have shown impressive capability in predicting a range of postoperative adverse events, from mortality to major complications. In fact, recent narrative analyses assert that ML algorithms are "superior to traditional models for predicting postoperative anemia, opioid dependence, diabetes complications, and mortality risks," thereby providing more precise risk stratifications which may elevate perioperative resource optimization plans (1,8). These algorithms can take into account complex interactions of variables (laboratory tests, vital trends, comorbid conditions, medications, etc.) that static risk scores cannot, and lead to more individualized risk profiles. The improved accuracy means fewer high-risk patients "fly under the radar" and fewer low-risk patients are subjected to unnecessary costly interventions, a better alignment of perioperative resources with patient needs. Importantly, many ML models now also incorporate techniques for interpretability (such as SHAP - Shapley Additive exPlanations (SHAP) is a model-agnostic interpretability framework that enables the explanation of predictions from any machine learning model, including complex "black-box" models such as neural networks. values or other explainable AI methods) to identify which factors are driving a given patient's risk score. This is critical for clinician acceptance: for example, AI might reveal that a patient's poorly controlled COPD, low albumin, and high ASA status are the top contributors to predicted risk, which aligns with clinical intuition and directs what needs to be optimized.

AI applications in preoperative anemia

Preoperative anemia is highly prevalent among surgical patients and is consistently associated

with increased rates of perioperative transfusion, postoperative complications, prolonged hospital stay, and mortality. Artificial intelligence–based models have recently been developed to improve the identification of patients at risk for significant postoperative anemia or transfusion requirements, enabling earlier and more targeted preoperative interventions. Kolin et al. developed machine learning predictive models for postoperative anemia and blood transfusion in patients undergoing orthopedic surgery, using routinely available clinical variables such as age, sex, baseline hemoglobin concentration, and comorbidities. Their models demonstrated strong discriminative performance, with area under the receiver operating characteristic curves ranging from 0.88 to 0.90 for both postoperative anemia and transfusion outcomes (9). Importantly, the identification of patients with a predicted probability greater than 5% for severe postoperative anemia allowed clinicians to individualize preoperative management strategies. High-risk patients could be directed toward iron supplementation, erythropoietin therapy, or proactive blood cross-matching, whereas patients classified as low risk could safely avoid unnecessary laboratory testing or iron treatment. Beyond single-outcome prediction, AI-driven decision support systems are increasingly capable of integrating longitudinal laboratory trends and patient-level clinical data to recommend standardized anemia optimization pathways within preoperative clinics (1). This approach facilitates early detection and treatment of anemia, a critical step given that untreated preoperative anemia substantially increases exposure to allogeneic blood transfusion and its associated risks.

AI application in medication management

It represents another important domain of preoperative optimization where AI has demonstrated significant potential. A particularly illustrative example is the problem of inaccurate penicillin allergy labeling. A substantial proportion of surgical patients carry a documented penicillin allergy, which frequently leads to the use of second-line perioperative antibiotic prophylaxis, such as vancomycin or clindamycin, instead of first-line beta-lactams like cefazolin. This practice has been associated with higher rates of surgical site infections and antimicrobial resistance. However, many penicillin allergy labels are outdated, imprecise, or reflect non-allergic adverse reactions rather than true immunoglobulin E–mediated hypersensitivity (10). Artificial intelligence can assist in identifying patients suitable for allergy reassessment or delabeling. Jiang et al. applied a machine learning algorithm to neurosurgical inpatients and demonstrated that approximately 22% of recorded penicillin allergies were inconsistent with true allergy criteria. Their model accurately differentiated allergy from intolerance with a reported accuracy of 98%, effectively flagging patients eligible for penicillin allergy testing and potential delabeling (11,12). When integrated into the preoperative workflow, such AI systems could automatically

AI applications in preoperative patient optimization (Table 1).

Beyond risk prediction, AI is increasingly being used to guide and enhance preoperative optimization strategies, that is, the process of improving a patient's condition prior to surgery. Once high-risk patients are identified, the next step is to mitigate those risks. AI tools can assist in several domains.

a) Screen patient histories and prompt clinicians with alerts suggesting allergy consultation. This would allow a greater proportion of patients to receive optimal perioperative antibiotics, thereby reducing infection risk and improving antimicrobial stewardship. This example highlights how AI can systematically interrogate complex electronic health records to uncover optimization opportunities that might otherwise be overlooked in routine clinical practice.

b) Postoperative Analgesia - Artificial intelligence has also been widely applied to the prediction and

Table 1. Representative AI applications in preoperative assessment and optimization

Study / domain	Population / setting	Data inputs (preop unless stated)	Model / approach	Outcome(s)	Performance / key result	Validation / implementation	Preop clinic "actionability"
Mahajan et al – global risk stratification	>1.4M surgical cases	"Only preoperative variables readily available in the EHR"	Gradient-boosted decision trees	30-day mortality	AUROC **0.95**; outperformed NSQIP (ΔAUROC **0.048**)	Prospective, point-of-care deployment	Earlier flagging for ICU planning, monitoring, specialty consults
Corey et al ("Pythia") – automated risk identification	Surgical patients (EHR-curated)	Automatically curated EHR features	ML risk models ("Pythia")	High-risk patient identification	Foundational demonstration of automated EHR curation for risk prediction	Validated models; informs later tools	Automated preop triage; reduces manual data extraction burden
Bai et al – frailty phenotyping	≥65 years; >150k surgical patients	Demographics; ASA/acuity & history (e.g., cancer); ICD-10→CCS; routine labs (Hb/Ht, biochem)	AI-based frailty index	Mortality, LOS, discharge disposition	Highest frailty tier: >4× odds of 30-day mortality; stepwise worse outcomes	External validation	Routes frail patients to geriatric co-management / prehab
Shelley et al – clinical utility framing	Commentary / periop risk	Emphasizes endpoint choice and timing	—	—	Predict the "right" endpoint when intervention is possible	—	Helps select deployable preop targets (e.g., PPC prevention)
Kolin et al – anemia / transfusion risk	Orthopedic surgery (TKA)	Routine clinical variables (age/sex, baseline Hb, comorbidities)	ML predictive models	Postop anemia; transfusion	AUROC 0.88–0.90	Retrospective modeling	Triggers iron/EPO, crossmatch planning; avoids low-yield testing
Jiang et al – penicillin allergy delabeling	Neurosurgical inpatients	EHR allergy history patterns	ML classifier	True allergy vs intolerance	22% labels inconsistent; reported accuracy 98%	Feasibility study	Prompts allergy consult/testing → better prophylaxis choices
Vydiswaran et al – risky alcohol detection	Preop patients (notes-based)	**Unstructured** preop clinical notes	NLP	Risky alcohol use	Detected 87% vs 29% with ICD codes	Retrospective NLP study	Earlier counseling, prophylaxis for withdrawal/delirium
Bishara et al – delirium prediction	Surgical patients	Preop EHR data	ML	Postop delirium	(Performance not detailed in current draft excerpt)	Published model	Preop geriatric pathway, medication review, non-pharm bundles
Nair et al – opioid needs prediction	Ambulatory surgery	Preop factors	ML (e.g., RF classifiers)	Postop opioid requirement	(Performance not detailed in current draft excerpt)	Published model	Guides multimodal analgesia, RA strategy, pain referral
Workflow integration (implementation principle)	Preop clinic / EHR	Risk scores + interpretability + prompts	Decision support integration	Action uptake	Needs seamless EHR integration + interpretable outputs	Real-world integration described for Mahajan model	Turns predictions into consults, optimization checklists, scheduling

prevention of other postoperative complications amenable to preoperative intervention. One important area is postoperative opioid use and the risk of prolonged opioid dependence. Nair et al. developed a machine learning model to predict postoperative opioid requirements in patients undergoing ambulatory surgery, demonstrating that algorithms such as random forest classifiers could reliably identify patients likely to require higher analgesic doses (13). Beyond immediate postoperative needs, multiple studies have shown that preoperative factors—including chronic pain syndromes, preoperative opioid exposure, and certain psychosocial variables—are strong predictors of persistent opioid use after surgery (3). AI-based clinical decision support tools could integrate these variables and provide automated alerts identifying patients at high risk for prolonged opioid use, thereby prompting early referral to pain specialists, implementation of multimodal analgesia strategies, or greater reliance on regional anesthesia techniques.

c) Diabetic Patient Optimization - Similar approaches have been explored for metabolic optimization, particularly in patients with diabetes mellitus. Machine learning models have demonstrated the ability to predict which diabetic patients are at highest risk for postoperative complications related to poor glycemic

control, such as surgical site infections or delayed wound healing. These predictions can guide intensified preoperative glycemic optimization, endocrine consultation, and individualized perioperative glucose management strategies (1).

d) Smoking Cessation & Life-style Optimization - Lifestyle-related risk factors represent another critical but frequently under-recognized component of preoperative assessment. Smoking and hazardous alcohol consumption are both independently associated with increased perioperative morbidity, including pulmonary complications, wound infections, delirium, and prolonged hospitalization. Artificial intelligence applications in this domain increasingly rely on conversational agents and natural language processing. Emerging evidence suggests that AI-powered chatbots or automated messaging platforms can engage patients in smoking cessation counseling tailored to the preoperative timeline, reinforcing behavioral change during a period when patients may be particularly receptive to intervention (1). Large language models, including tools such as ChatGPT, have also been explored as adjuncts for answering patient questions and providing personalized health education prior to surgery. With respect to alcohol use, Vinod Vydiswaran et al. demonstrated the power of natural language processing applied to preoperative clinical notes to detect risky alcohol consumption. In their study, NLP algorithms identified 87% of patients consuming more than two alcoholic drinks per day, compared with only 29% identified using conventional ICD diagnostic codes, effectively tripling detection rates (14,15). This finding underscores the ability of AI to extract clinically meaningful information from unstructured text that is often missed by structured data fields. Early identification of hazardous alcohol use allows clinicians to initiate preoperative interventions such as counseling, vitamin supplementation, or withdrawal prophylaxis, thereby reducing the risk of postoperative delirium, withdrawal syndromes, and ICU admission.

e) Perioperative Patient Education - Finally, artificial intelligence is beginning to play a role in patient education and engagement during the preoperative period. Adequate preparation of patients—both physically and psychologically—is essential for optimizing surgical outcomes. Conversational AI platforms can provide individualized education about planned procedures, perioperative expectations, and recovery pathways, while also reinforcing key instructions such as fasting requirements, medication adjustments, and prehabilitation exercises. Early reports suggest that these tools may improve patient comprehension, satisfaction, and anxiety levels. Jones et al. describe how AI systems, including large language models, have been piloted to enhance preoperative education and support behavioral interventions such as smoking cessation (1). Although these applications remain in early stages of implementation, they hold promise for extending the reach of preoperative optimization beyond the clinic visit and providing continuous, scalable patient support.

Integration into clinical workflow

For AI to truly improve preoperative care of complicated patients, it must integrate seamlessly into existing workflows. This means turning predictive insights into actionable clinical steps. Some leading medical centers have begun integrating ML risk scores into preoperative clinic software or the electronic record. For instance, the model by Mahajan et al. was deployed at the point of care in a prospective trial, meaning that when a patient was seen preoperatively, the system generated a risk score in the background and identified high-risk patients to clinicians (2). Such integration allowed the care team to “optimize perioperative care” by, for example, scheduling a high-risk patient for closer intraoperative monitoring, ICU admission post-op, or preemptive specialist consultations. Another domain of integration is scheduling and resource allocation: AI algorithms can help prioritize which patients should be seen in specialized pre-op clinics (e.g., a frail patient flagged

by an EHR-based frailty index might be routed to a multidisciplinary geriatric optimization program pre-surgery).

To facilitate adoption, AI outputs should be presented in a user-friendly, interpretable manner. Clinicians are more likely to trust and use an AI risk tool if it explains its reasoning (e.g., listing key risk factors contributing to a high risk score) and if it links to suggested actions (like "consider cardiology evaluation" or "optimize nutrition"). There are also efforts to incorporate AI-based checklists that automatically pull patient data and highlight gaps in optimization (for example: "Patient has Hgb 10 g/dL, anemia protocol recommended" or "BMI > 40, evaluate for weight loss program prior to elective bariatric surgery"). By acting as an ever-vigilant assistant, AI can ensure complex patients receive thorough evaluation and that modifiable issues are addressed systematically.

It's worth noting that AI doesn't act alone, but rather augments the clinician. The perioperative team (surgeons, anesthesiologists, internists) still makes the final decisions and engages patients in optimization strategies. AI's role is to provide a more informed foundation: identifying the silent risk factors, quantifying risk severity, and even predicting which interventions might yield the most benefit. In complex patients who often have numerous issues, this helps prioritize efforts on what will most improve surgical readiness and outcomes (16,17).

Challenges and future perspectives

While the promise of AI in preoperative assessment is great, there are important challenges and limitations to acknowledge.

Despite the growing enthusiasm surrounding artificial intelligence in perioperative medicine, several important challenges must be addressed before widespread clinical implementation in preoperative assessment and optimization can be achieved.

Data privacy and security - One of the foremost concerns relates to data privacy and security. Most AI models rely on large-scale datasets extracted from electronic health records, which contain highly sensitive personal and medical information. Ensuring patient privacy is therefore paramount, and AI systems must be developed and deployed in strict compliance with data protection regulations. Beyond regulatory compliance, the use of personal health data for algorithm training raises broader ethical concerns, particularly regarding secondary data use and long-term data storage. Robust anonymization techniques, secure data infrastructures, and advanced cybersecurity measures are essential to maintain institutional and patient trust in AI-driven clinical tools.

Amplification of Bias - Another major challenge is algorithmic bias and fairness. Machine learning models are inherently dependent on the data used for their training and may inadvertently reproduce or amplify existing biases present in historical healthcare data. For instance, if certain patient populations—such as women, ethnic minorities, or socioeconomically disadvantaged groups—have historically experienced poorer outcomes due to unequal access to care or systemic disparities, a naïvely trained algorithm may incorrectly assign higher risk to these groups and perpetuate inequities. This underscores the necessity of validating AI models across diverse populations and healthcare settings. Risk prediction tools must be carefully audited to ensure that they do not disproportionately penalize patients based on non-modifiable characteristics such as race or socioeconomic status. Ongoing efforts to improve fairness through bias detection, model recalibration, and transparent reporting are critical to the ethical adoption of AI in perioperative care.

Clinical skepticism and concerns about workflow disruption also represent significant barriers to adoption. Many clinicians remain cautious about integrating AI into routine practice, particularly when algorithms function as "black boxes" with limited interpretability. Fear of over-reliance on automated systems and erosion of clinical judgment is common. To address these concerns, developers increasingly

emphasize explainable AI approaches that provide clinicians with insight into how predictions are generated and which variables contribute most strongly to risk estimates. User-centered design and seamless integration into existing electronic health record workflows are equally important. Early success stories, such as AI tools that demonstrably prevent complications or reduce healthcare costs, may help build confidence among clinicians. Equally crucial is structured training for perioperative teams, enabling them to interpret AI outputs appropriately and to view these tools as decision-support systems rather than decision-makers. Demonstrating that AI can reduce cognitive burden and save time by automating repetitive aspects of risk assessment will likely be key to broader acceptance among busy clinicians.

Regulatory and legal considerations further complicate the implementation of AI in preoperative medicine. When AI systems provide patient-specific recommendations, questions inevitably arise regarding responsibility and liability in the event of an adverse outcome. Regulatory agencies, including the U.S. Food and Drug Administration and their international counterparts, are beginning to develop frameworks for evaluating and approving clinical AI tools. At present, most AI applications in preoperative assessment are positioned as advisory systems, with ultimate responsibility remaining firmly with the clinician. However, as models become increasingly autonomous and adaptive, clearer regulatory oversight and legal frameworks will be required. Establishing transparent standards for validation, monitoring, and accountability will be essential to ensure patient safety and clinician protection.

Finally, there remains a substantial need for prospective evidence. Although many AI models in perioperative medicine have demonstrated impressive performance in retrospective and observational studies, relatively few have been evaluated in prospective trials or real-world implementation studies. Future research should prioritize assessing whether AI-driven preoperative assessment and optimization strategies translate into meaningful improvements in patient-centered outcomes, such as reduced complication rates, shorter hospital stays, or decreased ICU utilization, as well as demonstrating cost-effectiveness. Encouraging early data exist, including the prospective validation of large-scale risk prediction models such as the UPMC preoperative risk model described by Mahajan et al., but broader evidence is needed to firmly establish the clinical value of these tools. Ongoing research should also focus on continuous model refinement using updated data and on defining optimal strategies for integrating AI recommendations into standardized preoperative clinical pathways, potentially through guidelines that incorporate AI-based risk stratification.

Despite these challenges, the trajectory is clearly toward greater AI involvement. The future likely holds increasingly sophisticated AI systems that can aggregate data from multiple sources (EHR, wearable devices, genomics, etc.) for a 360-degree preoperative assessment. These might even simulate outcomes under different scenarios, for example, predicting "if we improve this patient's pulmonary function by X, the risk of complication drops by Y%," thus guiding specific optimization interventions quantitatively. Furthermore, AI might help in surgical decision-making, identifying patients who are at the highest risk for a procedure and therefore alternatives to be made available. By continuously learning from each surgical outcome, AI systems can become smarter and more personalized over time (18).

Conclusion

Artificial intelligence is poised to become an invaluable ally in the preoperative assessment and optimization of complicated surgical patients. By leveraging vast datasets and advanced algorithms, AI can enhance risk stratification, identify high-risk patients with greater accuracy and granularity than traditional methods. It can also aid in focusing and addressing modifiable risk factors through innovative applications like NLP-driven substance use detection, predictive models for complications, and decision support for

optimization interventions (anemia management, allergy delabeling, etc.). For intensive care and perioperative professionals, these technologies offer the potential to improve patient outcomes: fewer complications, more efficient use of ICU resources, and tailored perioperative care plans. Early studies and implementations have shown promising results, such as improved predictive performance (2) and successful identification of hidden risk factors (14,19,20). Nevertheless, integrating AI into routine practice requires careful attention to ethics, bias, and user adoption. As we continue to validate these tools in diverse patient populations and refine their integration into clinical workflows, AI-driven preoperative assessment could markedly enhance the safety and effectiveness of surgery for our most vulnerable patients.

In summary, the collaboration of human clinical expertise with machine intelligence stands to optimize perioperative care, enabling precision medicine in surgical risk assessment and preparation. With ongoing research and responsible implementation, AI's full potential in perioperative medicine may transform how we evaluate and optimize complex surgical patients for the better.

Acknowledgements

The authors acknowledge Yassine Moussali and Richard Boyer for their involvement in an AI research and practice company (HoopCare); however, their review and contributions to this manuscript did not include any information related to their products or commercial activities

Author contribution

Study conception and design: YE, YM, RB; data collection: YE, YM, RB; analysis and interpretation of results: YE, YM, RB; draft manuscript preparation: YE, YM, RB. The author(s) reviewed the results and approved the final version of the article.

Source of funding

The authors declare the study received no funding.

Conflict of interest

Active participation to HoopCare development (commercial and research) for Yassine Moussali and Richard Boyer.

References

1. Jones JH, Sakai T. The Potential Impacts of Artificial Intelligence on Preoperative Optimization and Predicting Risks of Morbidity and Mortality: A Narrative Focused Review. A A Pract. 2025;19:e02061. [Crossref]
2. Mahajan A, Esper S, Oo TH, et al. Development and Validation of a Machine Learning Model to Identify Patients Before Surgery at High Risk for Postoperative Adverse Events. JAMA Netw Open. 2023;6:e2322285. [Crossref]
3. Lu Y, Forlenza E, Wilbur RR, et al. Machine-learning model successfully predicts patients at risk for prolonged postoperative opioid use following elective knee arthroscopy. Knee Surg Sports Traumatol Arthrosc. 2022;30:762-72. [Crossref]
4. Corey KM, Kashyap S, Lorenzi E, et al. Development and validation of machine learning models to identify high-risk surgical patients using automatically curated electronic health record data (Pythia): A retrospective, single-site study. PLoS Med. 2018;15:e1002701. [Crossref]
5. Fritz BA, King CR, Abdelhack M, et al. Effect of machine learning models on clinician prediction of postoperative complications: the Perioperative ORACLE randomised clinical trial. Br J Anaesth. 2024;133:1042-50. [Crossref]
6. Shelley B, Shaw M. Machine learning and preoperative risk prediction: the machines are coming. Br J Anaesth. 2024;133:925-30. [Crossref]
7. Bai C, Xiao F, Al-Ani M, Price CC, Manini TM, Mardini MT. External validation of an AI-based preoperative frailty index using real-world data. J Gerontol A Biol Sci Med Sci. 2025;80:glaf119. [Crossref]
8. Park S, Chung S, Kim Y, et al. A deep-learning algorithm using real-time collected intraoperative vital sign signals for predicting acute kidney injury after major non-cardiac surgeries: A modelling study. PLoS Med. 2025;22:e1004566. [Crossref]
9. Kolin DA, Lyman S, Della Valle AG, Ast MP, Landy DC, Chalmers BP. Predicting Postoperative Anemia and Blood Transfusion Following Total Knee Arthroplasty. J Arthroplasty. 2023;38:1262-1266.e2. [Crossref]

10. Murphy ZR, Muzaffar AF, Massih SA, et al. Examining cefazolin utilization and perioperative anaphylaxis in patients with and without a penicillin allergy label: A cross-sectional study. J Clin Anesth. 2024;94:111377. [Crossref]

11. Jiang M, Lam A, Lam L, et al. Artificial intelligence and the potential for perioperative delabeling of penicillin allergies for neurosurgery inpatients. Br J Neurosurg. 2025;39:40-3. [Crossref]

12. Bishara A, Chiu C, Whitlock EL, et al. Postoperative delirium prediction using machine learning models and preoperative electronic health record data. BMC Anesthesiol. 2022;22:8. [Crossref]

13. Nair AA, Velagapudi MA, Lang JA, et al. Machine learning approach to predict postoperative opioid requirements in ambulatory surgery patients. PLoS One. 2020;15:e0236833. [Crossref]

14. Vydiswaran VGV, Strayhorn A, Weber K, et al. Automated-detection of risky alcohol use prior to surgery using natural language processing. Alcohol Clin Exp Res (Hoboken). 2024;48:153-63. [Crossref]

15. Xue B, Li D, Lu C, et al. Use of Machine Learning to Develop and Evaluate Models Using Preoperative and Intraoperative Data to Identify Risks of Postoperative Complications. JAMA Netw Open. 2021;4:e212240. [Crossref]

16. Lee SW, Lee HC, Suh J, et al. Multi-center validation of machine learning model for preoperative prediction of postoperative mortality. NPJ Digit Med. 2022;5:91. [Crossref]

17. Graeßner M, Jungwirth B, Frank E, et al. Enabling personalized perioperative risk prediction by using a machine-learning model based on preoperative data. Sci Rep. 2023;13:7128. [Crossref]

18. Abraham J, Bartek B, Meng A, et al. Integrating machine learning predictions for perioperative risk management: Towards an empirical design of a flexible-standardized risk assessment tool. J Biomed Inform. 2023;137:104270. [Crossref]

19. Chung P, Fong CT, Walters AM, Aghaeepour N, Yetisgen M, O'Reilly-Shah VN. Large Language Model Capabilities in Perioperative Risk Prediction and Prognostication. JAMA Surg. 2024;159:928-37. [Crossref]

20. Ouyang D, Theurer J, Stein NR, et al. Electrocardiographic deep learning for predicting post-procedural mortality: a model development and validation study. Lancet Digit Health. 2024;6:e70-8. [Crossref]

Turk J Intensive Care 2026;24(1):11-20
DOI: 10.63729/TJIC.2026.684

REVIEW

Unraveling paroxysmal sympathetic hyperactivity syndrome; what is behind the storm?

Alkım Gizem Yılmaz Selimoğlu[1], Tuğhan Utku[2], Zeynep Fırat[3]

[1]Department of Anesthesiology and Reanimation, Prof. Cemil Taşçıoğlu City Hospital, University of Health Sciences, İstanbul, Türkiye
[2]Department of Anesthesiology and Reanimation, Yeditepe University Koşuyolu Hospital, İstanbul, Türkiye
[3]Department of Radiology, Yeditepe University Koşuyolu Hospital, İstanbul, Türkiye

ABSTRACT

Paroxysmal sympathetic hyperactivity syndrome (PSH) is a rarely diagnosed syndrome associated with acute brain injury which involves traumatic brain injury, stroke, infectious diseases, and encephalopathy, and results in cyclic episodes of sympathetic and motor hyperactivity (hypertension, tachypnea, hyperthermia, diaphoresis, dystonic posturing). Even though there are some theories regarding the pathophysiology of PSH, the main mechanism still remains unclear. However, it is mostly agreed upon that PSH is caused by an unbalanced activation of the autonomic nervous system caused by the loss of inhibition of excitation in the sympathetic nervous system. Although PSH has been well known for many decades there were misunderstandings regarding the nomenclature and the definition of this syndrome. The term "Paroxysmal Sympathetic Hyperactivity and a diagnostic tool consisted of two different components and named PSH-Assessment Measure (PSH-AM)," was developed to help guiding clinical management in 2014. These components are the diagnostic likelihood tool and the clinical features scale. To diagnose this syndrome first other neurological issues should be ruled out. Once diagnosed in order to treat and avoid secondary brain damage and other adverse outcomes of this syndrome an approach of both pharmacological (such as opioids, B-blockers, alfa2 agonists, benzodiazepines, gabapentin and muscle relaxants) and nonpharmacological should be combined. Pharmacological approach focuses on symptom abortion, prevention and refractory treatment.

Keywords: paroxysmal sympathetic hyperactivity syndrome, traumatic brain injury, acute brain injury

Introduction

Paroxysmal sympathetic hyperactivity (PSH) is a syndrome first identified in 1954 and characterized by episodes of sympathetic discharges, after an acute brain injury either traumatic or non-traumatic (1-4). During this sympathetic discharge episodes; tachycardia, transient fever (hyperthermia), arterial hypertension, tachypnea, diaphoresis, dystonia and posturing (extensor or flexor) may occur spontaneously or after a non-painful stimulus (such as endo-tracheal tube suctioning or passive body positioning) (1,3). PSH is frequently seen in critically ill patients on intensive care units (ICU), with acquired brain injury including traumatic brain injury (80%), hypoxic- ischemic encephalopathy (10%), autoimmune encephalitis associated with N-methyl-D-aspartate receptor antibodies, stroke (mainly hemorrhagic), tumors, cerebrovascular accidents, cerebral fat embolism and infectious diseases such as tuberculous meningitis and usually observed when the patient is started neurological rehabilitation (1-3,5-8).

PSH has been well known for many decades and recognizing this syndrome is very important due to its clinical burden such as longer stay in the ICU, infections, increased morbidity and lengthening of the rehabilitation process (1,9). Even though PSH is clinically very important; there were misunderstandings regarding the nomenclature, definition and the diagnostic criteria of this syndrome (1,9,10). Therefore, a committee came together in 2014

✉ Alkım Gizem Yılmaz Selimoğlu • alkimgizemyilmaz@gmail.com

Received: 10.07.2025 **Accepted:** 22.10.2025 **Published:** 26.03.2026

in order to develop a definition and set the diagnostic criteria for the syndrome. So the term “Paroxysmal Sympathetic Hyperactivity” was developed to identify the clinical state seen after severe acquired brain injury of any cause, and resulted in simultaneous paroxysmal transient increases in sympathetic and motor activity (1,3,9,10).

Epidemiology and Risk Factors of PSH

The worldwide yearly incidence of traumatic brain injury (TBI) is 69 million cases (11). While the prevalence of PSH after non-traumatic brain injuries is only 6%; the prevalence of PSH is shown to be between 7,7%- 33% of patients after severe traumatic brain injury, although the real incidence is thought to be much higher (2,4-6,10). Some of the risk factors for PSH include; male gender, young age, early onset of hyperthermia, GCS score, tracheostomy, the degree of diffuse axonal injury, mid-brain and pontine lesions, the cause and the severity of the brain injury (mostly after traumatic brain injury(79,4%), hypoxic encephalopathy and stroke (3-5,12-14).

Pathophysiology of PSH

Basically PSH is thought to be caused by the imbalance of the autonomic nervous system (ANS) (4). After damage to the brain ANS activation leads to immediate inflammation and metabolic response. This response results in the core sympathetic symptoms of PSH if the parasympathetic mechanisms cannot compensate (6). However, the main pathophysiologic mechanisms behind PSH, even though there are some theories, still remains unclear. These theories are the disconnection theory, excitatory/inhibitory ratio (EIR) model, the neuroendocrine dysregulation theory and the neutrophil extracellular traps theory (2,12).

Disconnection theory (Figure 1) supports a disconnection related to focal or diffuse brain damage, either anatomical or functional, between cortical inhibitory centers; which are the hippocampus, insular cortex, cingulate cortex, middle temporal cortex, amygdala, basal ganglia and the dorsolateral prefrontal cortex and the sympathetic centers which are; the hypothalamus, brain stem and mesencephalon (2,3,6,10,12). When there is a disconnection, losing the cortical inhibition results in an inflated sympathetic response to normally non-painful stimuli. However the problem with this model is that it does not explain the episodic nature of this syndrome (2).

Excitatory/inhibitory ratio model (Figure 2) helps explain the hypersensitivity of the reactions and the episodic nature of PSH (5,12). This theory, being the mostly agreed upon, supports an unbalanced relationship between inhibitory (brainstem and diencephalon) and the excitatory (spinal cord) pathways. In first place we witness the loss of descending inhibition which leads to excitation of the spinal circuits against non-painful stimuli resulting in hyperactive sympathetic responses (2,6,10,12). Other mechanisms try to compensate for the loss of inhibitory control, but they contain partial recovery of the descending pathways, and an increase in gamma-aminobutyric acid levels. Because these mechanisms are episodic in nature we can explain the paroxysmal characteristic of PSH (2).

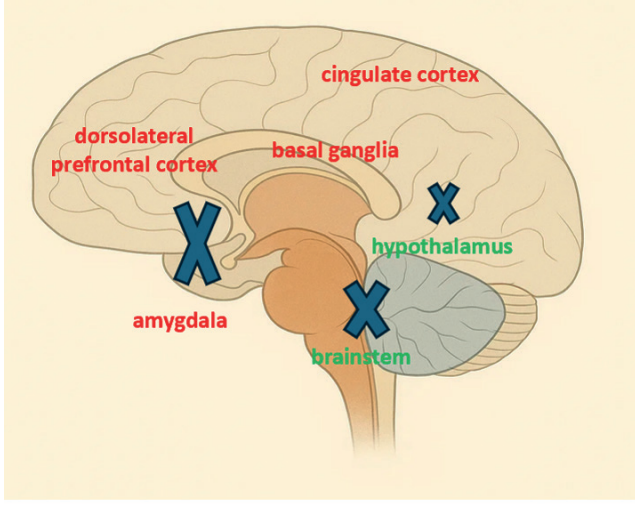

Figure 1. Schematic representation of disconnection theory

Neuroendocrine dysregulation theory refers to a dysfunction in the hypothalamic–pituitary–adrenal (HPA) axis. PSH causes overactivation of HPA axis resulting in an uncontrolled adrenergic outflow which in turn leads to an increased amount of catecholamines in the circulation (2,3). During the sympathetic discharge episodes blood levels of epinephrine, norepinephrine, dopamine and adrenocorticotropic hormone (nearly 40%) rises significantly, favoring the involvement of neuroendocrine system in the pathophysiology of PSH (2,12).

Neutrophil extracellular traps (NETs) theory explains the infiltration of paraventricular nucleus with neutrophils after TBI. The release of NETs leads to microglial activation and interleukin 1 B release resulting in sympathetic activation and a change in neurotransmitter levels (15). Cerebral contusion, brain edema, cerebral ischemia may also result in the release of excitatory amino acids at a cellular level intensifying the development of PSH (12).

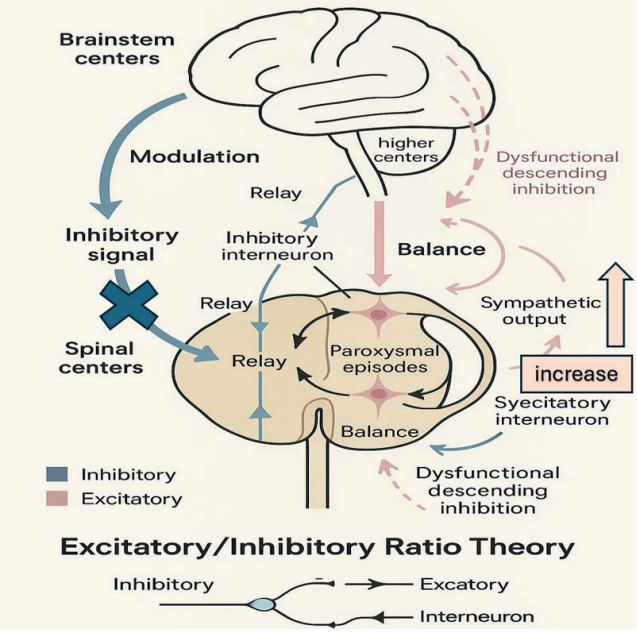

Figure 2. Schematic representation of excitatory / inhibitory ratio theory

Diagnosing PSH

In order to diagnose PSH, like all other syndromes, first one must have a strong degree of suspicion. First step of diagnosing PSH is excluding all the other causes of the symptoms such as sepsis, pulmonary embolism, epilepsy or hypoxic brain (1,2,6,10). As mentioned above these findings of sympathetic hyperactivity episodes are tachycardia, hypertension, hyperthermia, sweating, tachypnea, posturing (2,5,6,9,10). Moreover some of the less frequent symptoms are mydriatic pupils, altered consciousness, bowel disorders, alterations in blood glucose levels, increased bronchial secretions and hypersalivation, desynchrony with mechanical ventilator, excitation and horripilation (2,5,6). The duration of these episodes may vary between minutes, hours, and in severe cases it may occur a few times in a day. They may even become continuous in refractory cases (4). Because these symptoms may overlap with other TBI related pathological outcomes such as; seizures, sepsis, embolism, neuroleptic malignant syndrome, central fever, traumatic pain, different brain injuries, sedation withdrawal, hypoxia, rhabdomyolysis, and dehydration diagnosing PSH is often delayed or misdiagnosed resulting in complications in the management of the case (1,3,4). There is also another entity resembling paroxysmal sympathetic hyperactivity in nomenclature and that is autonomic dysreflexia. Autonomic dysreflexia patients have episodes of hypertension after a high spinal cord (above the level of thoracal 6 vertebra) injury, however they are usually bradycardic as a reflex response to hypertension, and they often have debilitating headaches; differentiating this syndrome from PSH (16-20).

Diagnosing PSH as early as possible has great importance because delayed recognition may result in unnecessary work-up and inappropriate use of medications may prolong hospitalization. Uncontrolled symptoms can lead to secondary brain injury caused by hypertension, hyperthermia and cardiac damage. It should also be kept in mind that

Table 1. Diagnostic likelihood tool (1 point for each feature)	
Clinical features occur simultaneously	1 point
Episodes are paroxysmal in nature	1 point
Sympathetic over – reactivity to normally non-painful stimuli	1 point
Features persist > 3 consecutive days	1 point
Features persist > 2 weeks post brain injury	1 point
Features persist despite treatment of alternative differential diagnosis	1 point
Medication administered to decrease sympathetic features	1 point
> 2 episodes daily	1 point
Absence of parasympathetic features during episodes	1 point
Absence of other presumed cause of features	1 point
Antecedent acquired brain injury	1 point

these other pathologies may coexist and even trigger episodes of PSH (4).

Therefore the intensivist should keep the possibility of PSH in mind, especially when the patient is coming out of a coma or when the patient is weaned from sedatives (4,10).

Neuro-imaging techniques like computerized tomography (for acute phase) and magnetic resonance images (in stable patients) are helpful to identify the anatomical place and the morphological structure of the injury and as in a case report from the literature, they often show diffuse axonal injury (3,6,10,12,21). Aside from these techniques, dysconnectivity in white matter; especially on the right posterior internal capsule, corpus callosum and the splenium shown on diffusion tensor imagings are associated with the early stages of PSH (2).

Even though there is no specific biomarker for PSH a study by Fernandez et al showed that plasma catecholamine (and to a lesser extend adrenocortical hormone) levels increased during the episodes of PSH (22). Moreover another study showed that procalcitonin levels can be used to differentiate between infectious pathologies and PSH (23).

A diagnostic tool named Paroxysmal Sympathetic Hyperactivity - Assessment Measure which consisted of two different components, was developed in order to help guiding the clinical management and to standardize the diagnostic criteria. One of the components, referring to the possibility of the diagnosis, is a diagnosis likelihood tool (DLT) (Table 1) derived from 11 characteristics of this syndrome, and the other one, evaluating the severity and intensity of the symptoms in each hyperactivity episode, is a clinical feature scale (CFS) (Table 2) (1,3,9). The DLT evaluates 11 main items with the presence of each scored as one point and absences are scored as zero. If the symptoms persist for three consecutive days, the diagnosis of PSH is more probable. Data to evaluate six main symptoms CFS is used. CFS has a value range between zero and three. A combined score of DLT and CFS gives us the Paroxysmal Sympathetic Hyperactivity Assessment Measure (PSH-AM) (Table 3). If the score is < 8 points the diagnosis is unlikely, if it is between 8-16 points the diagnosis is possible and if the score is > 17 points the diagnosis is probable (1,2,9).

Treatment Modalities in PSH

Treating PSH is challenging due to the lack of guidelines and the complicated etiology of the syndrome. That is why the treatment modalities mostly focus on controlling the symptoms and the episodes (2,4).

Treatment approach should include adequate sedation, analgesia and muscle relaxation. However, the clinician must be ready to treatment related scenarios like prolonged mechanical ventilation support and a delay in neurological rehabilitation

Table 2. Clinical feature scale

	0	1	2	3
Heart Rate	<100/per minute	100-119/per minute	120-139/per minute	>140/per minute
Respiratory Rate	<18/ per minute	18-23/per minute	24-29/per minute	>30/per minute
Systolic Blood Pressure	<140 mmHg	140-159 mmHg	160-179 mmHg	>180 mmHg
Temperature	<37oC	37oC-37.9oC	38oC-38.9oC	>39oC
Sweating	Nil	Mild	Moderate	Severe
Posturing During Episodes	Nil	Mild	Moderate	Severe

of the patient (3). Moreover, while treating PSH the possibility of multisystem organ dysfunction must also be considered and possible adverse events like cardiac hypertrophy, muscle wasting and dehydration must also be treated. We must also make sure that the patient is receiving enough calories and water-electrolyte levels are balanced (6,10). In order to treat this syndrome, an approach of both pharmacological and nonpharmacological should be combined (4).

Pharmacological Treatment

Medical treatments include a diversity of drug groups, each affecting or preventing different symptoms. Opioids, beta-blockers, dopamine agonists, alfa2 agonists (clonidine, dexmedetomidine), GABAergic agents, benzodiazepines, gabapentin, baclofen (can be given either enterally or intrathecal) and muscle relaxants are mostly used (1,3,4,10). Pharmacological approach focuses on three steps: symptom avoidance, prevention and refractory treatment. Symptom abortive medications should be administered as soon as the episodes are identified they focus on stopping the paroxysmal episodes (2). They have a rapid onset of action and a short half-life; for example, use of antipyretics to treat hyperthermia, sedatives for agitation, muscle relaxants to relieve spasticity and postures, and antihypertensive agents for hypertension. Morphine and short acting benzodiazepines are considered first line treatment (2,4).

Preventive medications aim to control the episodes and to reduce their frequency as well as severity, in order to avoid any arrhythmia, cardiac overload, dehydration, and loss of muscle mass. This approach includes the usage of non-selective beta-blockers, alfa 2 agonists bromocriptine, baclofen, gabapentin and long-acting benzodiazepines. Among these drugs, Propranolol a non-selective B-blocker has shown to reduce mortality rates when given 20-60mg doses in every 4-6 hours. Besides its cardiovascular effects, propranolol also helps lower the body temperature. Furthermore, dexmedetomidine, an alpha-2 agonist, can be administered as an intravenous infusion at a rate of 0.2–0.7 mcg/kg/h to provide sedation and analgesia, regardless of whether the patient is receiving ventilatory support or not. It is also preferred on TBI patients to prevent PSH (2,4).

Table 3. Paroxysmal sympathetic hyperactivity – assessment measure (PSH-AM)

Unlikely	<8 points
Possible	8-16 points
Probable	>17 points

Refractory treatment modalities aim to avoid secondary brain damage from hypertension, hyperthermia and cardiac damage. During the refractory period continues or bolus intravenous medications likes propofol, benzodiazepines, opioids or dexmedetomidine can be used. Also, intrathecal baclofen use may also be considered in some refractory cases in which posturing episodes persist. Dantrolene, a ryanodine receptor antagonist may also be used for posturing during the refractory period, but with close monitorization of liver function tests (3,4,6).

Because there is no treatment guideline, centers can prepare their own PSH treatment protocols according to clinical presentations of PSH (3,4). Besides, we can

also use the PSH-AM scores to combine treatment modalities. For patients with a score of <8 points only the dominant symptoms might be targeted, whereas for patients with a score of 8-16 points both symptomatic and preventive modalities might be used. Patients with a score of >17 points might need symptomatic, preventive treatment as well as baclofen, gabapentin and even dantrolene (6).

Non-pharmacological treatment

As mentioned above, the treatment of PSH should include both pharmacological and non-pharmacological approaches. Non-pharmacological approach aims to prevent any sympathetic hyperactivity episode triggering events, reduce sympathetic nervous activity and lighten any adverse effects (3).

Avoidance of excessive external stimuli while giving daily care, and controlling room temperature are of major importance (3,5).

During ICU management of patients with PSH it must be taken into account that energy consumption of these patients are increased during the episodes, therefore their caloric requirements are also increased because of a hyperfunctioning brain (24,25). Close monitorization of nutrition and hydration status as well as early initiation of enteral nutrition is of crucial importance (26).

Physiotherapy must also keep in mind in order to extend the motion range and prevent contractile postures (3).

Family support and their education are also very important for the management of these patients because the road to recovery is hard and long. Also, Salmani et al showed that family related stimulations are more effective than sensory stimulations in order to improve consciousness (24,27).

The relationship of PSH with cerebral hypoxia might bring hyperbaric oxygen therapy (HBOT) to mind. It was shown in a case series HBOT controlled autonomic discharges and posturing episodes in the subacute phase of TBI and is a good treatment option in refractory PSH with pharmacological therapy (28). Moreover, in a study conducted by Wang et al, two groups of PSH patients, one received HBOT, and the other group did not, were compared. The study revealed that the group which had HBOT had lower PSH-AM scores, more clear relief of PSH symptoms, more awake patients, higher Glasgow Coma Scale scores and shorter ICU stay (29).

Clinical Features and Intensive Care Management of PSH

Paroxysmal Sympathetic Hyperactivity syndrome is a complex disease in which the main symptoms consist of paroxysmal episodes of sympathetic and motor hyperactivity. Although these main symptoms are tachycardia, tachypnea, hypertension, hyperthermia, sweating and posturing, it should also be expected to see different symptoms in each patient (3). During the ICU stay these hyperactivity episodes occur in a cyclic pattern. Even though the episodes may occur spontaneously, they may also occur after non-painful stimuli such as endotracheal tube aspirating, exposure to touch or light or physiotherapy (6).

Another important approach is to remember that some of the symptoms might be masked by the therapeutic processes of TBI or may overlap with other neurological issues related to TBI (3,4). Number of symptoms rather than the duration of episodes are more indicative as to the severity of the disease. Non-adequate controlling of these symptoms may result in secondary brain damage and therefore leading to a poor prognosis (4,6).

The episodes may last a few minutes or as long as two hours, and they can even occur several times in a day or they may occur continuously in refractory cases (3,4). On the other hand the duration of PSH may also change between a few weeks and more than a year (3).

PSH occurs in three stages. First one, the hyperacute phase usually refers to the first week of admission in which the damage to the brain is maximum but the patient is usually asymptomatic due to heavy sedation, analgesia and neuromuscular blockers (if needed) in order to treat TBI and other related injuries. This results in a delay in diagnosis unless the patient awakens for some reason. The second phase is the one in which the patient shows paroxysmal episodes of sympathetic and motor discharges. The last phase starts when hyperhidrosis ends. During this stage declines in posturing episodes are seen. Furthermore, this stage represents the rehabilitation phase which can last for years but with less frequent and severe episodes (6,10).

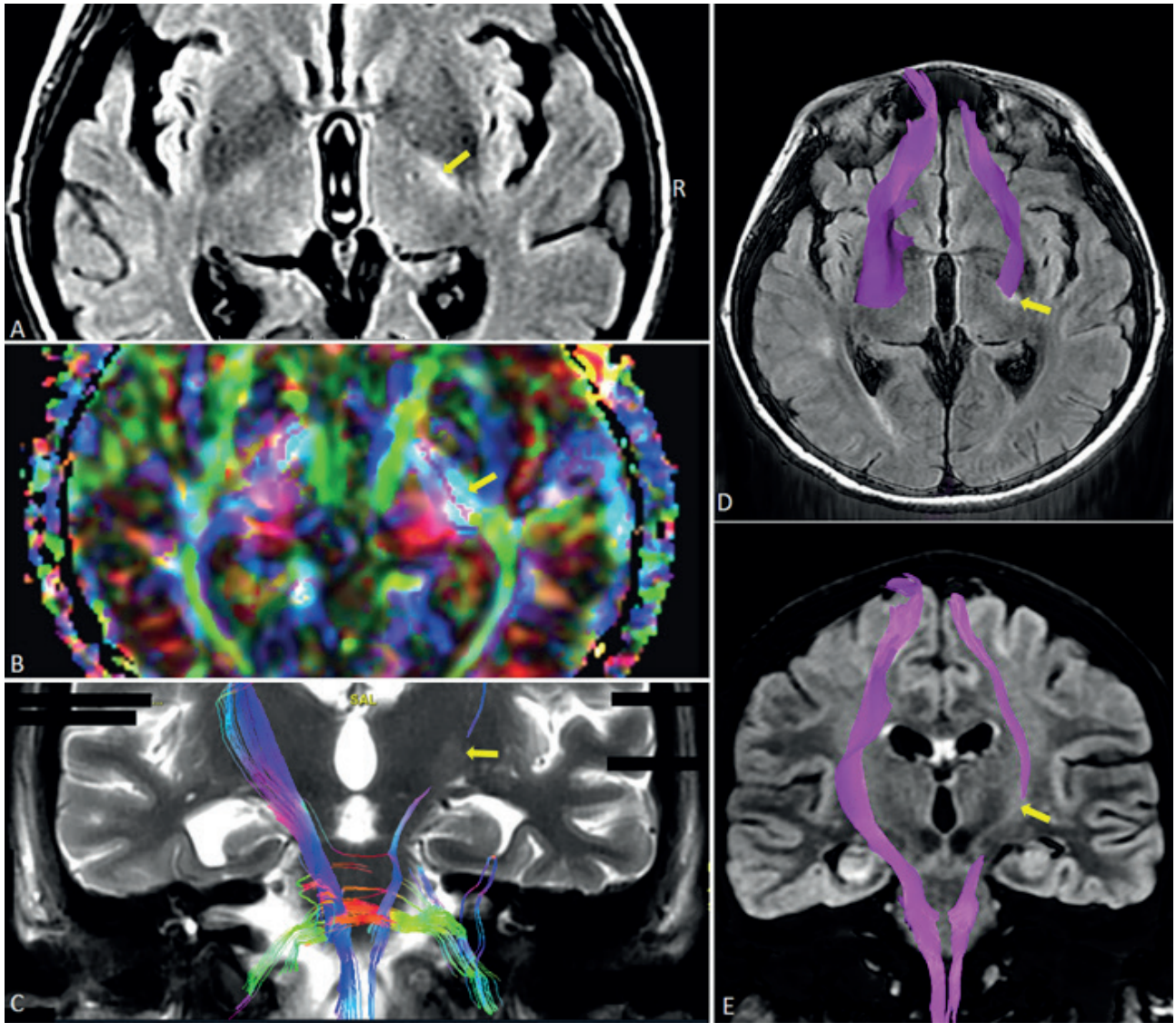

Figure 3. Diffusion tensor imaging (DTI) and tractography magnetic resonance imaging (MRI) findings of diffuse axonal injury

Axial FLAIR imaging (A) reveals a subtle hyperintense signal in the posterior limb of the right internal capsule (yellow arrow), consistent with chronic changes due to diffuse axonal injury. The color-coded fractional anisotropy (FA) map (B) demonstrates focal disruption, reflecting underlying microstructural damage and reduced white matter integrity. Tractography (C) reveals a noticeable reduction in the density and continuity of fibers passing through the affected region of the internal capsule. The background axial (D) and coronal (E) FLAIR images, combined with corticospinal tract (CST) visualization, confirm that the lesion spatially overlaps with the right CST, indicating trauma related degeneration or partial disruption along its trajectory.

It should also keep in mind that other medical conditions related to trauma and intensive care treatments may also cause delays in diagnosing PSH, as in a case reported by ourselves (21). In this case report it was stated that a 26-year-old female suffering from TBI was admitted to the ICU with diffuse axonal injury and deep coma. Even though she had episodes of sympathetic activities at early admission she also had other medical problems like sepsis and acute hypoxemic respiratory failure at the same time. During her stay in the ICU her magnetic resonance images showed diffuse axonal injury (Figure 3) and the sympathetic symptoms re-occurred while there were no other contemporaneous medical problems. Since PSH-AM was applied. Her CFS was 13, DLT was 9 and she had a total PSH-AM score of 22 and diagnosed with PSH. The diagnostic tool PSH-AM can help the clinician diagnose and treat PSH at early stages, if it begins to be used from the admission of the patient unless there are no other concurrent pathologies.

PSH is often recognized once the intravenous sedation infusions are stopped and the patient begins to awaken. In the case report mentioned above the patient was given metoprolol, gabapentin, tramadol, dexmedetomidine, amantadine sulfate, melatonin and modafinil as pharmacological treatment to control the symptoms (21).

Paroxysmal Sympathetic Hyperactivity syndrome is usually associated with poor long-term outcomes such as, low level of consciousness and low Glasgow Coma Scale scores, longer hospital stays, higher dependance to mechanical ventilation, tracheostomy indication, and more infectious complications (3,5,30). While managing these patients in the ICU it must be kept in mind that PSH results in a hypermetabolic state which leads to weight loss and dehydration as a result of hypercatabolism, heterotopic ossifications, inflammation, immunosuppression and infections, all of which resulting in excessive interventions, delayed rehabilitation, increase in morbidity, longer hospital and ICU stays (1-3,6,30). Even though there is no consensus on the relationship of PSH and weaning from mechanical ventilation, the intensivist should also evaluate the effects of PSH on the weaning process (2).

Conclusion

Prompt recognition of PSH is essential, because delayed diagnosis may result in unnecessary work-up, inappropriate use of medications, excessive interventions, and prolonged hospitalization. The occurrence of PSH after TBI should always be suspected especially if the patient is showing episodes of sympathetic hyperactivity while being weaned from sedative agents. Because PSH is often recognized once the intravenous sedation infusions are stopped and the patient begins to awaken. In order to treat this syndrome an approach of both pharmacological and nonpharmacological should be combined. It must be kept in mind that uncontrolled symptoms may also lead to secondary brain injury caused by hypertension, hyperthermia, cardiac damage and even death.

Author contribution

Study conception and design: TU, AGYS; data collection: AGYS, ZF; analysis and interpretation of results: AGYS, TU; draft manuscript preparation: AGYS, TU. The author(s) reviewed the results and approved the final version of the article.

Source of funding

The authors declare the study received no funding.

Conflict of interest

The authors declare that there is no conflict of interest.

References

1. Godo S, Irino S, Nakagawa A, et al. Diagnosis and management of patients with paroxysmal sympathetic hyperactivity following acute brain injuries using a consensus-based diagnostic tool: a single institutional case series. Tohoku J Exp Med. 2017;243:11-8. [Crossref]
2. Panjaitan JA, Ginting LF, Rajagukguk M, Sibagariang DB, Siahaan AM. Paroxysmal sympathetic hyperactivity: current update on diagnosis, treatments, and outcomes. Surg Neurol Int. 2025;16:163. [Crossref]
3. Zheng RZ, Lei ZQ, Yang RZ, Huang GH, Zhang GM. Identification and management of paroxysmal sympathetic hyperactivity after traumatic brain injury. Front Neurol. 2020;11:81. [Crossref]
4. Samuel S, Allison TA, Lee K, Choi HA. Pharmacologic management of paroxysmal sympathetic hyperactivity after brain injury. J Neurosci Nurs. 2016;48:82-9. [Crossref]
5. Totikov A, Boltzmann M, Schmidt SB, Rollnik JD. Influence of paroxysmal sympathetic hyperactivity on the functional outcome of neurological early rehabilitation patients: a case control study. BMC Neurol. 2019;19:162. [Crossref]
6. Godoy D, Panhke P, Guerrero Suarez PD, Murillo-Cabezas F. Paroxysmal sympathetic hyperactivity: an entity to keep in mind. Medicina Intensiva (English Edition). 2019;43:35-43. [Crossref]
7. Wang D, Su S, Tan M, Wu Y, Wang S. Paroxysmal sympathetic hyperactivity in severe Anti-N-Methyl-d-Aspartate receptor encephalitis: a single center retrospective observational study. Front Immunol. 2021;12:665183. [Crossref]
8. Li Z, Chen W, Zhu Y, et al. Risk factors and clinical features of paroxysmal sympathetic hyperactivity after spontaneous intracerebral hemorrhage. Auton Neurosci. 2020;225:102643. [Crossref]
9. Baguley IJ, Perkes IE, Fernandez-Ortega JF, et al. Paroxysmal sympathetic hyperactivity after acquired brain injury: consensus on conceptual definition, nomenclature, and diagnostic criteria. J Neurotrauma. 2014;31:1515-20. [Crossref]
10. Meyer KS. Understanding paroxysmal sympathetic hyperactivity after traumatic brain injury. Surg Neurol Int. 2014;5:490-2. [Crossref]
11. Burzynska M, Wozniak J, Urbanski P, et al. Heart rate variability and cerebral autoregulation in patients with traumatic brain injury with paroxysmal sympathetic hyperactivity syndrome. Neurocrit Care. 2025;42:864-77. [Crossref]
12. Xu SY, Zhang Q, Li CX. Paroxysmal sympathetic hyperactivity after acquired brain injury: an integrative review of diagnostic and management challenges. Neurol Ther. 2024;13:11-20. [Crossref]
13. Qian J, Min X, Wang F, Xu Y, Fang W. Paroxysmal sympathetic hyperactivity in adult patients with brain injury: a systematic review and meta-analysis. World Neurosurg. 2022;166:212-9. [Crossref]
14. Perkes I, Baguley IJ, Nott MT, Menon DK. A review of paroxysmal sympathetic hyperactivity after acquired brain injury. Ann Neurol. 2010;68:126-35. [Crossref]
15. Zhu K, Zhu Y, Hou X, et al. NETs lead to sympathetic hyperactivity after traumatic brain injury through the LL37-Hippo/MST1 pathway. Front Neurosci. 2021;15:621477. [Crossref]
16. Jafari AA, Shah M, Mirmoeeni S, et al. Paroxysmal sympathetic hyperactivity during traumatic brain injury. Clin Neurol Neurosurg. 2022;212:107081. [Crossref]
17. Morgan S. Management of autonomic dysreflexia in the community. Br J Community Nurs. 2020;25:496-501. [Crossref]
18. Solinsky R, Kirshblum SC, Burns SP. Exploring detailed characteristics of autonomic dysreflexia. J Spinal Cord Med. 2018;41:549-55. [Crossref]
19. Hou S, Rabchevsky AG. Autonomic consequences of spinal cord injury. Compr Physiol. 2014;4:1419-53. [Crossref]
20. Eldahan KC, Rabchevsky AG. Autonomic dysreflexia after spinal cord injury: systemic pathophysiology and methods of management. Auton Neurosci. 2018;209:59-70. [Crossref]
21. Gizem A, Selimoğlu Y, Aytaç E, Nizam B, Utku T. Diagnosing paroxsymal sympathetic hyperactivity syndrome after traumatic brain injury, an inspiring case report. Paper presented at: 24th International Intensive Care Symposium; 2023 May 2-3; İstanbul, Türkiye.
22. Fernandez-Ortega JF, Baguley IJ, Gates TA, Garcia-Caballero M, Quesada-Garcia JG, Prieto-Palomino MA. Catecholamines and paroxysmal sympathetic hyperactivity after traumatic brain injury. J Neurotrauma. 2017;34:109-14. [Crossref]
23. Bindra A, Chowdhary V, Dube SK, Goyal K, Mathur P. Utility of serum procalcitonin in diagnosing paroxysmal sympathetic hyperactivity in patients with traumatic brain injury. Indian J Crit Care Med. 2021;25:580-3. [Crossref]
24. Yin P, Pan Y, Chen D, et al. Diagnosis and management of paroxysmal sympathetic hyperactivity: a narrative review of recent literature. Eur J Med Res. 2025;30:349. [Crossref]
25. Mehta NM, Bechard LJ, Leavitt K, Duggan C. Severe weight loss and hypermetabolic paroxysmal dysautonomia following hypoxic ischemic brain injury: the role of indirect calorimetry in the intensive care unit. JPEN J Parenter Enteral Nutr. 2008;32:281-4. [Crossref]

26. Caldwell SB, Smith D, Wilson FC. Impact of paroxysmal sympathetic hyperactivity on nutrition management after brain injury: a case series. Brain Inj. 2014;28:370-3. [Crossref]

27. Salmani F, Mohammadi E, Rezvani M, Kazemnezhad A. The effects of family-centered affective stimulation on brain-injured comatose patients' level of consciousness: a randomized controlled trial. Int J Nurs Stud. 2017;74:44-52. [Crossref]

28. Lv LQ, Hou LJ, Yu MK, Ding XH, Qi XQ, Lu YC. Hyperbaric oxygen therapy in the management of paroxysmal sympathetic hyperactivity after severe traumatic brain injury: a report of 6 cases. Arch Phys Med Rehabil. 2011;92:1515-8. [Crossref]

29. Wang H, Li Y, Shen S, et al. Hyperbaric oxygen therapy for paroxysmal sympathetic hyperactivity syndrome after brain injury: a multicenter, retrospective cohort study. Med Gas Res. 2025;15:327-31. [Crossref]

30. Nasa P, Majeed NA, Juneja D. Paroxysmal sympathetic hyperactivity after traumatic brain injury: current understanding and therapeutic options. Indian J Crit Care Med. 2024;28:97-9. [Crossref]

Turk J Intensive Care 2026;24(1):21-29
DOI: 10.63729/TJIC.2026.685

ORIGINAL RESEARCH

Relationship between optic nerve sheath diameter, Glasgow Coma Scale, and the impact of PEEP in critically ill patients: a prospective observational study

Merve İkbal Göncü[1], Engin İhsan Turan[1], Ezgi Aydın İnan[1], Oktay İnan[1], Ebru Kaya[2], Ayça Sultan Şahin[1]

[1]Department of Anesthesiology, İstanbul Health Science University Kanuni Sultan Süleyman Education and Training Hospital, İstanbul, Türkiye
[2]Department of Intensive Care, İstanbul Health Science University Kanuni Sultan Süleyman Education and Training Hospital, İstanbul, Türkiye

ABSTRACT

Objective: Optic nerve sheath diameter (ONSD) has been increasingly recognized as a non-invasive surrogate marker for intracranial pressure (ICP) in critically ill patients. The Glasgow Coma Scale (GCS) is a widely used tool for assessing neurological status. However, the relationship between GCS and ONSD in intensive care unit (ICU) patients remains underexplored. This study aimed to investigate the association between ONSD and GCS scores in ICU patients, while also evaluating the impact of positive end-expiratory pressure (PEEP) on ONSD measurements.

Methods: This prospective observational study included 66 ICU patients. ONSD measurements were obtained using ultrasonography at 24 and 48–72 hours after ICU admission. Patients were categorized into three groups based on GCS scores (3–7, 8–11, 12–15). The effect of PEEP and other clinical parameters on ONSD was analyzed using linear mixed models, with a significance level of $p < 0.05$.

Results: ONSD was significantly higher in patients with lower GCS scores ($p < 0.001$). Additionally, PEEP application was strongly associated with increased ONSD ($p < 0.001$), whereas other factors such as mean arterial pressure, heart rate, and sepsis status did not show significant effects.

Conclusion: ONSD is significantly associated with GCS scores, supporting its role as a non-invasive marker of neurological deterioration. The influence of PEEP on ONSD suggests a potential impact of mechanical ventilation on ICP dynamics, warranting further investigation.

Keywords: optic nerve sheath diameter, Glasgow Coma Scale, intracranial pressure, ultrasonography, intensive care unit

Introduction

Optic nerve sheath diameter (ONSD) has emerged as a promising non-invasive indicator of increased intracranial pressure (ICP) in critically ill patients. Ultrasonographic assessment of ONSD allows for rapid and reliable detection of ICP changes, providing an alternative to invasive intracranial monitoring techniques. Recent studies have demonstrated that ultrasonographic ONSD measurements correlate with direct ICP measurements, making it a valuable tool for clinical decision-making in neurocritical care settings (1-3).

The Glasgow Coma Scale (GCS) is a widely used clinical scoring system for assessing consciousness and neurological function in patients with brain injuries or altered mental status. Several studies have reported a significant association between ONSD and GCS scores in traumatic brain injury, suggesting that patients with lower GCS scores tend to have increased ONSD, which may reflect elevated ICP (4,5). This relationship highlights the potential utility of ONSD measurements as a bedside tool for evaluating neurological deterioration in ICU patients.

✉ Engin İhsan Turan • enginihsan@hotmail.com

Received: 22.08.2025 **Accepted:** 11.11.2025 **Published:** 26.03.2026

Despite the growing body of literature on ONSD and its clinical implications, further research is needed to explore its correlation with various physiological parameters in critically ill patients. In particular, factors such as mechanical ventilation, sepsis, and comorbidities may influence ONSD measurements, warranting a more comprehensive analysis of its diagnostic value (3).

This study aims to investigate the relationship between ONSD and GCS scores in ICU patients while also assessing the impact of key clinical factors, including mechanical ventilation settings, hemodynamic parameters, and comorbidities. By examining these associations, we aim to determine the potential role of ONSD as a non-invasive biomarker for neurological monitoring and patient prognosis in intensive care settings.

Methodology

Ethical considerations

The study was conducted in accordance with the Declaration of Helsinki and ethical approval was obtained from the institutional ethics committee (IRB Number: 2020.12.208). Informed consent was obtained from all patients or their legal representatives before participation.

Study design and patient selection

This prospective observational study included adult patients (≥18 years old) who were admitted to the intensive care unit (ICU) for various reasons and received treatment between January 2021 and April 2021.

Inclusion and exclusion criteria

Patients were included if they were ≥18 years old and had a hospital stay of at least 24 hours. The exclusion criteria were:

- Age <18 or >75 years,
- Hospital stay <24 hours,
- Presence of conditions that could increase intracranial pressure, such as intracranial mass lesions or intracranial hemorrhage, (Patients with acute intracranial hemorrhage requiring neurosurgical intervention were excluded. However, patients with stable or chronic intracranial hemorrhage were included if no active ICP elevation was present.)
- History of ocular disease, including orbital tumors, optic neuritis, glaucoma, hyperthyroidism, or any condition affecting optic nerve sheath integrity.

Study hypothesis

The primary hypothesis of this study was that lower GCS scores would be associated with higher ONSD values in critically ill patients.

Collected data and study parameters

The study recorded the following parameters for each patient:

- Demographic characteristics (age, gender),
- Body mass index (BMI, kg/m^2),
- ICU admission indication,
- Comorbid conditions,
- Vital parameters,
- GCS score,
- Endotracheal intubation status,
- Ventilation mode and ventilation parameters,
- ONSD measurements (mm) at 24 hours and 48-72 hours.

ONSD measurement procedure

ONSD measurements were performed twice for each patient:

1. Within the first 24 hours of ICU admission,
2. Between 48-72 hours after admission.

Measurements were obtained using ultrasonography by an experienced researcher utilizing a MyLab™Six ultrasound system (Esaote SpA, Genoa, Italy) with a 4–15 MHz linear probe in B-mode. The patient was positioned supine with the head elevated at a 20–30° angle. A gel was applied to the temporal region of the closed eyelid to avoid direct pressure on the eye, and the ultrasound probe was gently placed over the eyelid (Figure 1a).

ONSD was measured 3 mm posterior to the retina along the perpendicular axis of the optic nerve using an electronic caliper (Figure 1b). Each measurement was performed twice, and the average value was recorded. All measurements were performed by the same investigator to ensure consistency and reduce interobserver variability.

All intubated patients were ventilated in SIMV mode with a standardized PEEP of 5 cmH_2O during ONSD measurements. The No-PEEP group consisted of non-intubated patients who were spontaneously breathing on room air or with supplemental oxygen via face mask without PEEP. All intubated patients received continuous sedation with midazolam (0.02–0.1 mg/kg/h) and remifentanil (0.05–0.2 μg/kg/min) infusions during measurements.

For intubated patients, the verbal component of the Glasgow Coma Scale was recorded as "1T" (for tube), while the eye-opening and motor responses were assessed based on the patient's reaction to verbal or painful stimuli.

We acknowledge that GCS assessment under sedation provides a suboptimal reflection of neurological status; therefore, to minimize potential bias, patients were analyzed using grouped GCS categories (3–7, 8–11, and 12–15) rather than relying on precise numeric scores. This approach allowed for more consistent interpretation across patients with varying sedation depths and ventilatory condition.

Figure 1. (a) Ultrasound measurement of the optic nerve sheath diameter (ONSD) was performed with the patient's head positioned at a 20-30° angle in the supine position, ensuring no pressure was applied to the eye. (b) ONSD measured at 3 mm in a patient.

Statistical analysis

The normality of the data was assessed using the Shapiro-Wilk test. We analyzed the relationship between ONSD and gender BMI and Sepsis using independent sample t test. We analyzed the relationship between ONSD and GCS, MAP, Heart Rate, SpO2, PEEP using a linear mixed-effects model with a random intercept for subjects and a compound symmetry covariance structure to account for repeated measurements at 24 and 72 hours. A p-value <0.05 was considered statistically significant.

Sample size calculation

This study aims to compare measurements across three groups based on the GCS levels. A preliminary study with 15 patients was conducted, and the mean values with standard deviations in each group were as follows:

- GCS 3-7 group: 4.1 mm (SD: 0.4)
- GCS 8-11 group: 3.8 mm (SD: 0.4)
- GCS 12-15 group: 3.5 mm (SD: 0.4)

Based on these values, the effect size was calculated as 0.61. To achieve 95% statistical power while maintaining a Type I error rate of 5% ($\alpha = 0.05$), a power analysis using G*Power determined that at least 45 patients should be included in the study.

However, considering potential patient losses and missing data during follow-up, the study is planned to be conducted with a total of 66 patients to ensure sufficient statistical power and reliability.

Results

Totally 66 patients were included in this study (Figure 2). In our cohort, the most common indication for intensive care admission was sepsis (n=19), followed by respiratory causes (n=18), including pneumonia, COPD exacerbations, and asthma attacks. Other frequent indications were postoperative close monitoring (n=12), multitrauma (n=8), cerebrovascular events (n=4), and intracranial hemorrhage (n=4). Less frequent causes included status epilepticus (n=1) and intoxication (n=1).

Table 1 presents demographic and clinical characteristics of the study population. Among the 66 patients, 60.6% were male and 39.4% were female. The mean age was 58.67 ± 18.84 years, while the mean BMI was 27.13 ± 5.74. Sepsis was present in 47% of the patients, while 53% had no sepsis.

Regarding comorbidities, 24.2% of patients had diabetes mellitus (DM), 31.8% had hypertension (HT), and 12.1% had a history of malignancy. Chronic obstructive pulmonary disease (COPD) was observed in 6.1% of patients, while 13.6% had chronic kidney disease (CKD). Parkinson's disease and Alzheimer's disease were present in 3% and 7.6% of patients, respectively. Additionally, 12.1% had a cardiac

Table 1. Demographical data of the patients

	Count	Percentage (%)/ Mean ± Std
Male	40	60,6
Female	26	39,4
Age (years)	66	58,67 ± 18,84
BMI (kg/m²)	66	27,13 ± 5,74
No Sepsis	35	53
Sepsis	31	47
Diabetes Mellitus (DM)	16	24,2
Hypertension (HT)	21	31,8
Any Malignancy History	8	12,1
COPD	4	6,1
Chronic Kidney Disease (CKD)	9	13,6
Parkinson's Disease	2	3
Alzheimer's Disease	5	7,6
Any Cardiac Condition	8	12,1
Patients with No Comorbidities	17	25,8

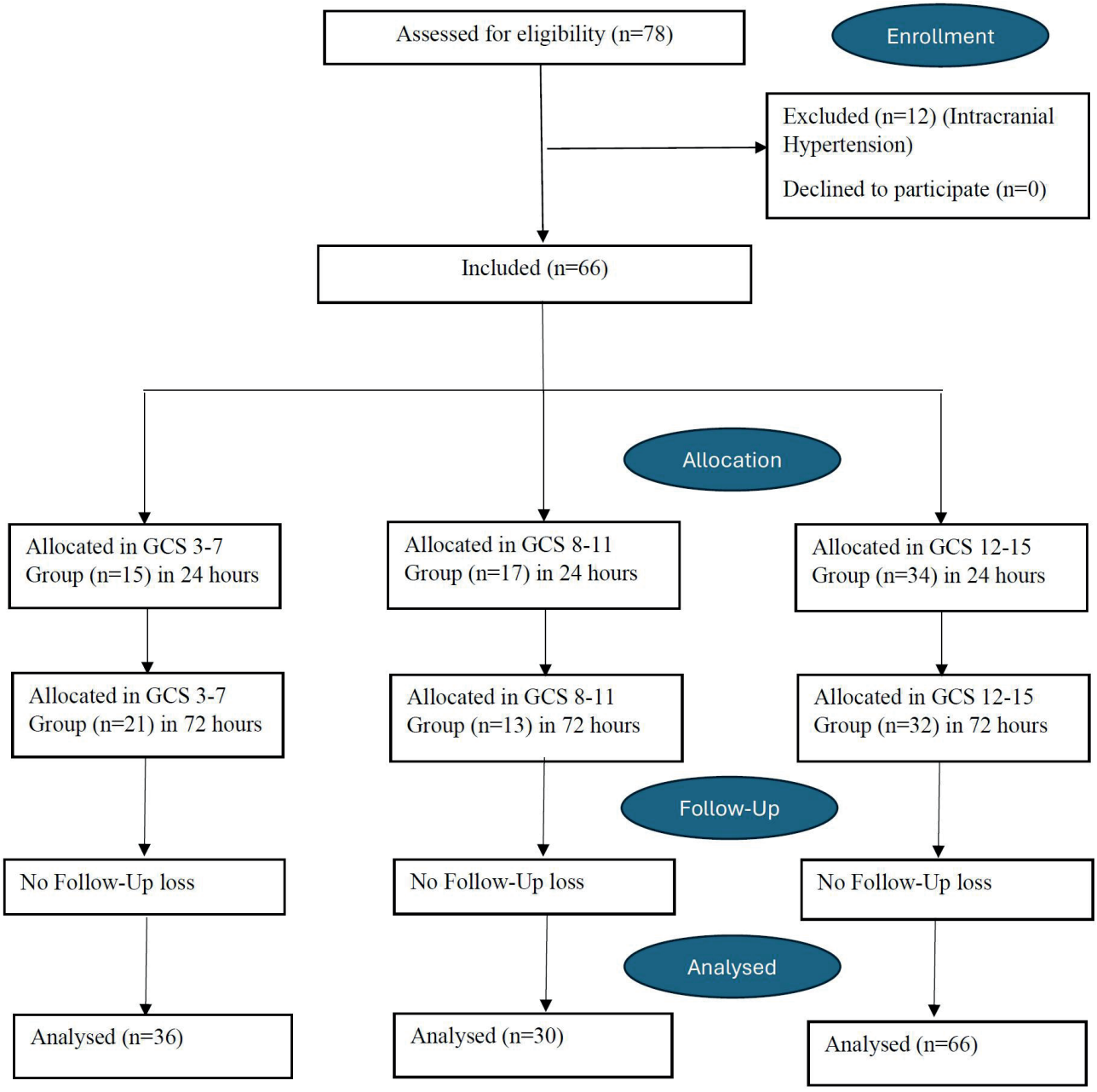

Figure 2. Flow diagram of patient population

condition. Notably, 25.8% of the patients had no comorbidities (Table 1).

Table 2 presents the comparison of optic nerve sheath diameter (ONSD) across selected patient characteristics. No statistically significant differences in ONSD were observed between male and female patients ($p = 0.655$), between patients with BMI < 30 and BMI ≥ 30 ($p = 0.191$), or between patients with and without sepsis ($p = 0.914$).

Table 3 summarizes the results of the linear mixed model analysis examining factors associated with ONSD. PEEP application was strongly associated with higher ONSD values ($F = 74.534$, $p < 0.001$). In contrast, mean arterial pressure (MAP), heart rate (HR),

Table 2. Comparison of optic nerve sheath diameter between patients characteristics

	ONSD (mm) (Mean ± Std)	p-value[1]
Male (n=40)	3.72 ± 0.36	0.655
Female (n=26)	3.76 ± 0.37	
BMI<30 (n=51)	3.71 ± 0.36	0.191
BMI>30 (n=15)	3.85 ± 0.36	
No-Sepsis (n=35)	3.74 ± 0.32	0.914
Sepsis (n=31)	3.73 ± 0.41	

[1] Independent Sample t Test has been applied.

Table 3. Comparison of optic nerve sheath diameter between variables

Fixed Effect	F (df)	p-value[1]
GCS (per 1-point change)	54.4	<0.001
Timepoint (24h vs 72h)	0.52	0.472
HR (beats/min) (<100 vs ≥100)	3.560	0.061
MAP (mmHg) (<65 vs ≥65)	0.929	0.337
SpO_2 (%) (≤97 vs >97)	1.092	0.298
PEEP (cmH_2O) (No vs Yes)	74.534	<0.001

[1] Linear Mixed Model has been applied.

and peripheral oxygen saturation (SpO_2) categories did not show statistically significant associations with ONSD (all $p > 0.05$). Timepoint of measurement (24h vs 72h) also had no significant effect on ONSD ($F = 0.52$, $p = 0.472$). Importantly, lower Glasgow Coma Scale (GCS) scores were significantly associated with higher ONSD values ($F = 54.4$, $p < 0.001$), supporting the primary study hypothesis.

Discussion

This study aimed to explore the relationship between ONSD and GCS scores in intensive care unit (ICU) patients, while also evaluating the impact of positive end-expiratory pressure (PEEP) on ONSD measurements. Our study demonstrated a significant association between ONSD and Glasgow Coma Scale GCS scores, with lower GCS scores corresponding to higher ONSD values, suggesting a potential role of ONSD as a non-invasive marker of intracranial pressure (ICP) changes in critically ill patients. Patients in the GCS 3–7 group had significantly higher ONSD measurements compared to the GCS 8–11 and GCS 12–15 groups, while the GCS 8–11 group also had significantly higher ONSD values than the GCS 12–15 group (all $p < 0.01$). Additionally, PEEP application was associated with significantly higher ONSD values compared to patients without PEEP ($p < 0.001$), supporting previous findings that mechanical ventilation settings may influence ICP dynamics by reducing cerebral venous outflow. In contrast, no significant associations were found between ONSD and MAP, heart rate (HR), SpO_2, gender, BMI, or sepsis status, suggesting that these factors do not substantially affect ONSD measurements in ICU patients.

Multiple studies have demonstrated a significant correlation between ONSD and intracranial pressure (ICP), supporting the use of ONSD as a reliable, noninvasive surrogate marker for ICP elevation (7-9). Research has consistently shown that increased ICP leads to ONSD distension due to the continuity of the subarachnoid space around the optic nerve (10,11).

A study by Kshirsagar et al. (2024) demonstrated a significant association between lower GCS scores and increased ONSD in traumatic brain injury (TBI) patients (12). Their findings showed that patients with severe TBI (GCS 2–8) had significantly higher mean ONSD values (6.4 ± 1.0 mm) compared to those with moderate TBI (GCS 9–12, 4.7 ± 0.4 mm), reinforcing the role of ONSD as a potential surrogate marker for elevated intracranial pressure (ICP). Similar to their findings, our study also found a significant correlation between GCS and ONSD, with lower GCS scores being associated with increased ONSD values. These results support the growing body of evidence that ONSD measurement via bedside ultrasonography may serve as a valuable, non-invasive tool for assessing ICP, particularly in critically ill and mechanically ventilated patients. However, while their study included only TBI patients, our study expands this association to a broader ICU population, suggesting that ONSD may be a useful indicator of neurological status beyond the trauma setting.

A study by Wang et al. (2019) demonstrated a strong correlation between ONSD and intracranial pressure (ICP) in traumatic brain injury (TBI) patients undergoing decompressive craniotomy (DC). The study found a significant linear relationship between ONSD and ICP values ($r = 0.771$, $p < 0.0001$), with ONSD progressively increasing as ICP rose. The authors identified ONSD cutoff values of 5.48 mm for detecting ICP >13 mmHg and 5.83 mm for ICP >22 mmHg, with high sensitivity and specificity. These findings highlight the utility of ONSD measurement as a noninvasive surrogate for ICP monitoring, offering a reliable alternative to invasive ICP monitoring methods. In line with these findings, our study also observed a significant association between ONSD and markers of neurological status, reinforcing the potential of bedside ultrasonographic ONSD measurement as an adjunctive tool for ICU patients at risk of intracranial hypertension, even in non-TBI populations (13).

A randomized trial by Yanatma et al. (2021) found that PEEP application at 10 cmH_2O did not significantly alter ONSD in laparoscopic cholecystectomy patients (14), contrasting with our findings where PEEP was associated with increased ONSD. This discrepancy may be due to differences in patient populations, surgical settings, and baseline intracranial compliance, as their study included healthy ASA I-II patients, whereas our cohort consisted of critically ill ICU patients who may have been more vulnerable to PEEP-induced changes in intracranial pressure. These findings highlight the need for further research in different clinical contexts to clarify the effects of PEEP on ICP.

A study by Fenerci et al. (2024) found that increasing PEEP levels led to a significant rise in ONSD, suggesting an increase in intracranial pressure (ICP), particularly at 10 cmH_2O PEEP in patients with midline shift, while PEEP up to 5 cmH_2O had no effect (15). Similarly, Balakrishnan et al. (2020) demonstrated that increasing PEEP from 5 to 10 cmH_2O and reducing $ETCO_2$ significantly altered ONSD and regional cerebral oxygen saturation ($rScO_2$) in patients with acute traumatic brain injury (TBI), with the highest ONSD observed at 10 cmH_2O PEEP and $ETCO_2$ at 40 mmHg (16). While both studies highlight the impact of ventilatory settings on ONSD, our findings suggest that even moderate PEEP levels (not exceeding 8 cmH_2O) were associated with increased ONSD in critically ill ICU patients without TBI or midline shift, indicating that ICP changes may not be limited to high PEEP levels or specific neurological conditions. These results emphasize the importance of individualized PEEP management in ICU patients at risk of intracranial hypertension and the need for further research to determine optimal ventilatory strategies across different patient populations.

The generalizability of our findings depends on several factors. First, our study suggests that even moderate levels of PEEP ($\leq$8 cmH_2O) can influence ONSD, indicating potential intracranial pressure (ICP) changes in critically ill patients. This finding may be applicable to ICU patients receiving mechanical ventilation, particularly those with impaired cerebral autoregulation. However, our results should be cautiously interpreted in patients with pre-existing neurological conditions, such as traumatic brain injury or intracranial pathology, as their baseline ICP dynamics may differ. Additionally, our study's methodology, including standardized ultrasound-based ONSD measurements performed by a single investigator, supports reproducibility in similar ICU settings with trained personnel. Given that no significant associations were found between ONSD and other hemodynamic parameters such as MAP, HR, and SpO_2, our findings suggest that PEEP-related ONSD changes may be independent of systemic hemodynamics, making them more likely to be generalizable across mechanically ventilated ICU populations. Nonetheless, external validation in larger, multi-center studies with direct ICP measurements is necessary to confirm the broader applicability of our findings across different patient groups and ventilatory conditions.

Our study has several limitations that should be acknowledged. First, the relatively small sample size may limit the generalizability of our findings, and larger studies are needed to confirm our results in a broader population of critically ill patients. Second, the observational nature of our study prevents us from establishing a causal relationship between PEEP application and changes in ONSD, as unmeasured confounding factors may have influenced our results. Third, ONSD measurements were not validated with direct intracranial pressure (ICP) monitoring, such as invasive intraparenchymal or intraventricular pressure measurements, which are considered the gold standard for ICP assessment. While ultrasonographic ONSD measurement is a well-established, non-invasive surrogate for ICP estimation, the lack of direct ICP validation may limit the accuracy of our findings. Fourth, we did not assess the potential impact of other ventilatory parameters, such as driving pressure or tidal volume, which may also influence cerebral hemodynamics and ONSD. Lastly, our study focused on ICU patients, and the applicability of our results to other clinical settings, such as the operating room or emergency department, remains uncertain. Future research should aim to address these limitations by conducting larger, multicenter, randomized controlled trials incorporating direct ICP monitoring and a comprehensive analysis of ventilatory and hemodynamic factors to further elucidate the relationship between PEEP, ONSD, and ICP dynamics.

Conclusion

In conclusion, our findings suggest that increased ONSD is associated with lower GCS scores in ICU patients, indicating a potential role for ONSD measurement in non-invasive ICP assessment. The influence of PEEP on ONSD warrants cautious interpretation, and clinicians should consider individual patient factors when managing ventilatory settings to mitigate potential impacts on intracranial dynamics.

Ethical approval

This study has been approved by the İstanbul S.B.U. Kanuni Sultan Süleyman Training and Research Hospital Clinical Research Ethics Committee (approval date: 10.12.2020, number: 2020.12.208). Written informed consent was obtained from the participants.

Author contribution

Study conception and design: MİG, EİT, EAİ, Oİ, EK, ASŞ; data collection: MİG, EİT, EAİ, Oİ; analysis and interpretation of results: MİG, EİT, EAİ, Oİ; draft manuscript preparation: MİG, EİT, EAİ, Oİ, EK, ASŞ. The author(s) reviewed the results and approved the final version of the article.

Source of funding

The authors declare the study received no funding.

Conflict of interest

The authors declare that there is no conflict of interest.

References

1. Netteland DF, Aarhus M, Smistad E, et al. Noninvasive intracranial pressure assessment by optic nerve sheath diameter: automated measurements as an alternative to clinician-performed measurements. Front Neurol. 2023;14:1064492. [Crossref]
2. Hirzallah MI, Lochner P, Hafeez MU, et al. Optic nerve sheath diameter point-of-care ultrasonography quality criteria checklist: an international consensus statement on optic nerve sheath diameter imaging and measurement. Crit Care Med. 2024;52:1543-56. [Crossref]
3. Lochner P, Czosnyka M, Naldi A, et al. Optic nerve sheath diameter: present and future perspectives for neurologists and critical care physicians. Neurol Sci. 2019;40:2447-57. [Crossref]
4. Zhang X, Ma D, Li W, et al. Correlation between optic nerve sheath diameter measured by bedside ultrasound and intracranial pressure in neurologically ill patients in a Chinese population. BMC Neurol. 2024;24:452. [Crossref]

5. Sekhon MS, McBeth P, Zou J, et al. Association between optic nerve sheath diameter and mortality in patients with severe traumatic brain injury. Neurocrit Care. 2014;21:245-52. [Crossref]

6. Magoon R, Jose J, Suresh V. Research trends in optic nerve sheath diameter monitoring - a bibliometric study. Indian J Anaesth. 2024;68:579-82. [Crossref]

7. Robba C, Santori G, Czosnyka M, et al. Optic nerve sheath diameter measured sonographically as non-invasive estimator of intracranial pressure: a systematic review and meta-analysis. Intensive Care Med. 2018;44:1284-94. [Crossref]

8. Kerscher SR, Schöni D, Neunhoeffer F, et al. The relation of optic nerve sheath diameter (ONSD) and intracranial pressure (ICP) in pediatric neurosurgery practice - part II: influence of wakefulness, method of ICP measurement, intra-individual ONSD-ICP correlation and changes after therapy. Childs Nerv Syst. 2020;36:107-15. [Crossref]

9. Fernando SM, Tran A, Cheng W, et al. Diagnosis of elevated intracranial pressure in critically ill adults: systematic review and meta-analysis. BMJ. 2019;366:l4225. [Crossref]

10. Sekhon MS, Griesdale DE, Robba C, et al. Optic nerve sheath diameter on computed tomography is correlated with simultaneously measured intracranial pressure in patients with severe traumatic brain injury. Intensive Care Med. 2014;40:1267-74. [Crossref]

11. Martínez-Palacios K, Vásquez-García S, Fariyike OA, Robba C, Rubiano AM; Noninvasive ICP Monitoring International Consensus Group. Using optic nerve sheath diameter for intracranial pressure (ICP) monitoring in traumatic brain injury: a scoping review. Neurocrit Care. 2024;40:1193-212. [Crossref]

12. Kshirsagar SJ, Pande AH, Naik SV, et al. Bedside ultrasonographic evaluation of optic nerve sheath diameter for monitoring of intracranial pressure in traumatic brain injury patients: a cross sectional study in level II trauma care center in India. Acute Crit Care. 2024;39:155-61. [Crossref]

13. Wang J, Li K, Li H, et al. Ultrasonographic optic nerve sheath diameter correlation with ICP and accuracy as a tool for noninvasive surrogate ICP measurement in patients with decompressive craniotomy. J Neurosurg. 2019;133:514-20. [Crossref]

14. Yanatma S, Polat R, Sayın MM, Karabayırlı S. The effects of positive end-expiratory pressure (PEEP) application on optic nerve sheath diameter in patients undergoing laparoscopic cholecystectomy: a randomized trial. Braz J Anesthesiol. 2023;73:769-74. [Crossref]

15. Fenerci A, Akcil EF, Tunali Y, Dilmen OK. Effect of different positive end expiratory pressure levels on optic nerve sheath diameter in patients with or without midline shift who are undergoing supratentorial craniotomy. Acta Neurochir (Wien). 2024;166:177. [Crossref]

16. Balakrishnan S, Naik S, Chakrabarti D, Konar S, Sriganesh K. Effect of respiratory physiological changes on optic nerve sheath diameter and cerebral oxygen saturation in patients with acute traumatic brain injury. J Neurosurg Anesthesiol. 2022;34:e52-6. [Crossref]

Turk J Intensive Care 2026;24(1):30-39
DOI: 10.63729/TJIC.2026.686

ORIGINAL RESEARCH

Retrospective analysis of the efficacy of molnupiravir and favipiravir in COVID-19 patients admitted to intensive care unit

Özlem Öner[1], Vildan Avkan Oğuz[2], Mehmet Çağatay Gürkok[3], Mehmet Nuri Yakar[4], Begüm Ergan[5], Volkan Hancı[6], Erdem Yaka[7], Ali Necati Gökmen[6]

[1]Division of Critical Care Medicine, Department of Anesthesiology and Reanimation, Buca Seyfi Demirsoy Training and Research Hospital, İzmir Demokrasi University, İzmir, Türkiye
[2]Department of Infectious Diseases, Faculty of Medicine, Dokuz Eylül University, İzmir, Türkiye
[3]Division of Critical Care Medicine, Department of General Surgery, Şanlıurfa Training and Research Hospital, Şanlıurfa, Türkiye
[4]Division of Critical Care Medicine, Department of Anesthesiology and Reanimation, Şişli Hamidiye Etfal Training and Research Hospital, İstanbul, Türkiye
[5]Division of Critical Care Medicine, Department of Pulmonary, Faculty of Medicine, Dokuz Eylül University, İzmir, Türkiye
[6]Division of Critical Care Medicine, Department of Anesthesiology and Reanimation, Faculty of Medicine, Dokuz Eylül University, İzmir, Türkiye
[7]Division of Critical Care Medicine, Department of Neurology, Faculty of Medicine, Dokuz Eylül University, İzmir, Türkiye

ABSTRACT

Objective: During the pandemic, molnupiravir and favipiravir treatments have been applied at different stages of the treatment of COVID-19 patients. However, their effectiveness in COVID-19 patients admitted to the ICU is not clear.

Methods: Patients who were admitted to the ICU between March 1, 2022, and December 31, 2023 and managed according to the guidelines of the Scientific Committee of the Turkish Ministry of Health were included.

Results: Data of 152 patients who met the inclusion criteria for the study were evaluated. Patients were divided into two groups according to the treatment modality applied. When both groups were compared in terms of median hospital stay; It was found to be statistically significant (p=0.025) in Group F and 16 (11) days in Group M. When respiratory support was examined in the entire cohort; the percentage of invasive mechanical ventilation application was found to be significant as 40 (60.5) in Group F and 61 (80.3) in Group M (p=0.008). Similarly, the number of days of invasive mechanical ventilation was found to be significant as 9 (14) in Group F and 12 (8) in Group M (p=0.010). On the other hand, when evaluated in terms of hospital mortality percentage; it was found to be 42 (55.3) in Group F and 39 (51.3) in Group M and no statistically significant difference was found (p=0.626).

Conclusion: In our study, no difference was found in terms of mortality rate between molnupiravir and favipiravir, two antiviral drugs used in COVID-19 treatment. However, further studies are needed to clarify this issue.

Keywords: intensive care unit, COVID-19, anti-viral drugs, mortality rate

Introduction

Coronavirus (CoV) is a member of a large family of viruses that can cause a wide range of illnesses, from mild, self-limiting infections like the common cold to more severe conditions such as Middle East Respiratory Syndrome (MERS) and Severe Acute Respiratory Syndrome (SARS) (1). The novel coronavirus 2019 (COVID-19) was declared a "Pandemic" by the World Health Organization (WHO) on March 9, 2020 (2). Unfortunately, since then, the COVID-19 outbreak has continued to cause significant morbidity and mortality both in our country and worldwide. According to WHO data as of January 19, 2025, there have been 777,335,228 confirmed cases globally, with 7,084,023 deaths (3). In our country, according to the Ministry of Health's data as of April 7, 2023, the total number of COVID-19 cases is reported to be 17,232,066, with

✉ Özlem Öner • namdaroner@yahoo.com

Received: 17.02.2025 **Accepted:** 21.11.2025 **Published:** 26.03.2026

102,174 deaths (4). Approximately 20% of patients diagnosed with COVID-19 require hospitalization, and about 10% of these patients need intensive care (5). Intensive care units (ICUs) play a critical role in the treatment of COVID-19 patients, with mortality rates among critically ill COVID-19 patients in ICUs being as high as 43% (5).

To combat this deadly situation, the medical community continues to develop and use effective antiviral agents, as has been done in other viral outbreaks. Among the most well-known antiviral agents are remdesivir, favipiravir, lopinavir, and oseltamivir (6). Favipiravir, an oral antiviral drug, gained popularity during the first wave of COVID-19 (7). However, this drug had to enter clinical use without approval from the U.S. Food and Drug Administration (6). In our country, favipiravir has been included in the Ministry of Health's COVID-19 treatment guidelines (8). Favipiravir is an RNA polymerase inhibitor with activity against a range of RNA viruses (9). It was initially licensed for the treatment of influenza viruses. Later, its inhibitory effects against COVID-19 were first identified in in vitro studies (10).

Subsequently, molnupiravir was added to these antiviral agents (11). Due to its significant inhibitory effects against Venezuelan, Eastern, and Western equine encephalitis viruses in cell cultures, it has been used for the treatment of influenza viruses and encephalitic alphaviruses. Initially developed for the treatment of influenza viral infections, this drug was later found to exhibit strong antiviral activity against SARS-CoV-2, leading to further research in this area (12). A reduction in viral RNA load has been demonstrated in in vivo studies, and the drug has been included in WHO treatment guidelines for COVID-19 (6). In our country, the Ministry of Health updated the COVID-19 adult patient guidelines on February 12, 2022, adding molnupiravir to the treatment protocols for patients over 65 years of age, those in risk groups, and hospitalized patients (8).

Both molnupiravir and favipiravir may reduce disease transmission and progression to severe illness (9). However, the safety and efficacy of these drugs in critically ill COVID-19 patients monitored in the ICU remain unclear (13). The aim of this study is to investigate the impact of molnupiravir and favipiravir use on treatment processes, clinical characteristics, and mortality rates in critically ill COVID-19 patients monitored in the ICU.

Materials and Methods

Study design and participants

This study was conducted as a retrospective analysis after obtaining approval from the University Ethics Committee (Approval ID: 2022/38-11). It involved a cohort of patients monitored in a tertiary intensive care unit (ICU) designated for COVID-19 patients between March 1, 2022, and December 31, 2023. Electronic medical records and laboratory data were obtained from the hospital database. Due to the retrospective nature of the study, written informed consent was waived.

Inclusion criteria

Patients admitted to the ICU who tested positive for COVID-19 via polymerase chain reaction (PCR), were over 18 years of age, and received either favipiravir or molnupiravir treatment were included in the study.

Exclusion criteria

Patients with negative PCR test results, those under 18 years of age, pregnant or lactating women, patients with incomplete health records, and those who did not receive favipiravir or molnupiravir treatment were excluded from the study.

Treatment protocol

In the tertiary ICU where the study was conducted, the treatment of COVID-19 patients followed the antiviral drug protocols outlined in the treatment guidelines of the Ministry of Health. According to these guidelines, favipiravir was the primary antiviral treatment used for COVID-19 in our country. Subsequently, the Ministry of Health updated the COVID-19 adult patient guidelines on February 12, 2022, adding molnupiravir to the

treatment protocol for patients over 65 years of age, those in risk groups, hospitalized patients, and those monitored in the ICU (8).

In the ICU, treatment dosages were administered according to the doses specified in the Ministry of Health guidelines. Favipiravir treatment was administered at 1600 mg twice daily on the first day, followed by 600 mg twice daily for the next 4 days. In rare cases, the treatment duration was extended to 10 days. Similarly, after the addition of molnupiravir to the guidelines, the drug was administered at 800 mg twice daily for a total of 5 days. Patients who completed both treatment protocols at the specified doses and durations were included in our study. Below is a chronological summary of the Ministry of Health COVID-19 treatment guidelines and the sequence of drug administration (14) (Figure 1).

Patient characteristics

We evaluated 205 patients (the total number of patients before matching) with critical illness due to COVID-19 and who were monitored in the intensive care unit during the specified period. Of these patients, 177 patients (the number of patients in both groups before matching) received either Favipiravir or Molnupiravir treatment. When these patients were examined, it was determined that 96 patients in the Favipiravir group and 81 patients (the number of patients in both groups before matching) met the study inclusion criteria. Patients receiving molnupiravir and favipiravir were matched according to baseline characteristics such as age, gender, body mass index, smoking status, hospitalization duration, laboratory values, respiratory support therapies (such as non-invasive or invasive mechanical ventilation), comorbidities, and intensive care unit scores. Patients with dissimilar characteristics were excluded from the analysis. Unmatched patients were not analyzed separately. Propensity Score Matching (PSM) was used to create balanced groups, and this matching was performed using a 1:1 nearest neighbor matching algorithm. Of these patients, 76 (50%) received favipiravir, and 76 (50%) received molnupiravir. Patients were divided into two groups according to the treatment modality: Favipiravir Group (Group-F) and Molnupiravir Group (Group-M).

Data collection

The following data were scanned from the electronic hospital database for each patient: age, gender, body mass index, Charlson comorbidity index (CCI), Acute Physiology and Chronic Health Evaluation (APACHE)

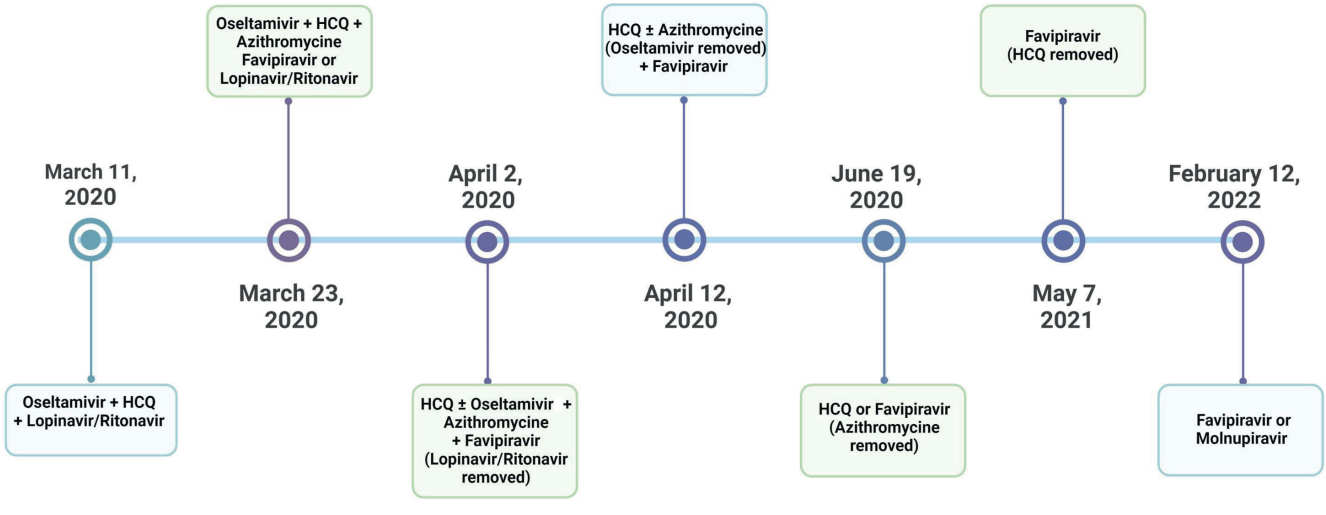

Figure 1. The timeline for the treatment protocols applied by the guidelines by the Scientific Board of the Ministry of Health (SBMH) of Türkiye (14).

II, and SOFA scores at ICU admission. CT-SS, arterial blood gas analysis (arterial partial pressure of oxygen (PaO_2); arterial partial pressure of carbon dioxide ($PaCO_2$); FiO_2; PaO_2/FiO_2 ratio; bicarbonate; SpO_2 (peripheral oxygen saturation)), laboratory data including hemogram parameters, C-reactive protein (CRP), procalcitonin, lactate dehydrogenase (LDH), alanine aminotransferase (ALT), aspartate aminotransferase (AST), D-dimer, serum creatinine (sCr), total bilirubin, ferritin, high-sensitive (HS) troponin I, length of hospital stay, length of intensive care unit stay, and intensive care unit and hospital mortality (Table 1).

Statistical analysis

All analyses were performed using the Statistical Package for Social Sciences (SPSS) version 24.0. Propensity score matching (PSM) was employed to create balanced groups by matching patients receiving molnupiravir and favipiravir based on baseline characteristics, including age, gender, and comorbidities, using a nearest-neighbor matching algorithm with a 1:1 ratio. The Kolmogorov-Smirnov and Shapiro-Wilk tests were used to assess normality. Parametric continuous variables were compared using Student's t-test, while non-parametric continuous variables were compared using the Mann-Whitney U test. Results are presented as mean ± standard deviation (SD) and median (interquartile range). Categorical variables were compared using the Chi-square test or Fisher's exact test, with results presented as frequencies (%). Variables were first evaluated using univariate analysis, followed by multivariate Cox regression analysis to predict in-hospital mortality. The Kaplan-Meier test was used to evaluate factors related to survival. Statistical significance was defined as $p < 0.05$.

Results

Patients characteristics

We evaluated 177 patients with critical illness due to COVID-19 being followed up in the intensive care unit. Data of 152 patients who met the inclusion criteria for the study were evaluated. Of these patients, 76 (50%) were found to have received favipiravir and 76 (50%) were found to have received molnupiravir treatment. Patients were divided into two groups according to the treatment modality applied: Group Favipiravir (Group-F) and Group Molnupiravir (Group-M). No statistically significant difference was found between the two groups in terms of demographic data, laboratory results and clinical results of the patients (Table 1).

Mean age was 69.9±12.6 in Group F and 66.1±11.4 in Group M, and no statistically significant difference was found between the two groups (p=0.051). The number of female patients in Group-F was 40 (52.3%) and the number of female patients in Group-M was 38 (50%), and no statistical difference was found between them (p=0.067). When the two groups were compared in terms of the time from diagnosis to hospitalization, the median was 4 (5) days in Group F and 3 (4) days in Group M, with no statistically significant difference between the two groups (p=0.743). When both groups were compared in terms of pre-ICU stay (pre-ICU days), the median was 6 (7) days in Group F and 5 (6) in Group M, and no statistically significant difference was found between the two groups (p=0.897). The most common comorbidities were hypertension (65.1%), diabetes mellitus (35.5%) and coronary artery disease (29.6%), respectively. The APACHE II score was 20 (15.5) in the entire cohort, 22 (15) in Group F and 19 (13) in Group M (p=0.093). Median hemoglobin values were 12.9 (12) g/dl in Group F and 12.8 (12.7) g/dl in Group M, with a p-value of 0.935 (Table 1).

Treatments and outcomes

When both groups were compared in terms of median hospital stay, it was found to be statistically significant (p=0.025) in Group F and 16(11) days in Group M. When respiratory support was examined in the entire cohort, the percentage of invasive mechanical ventilation application was found to be significant as 40 (60.5) in Group F and 61 (80.3) in Group M (p=0.008). Similarly, the number of days of invasive mechanical ventilation was found to be significant as

Table 1. Characteristics of patients who received molnupiravir versus favipiravir

	Total (n: 152)	Favipiravir (n: 76)	Molnupiravir (n: 76)	p-value
Age *mean±sd*	68.1±12.1	69.9±12.6	66.1±11.4	0.051
Gender (*female*) n (%)	76 (50)	40 (52.3)	38 (50)	0.067
BMI *median (IQR)*	26.2 (5.7)	26.0 (7.9)	26.3 (5.2)	0.935
Ex-Smoker* *n (%)*	29 (19.1)	10 (13.2)	19 (25.0)	0.063
Smoker 2* *n (%)*	15 (9.9)	8 (10.5)	7 (9.2)	0.786
Hospitalization duration *days median (IQR)*	14 (11)	13 (10)	16 (11)	**0.025**
Comorbidities, *n (%)*				
HT	99 (65.1)	51 (67.1)	48 (63.2)	0.610
DM	54 (35.5)	28 (36.8)	26 (34.2)	0.735
CAD	45 (29.6)	27 (35.5)	18 (23.7)	0.110
COPD	24 (15.8)	10 (13.2)	14 (18.4)	0.374
CKD (*)	18 (11.8)	11 (14.5)	7 (9.2)	0.315
RRT (*)	24 (15.8)	14 (18.4)	10 (13.2)	0.374
AFIB	9 (5.9)	4 (5.3)	5 (6.6)	N/A
Liver Cirrhosis	2 (1.3)	1 (1.3)	1 (1.3)	N/A
Dyslipidemia	45 (29.6)	19 (25.0)	26 (34.2)	0.214
DVT	1 (0.7)	(1.3)	0 (0)	N/A
PTE	3 (2.0)	2 (2.6)	1 (1.3)	N/A
CVD (*)	8 (5.3)	4 (5.3)	4 (5.3)	N/A
Neurodegenerative Disorder	13 (8.6)	6 (7.9)	7 (9.2)	0.772
Parkinson Disease	8 (5.3)	7 (9.2)	1 (1.3)	0.063*
Malignancy (*)	13 (8.6)	7 (9.2)	6 (7.9)	0.772
Scores *median (IQR)*				
APACHE II	20 (15.5)	22 (15)	19 (13)	0.093
SOFA	5 (4)	5 (4)	5 (4)	0.505
CCI	4 (4)	5 (4)	4 (4)	0.366
Laboratory findings *median (IQR)*				
Creatinine *(mg/dl)*	1.00 (0.71)	1.12 (0.78)	0.99 (0.69)	0.371
BUN *(mg/dl)*	30 (27)	32 (27)	28 (24)	0.071
AST *U/L*	52 (53)	55 (52)	51 (48)	0.170
ALT *U/L*	37 (39)	35 (44)	38 (37)	0.645
LDH *U/L*	575 (305)	565 (244)	576 (333)	0.922
CRP *mg/L*	150 (149)	140 (164)	162 (141)	0.264
Ferritine *µg/L*	614 (775)	579 (788)	635 (767)	0.863
D-Dimer *µ/mL*	1.50 (3.35)	1.45 (4.83)	1.50 (2.75)	0.630
BLB*	0.9 (0.5)	0.9 (0.5)	0.9 (0.5)	0.463
WBC *10*3/uL*	11.1 (7.0)	11.5 (6.4)	10.3 (8.3)	0.580

BMI: Body Mass index, ABG: Arterial blood gas, ACI: Acute cardiac injury, ARDS: Acute respiratory distress syndrome, AFIB: Atrial fibrillation, AKI: Acute kidney injury, ALT: Alanine transferase, AST: Aspartate transferase, BUN: Blood urea nitrogen, CAD: Coronary artery disease, CCI: Charlson comorbidity index, CKD: Chronic kidney disease, CRP: C-reactive protein, COPD: Chronic obstructive pulmonary disease, CVD: Cerebrovascular disease; DM: Diabetes mellitus, DVT: Deep vein thrombosis, ECMO: Extracorporeal membrane oxygenation, HT: hypertension, IQR: Interquartile range, LDH: Lactate dehydrogenase, MV: Mechanical ventilation, N/A: Not applicable, PTE: Pulmonary thromboembolism, SOFA: Sequential organ failure assessment, RRT: Renal replacement therapy, VAP: Ventilator-associated pneumonia, WBC: White blood cell.

*Fisher-exact test was used.

Table 1. Continued

	Total (n: 152)	Favipiravir (n: 76)	Molnupiravir (n: 76)	p-value
Lymphocyte *10*3/uL*	0.5 (0.6)	0.5 (0.6)	0.5 (0.6)	0.833
Hemoglobin *g/dl*	12.9 (2.3)	12.9 (2.0)	12.8 (2.7)	0.935
Platelet *10*3/uL*	255 (190)	296 (196)	242 (166)	0.098
Platokrit %	0.32 (0.97)	0.31 (0.89)	0.33 (1.37)	0.346
ABG analysis *median (IQR)*				
pH	7.42 (0.14)	7.43 (0.17)	7.42 (0.13)	0.744
Lactate *mmol/L*	1.9 (1.6)	1.8 (1.4)	2.7±1.7	0.370
pCO_2 *mmHg*	34 (10)	34 (9)	34 (12)	0.335
pO_2 *mmHg*	64 (25)	65 (25)	64 (23)	0.421
Bicarbonate *mmol/L*	22.9 (5.0)	22.0 (5.0)	23.3 (5.0)	0.348
FiO_2 *median (IQR)*	0.6 (0.1)	0.6 (0.1)	0.6 (0.1)	0.685
ICUP/F* *median (IQR)*	112 (52)	111 (47)	115 (54)	0.892
ICUvasopressor* *median (IQR)*	9900 (7000)	10350 (6325)	9250 (8325)	0.636
Airway access, *n (%)*				
Tracheostomy	3 (2)	0 (0)	3 (3.9)	0.254*
Respiratory Support, *n (%)*				
High-Flow Nasal Cannula	124 (81.6)	65 (85.5)	59 (77.6)	0.209
Noninvasive MV	121 (79.6)	61 (80.3)	60 (78.9)	0.840
Invasive MV	107 (70.4)	46 (60.5)	61 (80.3)	**0.008**
Respiratory Support duration by modalities *(day) median (IQR)*				
High-Flow Nasal Cannula	4 (5)	4 (4)	4 (5)	0.562
Noninvasive MV	3 (5)	3 (3)	3 (5)	0.939
Invasive MV	11 (15)	9 (14)	12 (8)	**0.010**
ECMO Treatment, *n (%)*	1 (0.7)	1 (1.3)	0 (0)	N/A
Positive Inotropic Therapy, *n (%)*	99 (65.1)	49 (64.5)	50 (65.8)	0.865
The time diagnosis in hospital (*days median) (IQR)*	4 (5)	3 (4)	4 (4)	0.743
Pre-ICU Stay Duration (*days median) (IQR)*	6 (7)	5 (6)	5 (6)	0.897
Complication, *n (%)*				
VAP	76 (50)	36 (47.4)	40 (52.6)	0.516
ARDS	75 (49.3)	38 (50.0)	37 (48.7)	0.871
AKI	82 (53.9)	47 (61.8)	35 (46.1)	0.051
ACI	44 (28.9)	23 (30.3)	21 (27.6)	0.721
Septic Shock	97 (63.8)	49 (64.5)	48 (63.2)	0.866
Mortality, *n (%)*	81 (53.3)	42 (55.3)	39 (51.3)	0.626

BMI: Body Mass index, ABG: Arterial blood gas, ACI: Acute cardiac injury, ARDS: Acute respiratory distress syndrome, AFIB: Atrial fibrillation, AKI: Acute kidney injury, ALT: Alanine transferase, AST: Aspartate transferase, BUN: Blood urea nitrogen, CAD: Coronary artery disease, CCI: Charlson comorbidity index, CKD: Chronic kidney disease, CRP: C-reactive protein, COPD: Chronic obstructive pulmonary disease, CVD: Cerebrovascular disease; DM: Diabetes mellitus, DVT: Deep vein thrombosis, ECMO: Extracorporeal membrane oxygenation, HT: hypertension, IQR: Interquartile range, LDH: Lactate dehydrogenase, MV: Mechanical ventilation, N/A: Not applicable, PTE: Pulmonary thromboembolism, SOFA: Sequential organ failure assessment, RRT: Renal replacement therapy, VAP: Ventilator-associated pneumonia, WBC: White blood cell.

*Fisher-exact test was used.

9 (14) in Group F and 12 (8) in Group M (p=0.010). On the other hand, when evaluated in terms of hospital mortality percentage, it was found to be 42 (55.3) in Group F and 39 (51.3) in Group M, and no statistically significant difference was found (p=0.626) (Table 1).

Risk factors for hospital mortality

When Cox regression univariate analysis was performed on risk factors affecting hospital mortality, for age: HR: 1.032, 95%CI: 1.011-1.054 and p=0.003; for Charlson comorbidity index: HR: 1.149, 95%CI: 1.060-1.247 and p=0.001; for APACHE II: HR: 1.096, 95%CI: 1.065-1.127 and p<0.001; for SOFA score: HR: 1.131, 95%CI: 1.061-1.1205 and p<0.001. When multivariate analysis was performed for favipiravir, one of the antiviral agents: HR: 1.161, 95%CI: 1.018-2.517 and p=0.041; for hemoglobin: HR: 0.882, 95%CI: 0.788-0.987 and p=0.029; for D-Dimer: HR: 1.028, 95%CI: 1.008-1.048 and p=0.005; for acute kidney injury: HR: 2.420, 95%CI: 1.458-4.015 and p=0.001; for septic shock: HR: 3.410, 95%CI: 1.700-6.842 and p=0.001 (Table 2).

Discussion

In this study, we investigated clinical outcomes, including mechanical ventilation duration, ICU length of stay, and mortality rates, in COVID-19 patients admitted to the ICU and treated with either favipiravir or molnupiravir. We found that patients treated with molnupiravir had significantly longer ICU stays, higher rates of invasive mechanical ventilation, and longer durations of mechanical ventilation compared to those treated with favipiravir. However, there were no statistically significant differences in ICU mortality or other clinical outcomes between the two treatment groups.

The need for safe and effective treatment options for COVID-19 patients has kept antiviral drugs at the forefront of clinical research. Antiviral agents can be used to minimize transmission and suppress the development of more virulent strains by reducing viral load (15). Molnupiravir, which acts by inhibiting RNA replicase, has been approved by infectious disease committees in many countries, including

Table 2. Evaluation of factors related to in hospital mortality by Cox Regression analysis

	Univariate analysis			Multivariate analysis		
	HR	95% CI	P-value	HR	95% CI	P-value
Age	1.032	1.011-1.054	**0.003**	1.006	0.977-1.035	0.697
Female sex	0.966	0.621-1.503	0.879	1.032	0.660-1.613	0.891
Smoking	1.214	0.605-2.437	0.585			
CCI	1.149	1.060-1.247	**0.001**	1.098	0.988-1.222	0.083
APACHE II	1.096	1.065-1.127	**<0.001**			
SOFA	1.131	1.061-1.205	**<0.001**			
Antiviral medicine (*Favipiravir*)	1.559	0.998-2.436	0.051	1.601	1.018-2.517	**0.041**
pH	0.246	0.053-1.140	0.073			
Lactate	1.097	0.991-1.215	0.074			
Hemoglobin	0.882	0.788-0.987	**0.029**			
D-Dimer	1.028	1.008-1.048	**0.005**			
AKI	2.420	1.458-4.015	**0.001**	1.575	0.871-2.850	0.133
VAP	1.233	0.768-1.977	0.386			
ARDS	1.061	0.677-1.664	0.797			
ACI	1.119	0.705-1.777	0.633			
Septic shock	3.410	1.700-6.842	**0.001**	1.996	0.861-4.625	0.107

CCI: Charlson comorbidity index, AKI: Acute kidney injury; HR: Hazard ratio; CI: Confidence interval, ACI: Acute cardiac injury, ARDS: Acute respiratory distress syndrome, AKI: Acute kidney injury, VAP: Ventilator-associated pneumonia, SOFA: Sequential organ failure assessment.

ours, for use in adults at high risk of progressing to severe COVID-19, which is associated with significant morbidity and mortality (16). Favipiravir, a purine nucleic acid analog that inhibits RNA-dependent RNA polymerase, was initially used as an anti-influenza drug in Japan and was later approved in China for the treatment of COVID-19 patients in March 2020 after Wang et al. demonstrated its in vitro efficacy against SARS-CoV-2 (17,18).

The efficacy of both drugs in COVID-19 patients remains unclear (19). In a study by Babayiğit et al. (14), no improvement in clinical parameters was observed in patients treated with favipiravir. These findings are consistent with other research indicating that the clinical recovery of patients receiving favipiravir was not superior to those receiving lopinavir/ritonavir in terms of hospital length of stay, ICU admission, or intubation rates (20). A meta-analysis on this topic also found no significant difference in mortality rates or the need for mechanical ventilation between favipiravir treatment and standard care (21). However, Guner et al. (22) reported that the addition of favipiravir to the treatment regimen reduced ICU admission and intubation rates in COVID-19 patients.

Similarly, there are various studies in the literature on patients treated with molnupiravir. In the MOVe-OUT study, molnupiravir treatment was associated with an 8% lower hospitalization rate in COVID-19 patients at high risk of progressing to severe disease (23). Another study also found that molnupiravir demonstrated favorable outcomes by reducing hospitalizations (24). A meta-analysis by Kamal et al. (25) confirmed the efficacy and safety of molnupiravir as an antiviral treatment for mild to moderate COVID-19 infections in high-risk patients.

Based on the available evidence from these clinical studies, it can be concluded that Molnupiravir is safe and effective in high-risk patients with mild to moderate COVID-19 infection when administered within the first five days of symptom onset. It is considered to delay disease progression by reducing hospitalization and/or mortality. Conversely, in the PANORAMIC study conducted in the United Kingdom (Adaptive Trial of Novel Antivirals for Early Treatment of COVID-19 in the Community), the lack of clinical benefits of Molnupiravir compared to standard care in non-hospitalized patients raised concerns. Furthermore, although the MOVe-OUT study demonstrated that Molnupiravir reduced hospitalization and mortality rates in non-hospitalized patients, the MOVe-IN study failed to show a survival advantage in the inpatient setting. However, another study found a lower risk of death among hospitalized patients treated with Molnupiravir, attributing the difference in findings between the MOVe-IN study and the present study to the inclusion of patients who initiated treatment more than five days after symptom onset.

In our study, we observed that in patients treated with Molnupiravir, the intensive care unit (ICU) length of stay, the percentage of patients requiring invasive mechanical ventilation, and the duration of ventilation were significantly higher compared to those treated with Favipiravir. However, no significant difference was detected between the two drug groups regarding ICU mortality rates. This finding may be explained by the initiation of both drugs only after hospitalization and/or ICU admission. Unfortunately, COVID-19 is a disease with a high potential for both vertical and horizontal transmission. Asymptomatic individuals play a crucial role in ongoing transmission, accounting for 25% to 50% of all new infections, which supports the recommendation for universal masking. Viral shedding begins one to two days before symptom onset, with viral titers in respiratory secretions reaching peak levels in the early stages of infection and decreasing over time. Consequently, in our study, the inability to administer the drugs during the early pre-symptomatic phase may have resulted in the loss of this critical therapeutic window. In alignment with our findings, a randomized controlled trial comparing these two drugs in COVID-19 patients also failed to demonstrate an improvement in clinical outcomes.

Limitations

Our study has inherent limitations due to its retrospective nature. Additionally, there are other constraints. Firstly, this is a single-center study with a relatively small patient population. Secondly, the exact timing of symptom onset was not clearly documented for each patient. Thus, the treatment doses and durations analyzed in this study reflect those administered at the hospital or ICU level. As a result, evaluating the clinical recovery process in cases where Favipiravir or Molnupiravir was administered during the early symptomatic phase remains insufficient. On the other hand, we think that our study is important in that it reflects the treatment processes of COVID-19 patients treated with antiviral drugs in the COVID intensive care unit of a university hospital during the pandemic.

Conclusion

In our study, no difference in mortality rates was found between the two antiviral drugs, Molnupiravir and Favipiravir, used for COVID-19 treatment. However, compared to Favipiravir-treated patients, those treated with Molnupiravir had significantly longer ICU stays, higher rates of invasive mechanical ventilation, and prolonged ventilation duration. We hypothesize that this finding may be related to the delayed administration of these drugs rather than their early use in the disease course. Nevertheless, further studies are needed to validate this observation.

Ethical approval

This study has been approved by the Dokuz Eylül University Non-Interventional Research Ethics Committee (approval date: 30.11.2022, number: 2022/38-11). Written informed consent was obtained from the participants.

Author contribution

Study conception and design: ÖÖ; data collection: MÇG, NY; analysis and interpretation of results: BE; draft manuscript preparation: VH, ANG, EY. The author(s) reviewed the results and approved the final version of the article.

Source of funding

The authors declare the study received no funding.

Conflict of interest

The authors declare that there is no conflict of interest.

References

1. V'kovski P, Kratzel A, Steiner S, Stalder H, Thiel V. Coronavirus biology and replication: implications for SARS-CoV-2. Nat Rev Microbiol. 2021;19:155-70. [Crossref]
2. Attwood SW, Hill SC, Aanensen DM, Connor TR, Pybus OG. Phylogenetic and phylodynamic approaches to understanding and combating the early SARS-CoV-2 pandemic. Nat Rev Genet. 2022;23:547-62. [Crossref]
3. World Health Organization (WHO). Coronavirus disease (COVID-19) pandemic. WHO; 2019. Available at: https://www.who.int/emergencies/diseases/novel-coronavirus-2019
4. T.C. Sağlık Bakanlığı. Genel koronavirüs tablosu. Ankara: T.C. Sağlık Bakanlığı; 2022. Available at: https://covid19.saglik.gov.tr/TR-66935/genel-koronavirus-tablosu.html
5. Öner Ö, Ergan B, Gürkök MÇ, et al. Is there a relationship between mortality rates and nutritional factors in critical ill patients with COVID-19? Turk J Intensive Care. 2023;21:74-82. [Crossref]
6. Mali KR, Eerike M, Raj GM, et al. Efficacy and safety of molnupiravir in COVID-19 patients: a systematic review. Ir J Med Sci. 2023;192:1665-78. [Crossref]
7. Singh AK, Singh A, Singh R, Misra A. Molnupiravir in COVID-19: a systematic review of literature. Diabetes Metab Syndr. 2021;15:102329. [Crossref]
8. T.C. Sağlık Bakanlığı. Ağır pnömoni, ARDS, sepsis ve septik şok yönetimi. Ankara: T.C. Sağlık Bakanlığı; 2025. Available at: https://covid19.saglik.gov.tr/TR-66340/agir-pnomoni-ards-sepsis-ve-septik-sok-yonetimi.html
9. Yasri S, Wiwanitki V. Molnupiravir, favipiravir and other antiviral drugs with proposed potentials for management of COVID-19: a concern on antioxidant aspect. Int J Biochem Mol Biol. 2022;13:1-4.
10. Ghasemnejad-Berenji M, Pashapour S. Favipiravir and COVID-19: a simplified summary. Drug Res (Stuttg). 2021;71:166-70. [Crossref]

11. Tian L, Pang Z, Li M, et al. Molnupiravir and its antiviral activity against COVID-19. Front Immunol. 2022;13:855496. [Crossref]

12. Agostini ML, Pruijssers AJ, Chappell JD, et al. Small-molecule antiviral β-d-N4-Hydroxycytidine inhibits a proofreading-intact coronavirus with a high genetic barrier to resistance. J Virol. 2019;93:e01348-19. [Crossref]

13. Jean SS, Lee PI, Hsueh PR. Treatment options for COVID-19: the reality and challenges. J Microbiol Immunol Infect. 2020;53:436-43. [Crossref]

14. Babayigit C, Kokturk N, Kul S, et al. The association of antiviral drugs with COVID-19 morbidity: the retrospective analysis of a nationwide COVID-19 cohort. Front Med (Lausanne). 2022;9:894126. [Crossref]

15. Panda PK, Bandyopadhyay A, Singh BC, et al. Safety and efficacy of antiviral combination therapy in symptomatic patients of Covid-19 infection - a randomised controlled trial (SEV-COVID Trial): a structured summary of a study protocol for a randomized controlled trial. Trials. 2020;21:866. [Crossref]

16. Wen W, Chen C, Tang J, et al. Efficacy and safety of three new oral antiviral treatment (molnupiravir, fluvoxamine and Paxlovid) for COVID-19: a meta-analysis. Ann Med. 2022;54:516-23. [Crossref]

17. Korula P, Alexander H, John JS, et al. Favipiravir for treating COVID-19. Cochrane Database Syst Rev. 2024;2:CD015219. [Crossref]

18. WHO Solidarity Trial Consortium , Pan H, Peto R, et al. Repurposed antiviral drugs for Covid-19 - interim WHO solidarity trial results. N Engl J Med. 2021;384:497-511. [Crossref]

19. Eloy P, Le Grand R, Malvy D, Guedj J. Combined treatment of molnupiravir and favipiravir against SARS-CoV-2 infection: one + zero equals two? EBioMedicine. 2021;74:103663. [Crossref]

20. Amani B, Khanijahani A, Amani B, Hashemi P. Lopinavir/ritonavir for COVID-19: a systematic review and meta-analysis. J Pharm Pharm Sci. 2021;24:246-57. [Crossref]

21. Özlüşen B, Kozan Ş, Akcan RE, et al. Effectiveness of favipiravir in COVID-19: a live systematic review. Eur J Clin Microbiol Infect Dis. 2021;40:2575-83. [Crossref]

22. Guner AE, Surmeli A, Kural K, et al. ICU admission rates in Istanbul following the addition of favipiravir to the national COVID-19 treatment protocol. North Clin Istanb. 2021;8:119-23. [Crossref]

23. Guan Y, Puenpatom A, Johnson MG, et al. Impact of molnupiravir treatment on patient-reported COVID-19 symptoms in the phase 3 MOVe-OUT trial: a randomized, placebo-controlled trial. Clin Infect Dis. 2023;77:1521-30. [Crossref]

24. Karniadakis I, Mazonakis N, Tsioutis C, Papadakis M, Markaki I, Spernovasilis N. Oral molnupiravir and nirmatrelvir/ritonavir for the treatment of COVID-19: a literature review with a focus on real-world evidence. Infect Dis Rep. 2023;15:662-78. [Crossref]

25. Kamal L, Ramadan A, Farraj S, Bahig L, Ezzat S. The pill of recovery; molnupiravir for treatment of COVID-19 patients; a systematic review. Saudi Pharm J. 2022;30:508-18. [Crossref]

Turk J Intensive Care 2026;24(1):40-48
DOI: 10.63729/TJIC.2026.687

ORIGINAL RESEARCH

The prognostic value of the early brain edema score (SEBES) in traumatic and non-traumatic subarachnoid hemorrhage

Ali Çayır[1], Yıldız Arslan[2], Sevinj Namazova[2], İzzet Durmuşalioğlu[3], Aysen Evkan Öztürk[1], Nimet Şenoğlu[1]

[1]Intensive Care Unit, İzmir Bakırçay University Çiğli Training and Research Hospital, İzmir, Türkiye
[2]Department of Neurology, İzmir Bakırçay University Çiğli Training and Research Hospital, İzmir, Türkiye
[3]Department of Neurosurgery, İzmir Bakırçay University Çiğli Training and Research Hospital, İzmir, Türkiye

ABSTRACT

Background: Subarachnoid hemorrhage (SAH) is a life-threatening cerebrovascular event with high morbidity and mortality. Early brain edema is a key determinant of prognosis and can be quantified using the Subarachnoid Hemorrhage Early Brain Edema Score (SEBES). Although SEBES has demonstrated prognostic value in spontaneous SAH, its utility in traumatic SAH remains underexplored. This study aimed to evaluate the relationship between SEBES and clinical outcomes in both traumatic and non-traumatic SAH patients.

Methods: In this retrospective cohort study, 50 SAH patients (30 traumatic, 20 non-traumatic) admitted to the intensive care unit (ICU) between January 2023 and May 2024 were analyzed. SEBES scores were calculated from brain CT scans obtained within 24 hours of SAH onset. Patients were classified by etiology and SEBES grade (≤2 vs. >2). Demographic data, clinical scores, laboratory parameters, and mortality at 1 and 3 months were compared. A subgroup analysis was performed to assess SEBES-associated outcomes within each SAH etiology.

Results: SEBES scores were markedly higher in non-traumatic SAH patients. Higher SEBES (>2) was associated with lower admission and discharge neurological scores (GCS, FOUR), longer ICU and ventilator duration, and higher 1- and 3-month mortality (all $p < 0.05$). Subgroup analysis revealed that the negative prognostic impact of elevated SEBES was evident in both traumatic and non-traumatic SAH groups, particularly regarding mortality and ICU burden.

Conclusion: SEBES is a valuable and simple radiological prognostic tool applicable to both traumatic and non-traumatic SAH. A SEBES score >2 may predict worse neurological outcomes, higher mortality, and increased ICU resource utilization. Its early application may aid in risk stratification and critical care planning.

Keywords: subarachnoid hemorrhage, early brain edema score, prognosis, SEBES, traumatic SAH, non-traumatic SAH, neurocritical care

Introduction

Subarachnoid hemorrhage (SAH) is a severe cerebrovascular condition that accounts for approximately 5% of all strokes and is associated with high rates of mortality and morbidity. The majority of SAH cases result from trauma, while in 80–85% of non-traumatic cases, aneurysmal rupture is identified as the underlying cause (1). SAH patients frequently require intensive care and constitute a significant proportion of the patient population in intensive care units (ICUs). Common complications occurring within the first 72 hours after SAH include early brain injury, early brain edema, and symptomatic vasospasm (2). Intracranial edema increases intracranial pressure, further impairing cerebral perfusion and increasing the risk of neuronal ischemia, ultimately leading to poor neurological outcomes.

Early brain edema refers to the immediate pathophysiological processes that occur following aneurysmal rupture. The extravasation of blood into the subarachnoid space leads to increased intracranial pressure, followed by a reduction in

✉ Yıldız Arslan • dryildizarslan@yahoo.com

Received: 11.07.2025 **Accepted:** 17.12.2025 **Published:** 26.03.2026

cerebral perfusion pressure, disruption of cerebral autoregulation, and transient or permanent ischemia (3,4,5). The persistence of brain edema after aneurysmal SAH, also referred to as persistent edema (PE), is considered an indicator of early brain injury (EBI) (6).

The Subarachnoid Hemorrhage Early Brain Edema Score (SEBES) is a radiographic assessment tool used to evaluate early brain edema in patients with spontaneous SAH (3,7). Studies have demonstrated that patients with high SEBES scores have an increased likelihood of delayed cerebral ischemia and poor clinical outcomes. Furthermore, SEBES has been shown to be a stronger prognostic indicator compared to other scoring systems (3,5). The SEBES system has been proposed as a reliable prognostic factor for both clinical outcomes and mortality in spontaneous SAH patients (1,3,7). Early application of SEBES may be beneficial in identifying high-risk patients and optimizing treatment strategies accordingly (7).

This study aimed to evaluate all SAH patients (both traumatic and non-traumatic) admitted to the ICU using the SEBES scoring system to predict those at risk of poor neurological outcomes. Additionally, we aim to investigate the prognostic relationship between SEBES and traumatic SAH in comparison with other commonly used scoring methods.

Materials and Methods

Ethical approval

This study was conducted in accordance with the ethical principles of the Declaration of Helsinki and was approved by the Institutional Review Board of the Local University (Decision No: 1670 / 03.07.2024). Due to its retrospective design and the use of anonymized clinical data, the requirement for written informed consent was waived by the ethics committee.

Study population

This study included all patients over the age of 18 who were diagnosed with subarachnoid hemorrhage (SAH), regardless of etiology, and were monitored and treated in the general intensive care unit (ICU) of our hospital between January 2023 and May 2024. The study was designed as a retrospective observational cohort study.

Inclusion criteria: Patients who underwent brain computed tomography (CT) within the first 24 hours after SAH onset, had a brain CT angiography performed for the detection of aneurysms or other vascular anomalies, and were assessed using all scoring systems specified in our study were included. Additionally, patients with follow-up data available for the first and third months were included in the study.

Exclusion criteria: Patients with multiorgan failure, multiple trauma, pregnancy, sepsis, or severe infections, as well as those with concurrent subdural and/or epidural hematomas or ischemic stroke at the time of SAH diagnosis, and patients with perimesencephalic subarachnoid hemorrhage were also excluded.

A total of 50 patients who met the specified criteria were included in the study. Among them, 20 had non-traumatic SAH (aneurysm detected in 9 patients, spontaneous SAH in 8 patients, and hypertension-related SAH in 3 patients), while 30 had traumatic SAH.

Patients were divided into two groups: non-traumatic SAH and traumatic SAH, and statistical comparisons were made. Additionally, patients were classified into two subgroups based on SEBES scores: those with SEBES >2 and those with SEBES ≤2, and their prognosis and other clinical parameters were compared.

Scoring systems

The following scoring systems were recorded for all patients at the time of ICU admission and discharge using hospital records and patient files: Glasgow Coma Scale (GCS), Full Outline of UnResponsiveness (FOUR), modified Fisher scale, World Federation of Neurosurgical Societies (WFNS) scale, Hunt and Hess scale, and modified Rankin Scale (mRS). The SEBES was calculated by the investigators. Radiological imaging of the patients was evaluated according to the recommended two-section method for SEBES assessment. The SEBES score ranged from 0 to 4, with 4 indicating the most severe condition.

Laboratory tests

Following an 8-hour fasting period, 5 mL of venous blood was drawn from the antecubital fossa for complete blood count (hemoglobin, hematocrit, leukocytes, lymphocytes, neutrophils, platelets). Routine biochemical blood tests (glucose, urea, creatinine, albumin), C-reactive protein (CRP), and procalcitonin levels were also measured. In addition, sodium levels were recorded on days 1, 3, and 7.

Statistical analysis

All values were expressed as mean ± standard deviation, mean (95% confidence interval), percentage (95% confidence interval), or median (interquartile range). The sample size of our study was determined based on a power analysis with a significance level of $\alpha=0.05$ and a power $(1-\beta)$ of 0.95. Differences between groups were analyzed using the Student's t-test, Mann–Whitney U test, chi-square test, Fisher's exact test, or analysis of variance (ANOVA). Statistical significance was defined as $p < 0.05$. Continuous variables were expressed as mean ± standard deviation and compared using the Student's t-test, assuming approximate normality. Categorical variables were expressed as counts and percentages and compared using the chi-square test. No normality testing was required for categorical data. For all significant parameters, logistic regression analyses were performed. All statistical analyses were conducted using SPSS version 22.0. Multiple comparisons were adjusted using the Holm–Bonferroni correction.

Results

In the non-traumatic SAH group (n=20), the mean age was 60.25 ±, whereas in the traumatic SAH group (n=30), it was 51.03 ±. In the non-traumatic group, 14 patients were male, while in the traumatic group, 27 patients were male. There was no statistically significant difference between the groups in terms of age and gender ($p>0.05$).

Among vascular risk factors, hypertension (HT) was more prevalent in the non-traumatic SAH group, showing borderline statistical significance ($p=0.05$). Other risk factors, including diabetes mellitus (DM), previous cerebrovascular disease (CVD), and coronary artery disease (CAD), did not show statistically significant differences between the groups.

The mortality rate at the first month was similar between the groups. However, by the third month, the mortality rate was higher in the non-traumatic group, though this difference was not statistically significant ($p=0.07$). The data presented above are summarized in Table 1.

When the groups were compared based on scoring systems, the SEBES score was markedly higher in the non-traumatic SAH group ($p = 0.00$). Although the FOUR scores at ICU admission were higher in the traumatic SAH group, the difference between the groups was not statistically significant ($p = 0.07$).

Additionally, no statistically significant differences were observed between the groups in terms of GCS, mRS, modified Fisher scale, WFNS, and Hunt-Hess

Table 1. Comparison of demographic characteristics, vascular risk factors, and clinical outcome between non-traumatic and traumatic SAH groups

Variable	Non-Traumatic SAH (n: 20)	Traumatic SAH (n: 30)	p-value
Age (years)	60.25 ± 14.46	51.03 ± 21.46	0.08
Gender (Male, n)	14	27	0.13
HT (n)	14	12	**0.05**
DM (n)	4	2	0.20
CVD (n)	0	2	0.51
CAD (n)	5	7	1.00
1st-Month Mortality (n)	9	8	0.23
3rd-Month Mortality (n)	11	8	0.07

HT: Hypertension, DM: Diabetes Mellitus, CVD: Cerebrovascular Disease, CAD: Coronary Artery Disease.

scores at admission. Similarly, ICU length of stay and ventilator support duration did not differ markedly between the two groups. However, at discharge, the GCS and FOUR scores were markedly higher in the traumatic SAH group (p=0.03), whereas the mRS score was higher in the non-traumatic SAH group (p=0.03). These comparisons are summarized in Table 2.

No statistically significant differences were found between the traumatic and non-traumatic SAH groups regarding laboratory test results. The mean values and corresponding p-values for each parameter are presented in Table 3.

When patients were categorized based on SEBES scores, in the non-traumatic SAH group, 13 patients had a high SEBES score (SEBES >2), while 7 patients had a low SEBES score (SEBES ≤2). In the traumatic SAH group, 10 patients had a high SEBES score, whereas 20 patients had a low SEBES score.

Table 2. Comparison of admission and discharge clinical scores, ICU length of stay, and duration of ventilator support between non-traumatic and traumatic SAH groups

Variable	Non-Traumatic SAH (n: 20)	Traumatic SAH (n: 30)	p-value
Admission GCS	8.70 ± 5.11	9.10 ± 4.80	0.78
Admission FOUR	8.25 ± 6.81	8.97 ± 6.79	0.72
Admission mFISHER	3.15 ± 0.87	2.70 ± 0.75	0.07
Admission mRS	3.40 ± 1.63	3.23 ± 1.48	0.72
Admission WFNS	3.50 ± 1.67	3.53 ± 1.36	0.94
Admission Hunt-Hess	3.45 ± 1.70	3.53 ± 1.41	0.86
SEBES	3.05 ± 1.10	2.10 ± 0.92	**0.001**
ICU Length of Stay (days)	18.25 ± 16.51	11.17 ± 11.02	0.10
Ventilator Support Duration (days)	11.50 ± 17.35	3.43 ± 5.54	0.06
Discharge GCS	8.15 ± 5.86	11.80 ± 5.02	**0.03**
Discharge FOUR	7.15 ± 8.11	12.20 ± 6.85	**0.03**
Discharge mRS	4.1 ± 2.24	2.73 ± 1.91	**0.03**

GCS: Glasgow Coma Scale, FOUR: Full Outline of UnResponsiveness, WFNS: World Federation of Neurosurgical Societies, mRS: Modified Rankin Scale, mFISHER: Modified Fisher Scale.

Table 3. Comparison of admission and follow-up laboratory findings between non-traumatic and traumatic SAH groups

Laboratory Parameter	Non-Traumatic SAH (n: 20)	Traumatic SAH (n: 30)	p-value
Albumin (g/L)	38.40 ± 5.19	37.10 ± 7.05	0.46
Creatinine (mg/dL)	1.11 ± 0.87	1.00 ± 0.56	0.61
Hemoglobin (g/dL)	12.95 ± 2.17	11.84 ± 2.18	0.08
Platelet Count (10^9/L)	249.05 ± 79.12	214.10 ± 77.72	0.13
Leukocyte Count (10^9/L)	15.10 ± 5.35	15.63 ± 5.55	0.74
Neutrophil (%)	85.55 ± 13.07	87.65 ± 10.67	0.55
Lymphocyte (%)	7.88 ± 4.75	7.64 ± 9.76	0.91
Neutrophil/Lymphocyte Ratio	15.11 ± 9.32	21.36 ± 15.09	0.08
C-Reactive Protein (CRP, mg/L)	41.78 ± 71.17	53.25 ± 50.01	0.54
Procalcitonin (ng/mL)	6.53 ± 22.73	2.19 ± 6.08	0.41
Admission Sodium (mmol/L)	138.38 ± 3.92	139.95 ± 5.36	0.24
Day 3 Sodium (mmol/L)	142.91 ± 9.39	141.39 ± 7.99	0.55
Day 7 Sodium (mmol/L)	142.88 ± 8.32	140.63 ± 11.79	0.43

Overall, 23 patients had high SEBES scores, while 27 had low SEBES scores. A comparison of these groups based on demographic characteristics, vascular risk factors, and prognosis is summarized in Table 4. Among patients with low SEBES scores, none had a history of diabetes mellitus (DM), whereas 6 patients in the high SEBES group had DM, a difference that was statistically significant (p = 0.01). Furthermore, non-traumatic SAH was markedly more prevalent in the high SEBES group (p = 0.03). Mortality rates at both one and three months were also markedly higher in the SEBES >2 group.

The groups were also compared based on their scoring systems, with the results summarized in Table 5. In the SEBES >2 group, admission GCS and FOUR scores were markedly lower compared to the SEBES ≤2 group (p = 0.00). Conversely, m FISHER, WFNS, Hunt-Hess, and mRS scores were markedly higher in the SEBES >2 group (p = 0.00).

Regarding prognosis, discharge GCS and FOUR scores were lower in the SEBES >2 group, whereas the mRS score was higher (p = 0.00). Additionally, 1st-month and 3rd-month mortality rates were markedly higher in the SEBES >2 group compared to the SEBES ≤2 group (p = 0.03 and p<0.001, respectively). Furthermore, the duration of ventilator support in the ICU was markedly longer in the high SEBES group (p = 0.01).

Table 4. Comparison of demographic characteristics, vascular risk factors, and mortality outcomes between patients with higher (SEBES >2) and lower (SEBES ≤2) subarachnoid early brain edema scores

Variables	SEBES ≤2 (Group 1, n=27)	SEBES >2 (Group 2, n=23)	p-value
Age (years)	53.18 ± 22.05	56.52 ± 15.91	0.54
Gender (Male, n)	22	19	1.00
HT (n)	14	12	0.60
DM (n)	0	6	**0.01**
Previous CVD (n)	1	1	0.71
CAD (n)	8	4	0.25
Spontaneous SAH (n)	7	13	**0.03**
1st-Month Mortality (n)	3	14	**0.001**
3rd-Month Mortality (n)	3	16	**0.001**

HT: Hypertension, DM: Diabetes mellitus, CVD: Cerebrovascular disease, CAD: Coronary artery disease.

Table 5. Comparison of admission and discharge clinical scores, ICU length of stay, and duration of ventilator support between patients with higher (SEBES >2) and lower (SEBES ≤2) subarachnoid early brain edema scores

Variables	SEBES ≤2 (Group 1, n=27)	SEBES >2 (Group 2, n=23)	p-value
Admission GCS	11.70 ± 3.91	5.69 ± 3.82	**0.001**
Admission FOUR	12.44 ± 5.06	4.26 ± 5.76	**0.001**
Admission FISHER	2.40 ± 0.69	3.43 ± 0.59	**0.001**
Admission mRS	2.44 ± 1.31	4.30 ± 1.105	**0.001**
Admission WFNS	2.74 ± 1.37	4.43 ± 0.99	**0.001**
Admission Hunt-Hess	2.70 ± 1.44	4.43 ± 0.99	**0.001**
ICU Length of Stay (days)	12.52 ± 12.57	15.74 ± 15.18	0.42
Ventilator Support Duration (days)	1.81 ± 3.96	12.35 ± 15.96	**0.01**
Discharge GCS	13.77 ± 3.24	6.30 ± 5.12	**0.001**
Discharge FOUR	14.74 ± 4.26	4.83 ± 7.46	**0.001**
Discharge mRS	2.07 ± 1.46	4.69 ± 1.94	**0.001**

GCS: Glasgow Coma Scale, FOUR: Full outline of UnResponsiveness, WFNS: World Federation of Neurosurgical Societies, mRS: Modified Rankin Scale, mFISHER: Modified Fisher Scale.

Table 6. Comparison of admission and follow-up laboratory findings between patients with higher (SEBES >2) and lower (SEBES ≤2) subarachnoid early brain edema scores

Laboratory Parameter	SEBES ≤2 (Group 1, n=27)	SEBES >2 (Group 2, n=23)	p-value
Albumin (g/L)	37.44 ± 5.52	37.82 ± 7.33	0.84
Creatinine (mg/dL)	0.92 ± 0.56	1.18 ± 0.81	0.20
Hemoglobin (g/dL)	11.88 ± 2.05	12.77 ± 2.36	0.16
Platelet Count (10^9/L)	223.22 ± 71.38	233.78 ± 89.17	0.65
Leukocyte Count (10^9/L)	14.26 ± 5.52	16.77 ± 5.09	0.10
Neutrophil (%)	88.09 ± 6.24	85.31 ± 15.80	0.43
Lymphocyte (%)	7.40 ± 4.75	8.14 ± 10.87	0.76
Neutrophil/Lymphocyte Ratio	18.09 ± 12.61	19.77 ± 14.39	0.66
C-Reactive Protein (CRP, mg/L)	39.73 ± 42.57	59.15 ± 73.40	0.27
Procalcitonin (ng/mL)	0.60 ± 0.87	7.83 ± 21.79	0.13
Admission Sodium (mmol/L)	138.74 ± 3.05	140.00 ± 6.37	0.39
Day 3 Sodium (mmol/L)	137.85 ± 4.26	146.87 ± 9.71	**0.001**
Day 7 Sodium (mmol/L)	136.82 ± 3.65	147.06 ± 13.07	**0.001**

Table 7. Multivariable logistic regression analysis for 3-month mortality

Variable	B	SE	Wald	p-value	Exp (B)	95% CI for Exp (B)
Age	−0.291	0.153	3.618	0.057	0.747	0.554 – 1.009
Gender	−4.075	3.608	1.275	0.259	0.017	0.000 – 20.024
Hypertension (HT)	3.801	2.583	2.165	0.141	44.736	0.283 – 7068.294
Subarachnoid Hemorrhage (SAH)	−2.810	2.784	1.019	0.313	0.060	0.000 – 14.105
SEBES	−0.253	2.404	0.011	0.916	0.777	0.007 – 86.449
GCS	0.375	0.415	0.815	0.367	1.455	0.645 – 3.285
Fisher Score	−1.541	1.783	0.747	0.388	0.214	0.007 – 7.058
ICU Length of Stay (days)	0.326	0.249	1.708	0.191	1.385	0.850 – 2.258
Ventilator Support Duration (days)	−1.239	0.999	1.539	0.215	0.290	0.041 – 2.052

Laboratory test results of the patients were compared. No significant difference was found between the groups in terms of admission sodium levels. However, serum sodium levels on days 3 and 7 were markedly higher in the SEBES >2 group ($p<0.001$). No other statistically significant differences were observed in the remaining laboratory parameters. The laboratory test values and corresponding p-values are presented in Table 6.

Multivariable logistic regression analysis for 3-month mortality showed that age demonstrated a trend toward higher risk (OR 0.75, 95% CI 0.55–1.01, $p=0.057$). None of the other variables, including gender, hypertension, subarachnoid hemorrhage type, SEBES score, GCS, Fisher score, ICU length of stay, or ventilator support duration, were significantly associated with mortality. Some variables showed very wide confidence intervals, reflecting limited event numbers or variable distribution, and should be interpreted with caution (Table 7).

Figure 1 illustrates the Exp(B) values and their 95% confidence intervals for each variable included in the regression analysis. A logarithmic scale was used to better visualize the large differences in Exp(B) values. The red dashed line represents the point of no effect (Exp(B) = 1); variables with values below this line indicate a negative association, while those above the line suggest a positive association.

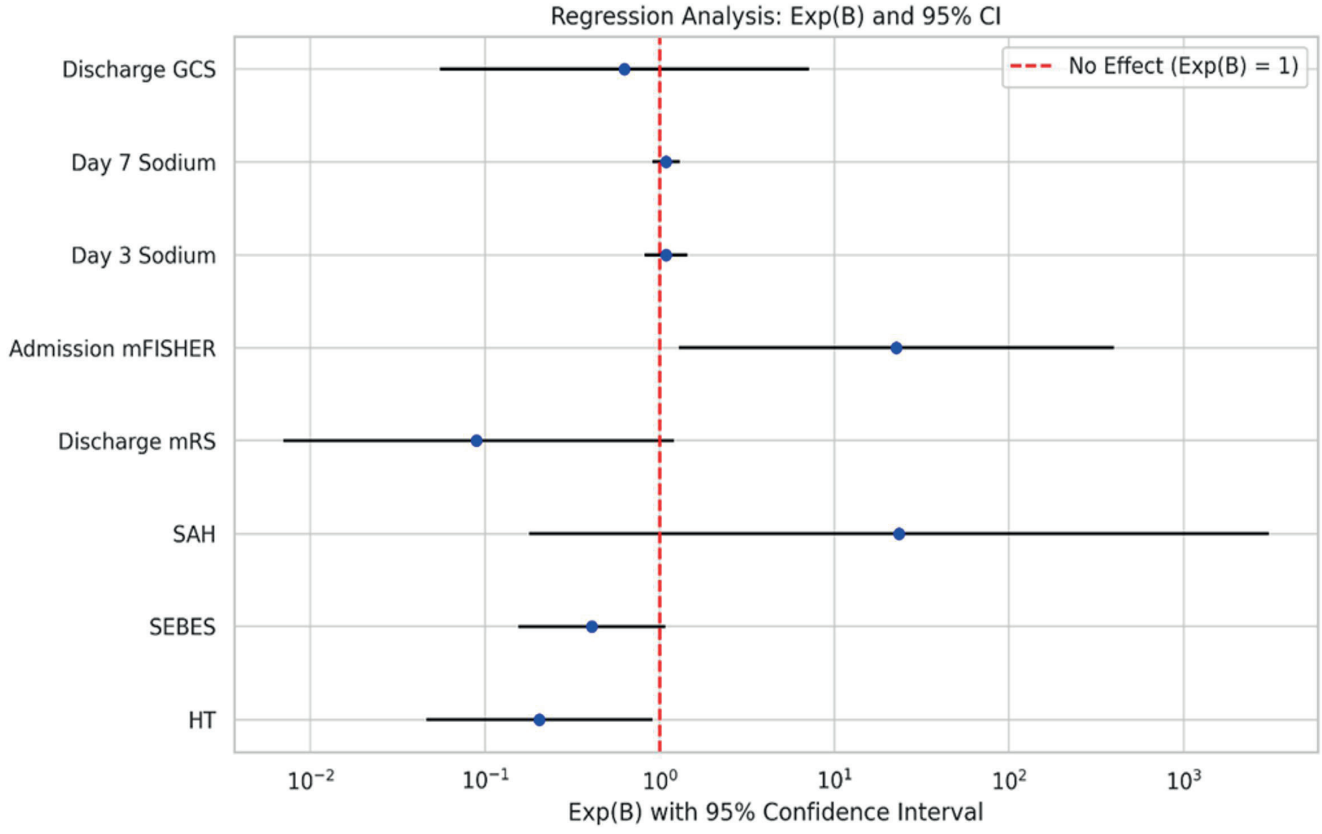

Figure 1. Logistic regression analysis of variables

To account for multiple testing, the Holm–Bonferroni correction was applied. After adjustment, only SEBES remained significantly different between groups in Table 2. In Table 4, 1- and 3-month mortality continued to show significant associations, whereas other variables lost significance. In Table 5, all admission and discharge clinical severity scores retained their significance after correction, while ventilator support duration did not. In Table 6, only Day 3 and Day 7 sodium levels remained significantly different between SEBES groups following adjustment.

Discussion

Predicting the prognosis of patients with SAH remains a fundamental yet challenging aspect of clinical neurocritical care. Accurate and early prediction allows clinicians to tailor interventions, monitor complications effectively, and improve overall patient outcomes. Despite the existence of various clinical and radiological scoring systems, a universally accepted, highly predictive tool remains elusive (8,9). Among the established prognostic indicators, cerebral edema and initial neurological status stand out for their strong correlation with delayed cerebral ischemia and infarcts (7). EBI, encompassing the cascade of pathophysiological changes occurring immediately after aneurysmal rupture, including increased intracranial pressure (ICP), disruption of cerebral autoregulation, and ischemia—has gained prominence as a critical determinant of outcome (2,4).

The SEBES has emerged as a simple, reproducible radiological tool designed to assess early brain edema severity on initial CT imaging in spontaneous SAH patients (3,7). This scoring system evaluates two predefined CT slices for evidence of cerebral edema, producing an objective numerical value indicative of brain injury severity. While initially validated in aneurysmal SAH, recent studies have suggested SEBES's applicability in non-aneurysmal and even

traumatic SAH populations (1,8). Our study uniquely applies the original SEBES system across both traumatic and non-traumatic SAH cases, confirming its prognostic utility beyond its initial scope.

Our analysis revealed that non-traumatic SAH patients had markedly higher early SEBES scores compared to their traumatic counterparts, with a notable prevalence of hypertension in this group ($p=0.05$). This finding aligns with previous research emphasizing hypertension as a risk factor for worse outcomes in non-traumatic SAH (10). The non-traumatic group also demonstrated worse discharge neurological status ($p=0.03$) and markedly higher mortality rates at one and three months ($p<0.001$). These observations corroborate the prognostic significance of early brain edema quantified by SEBES, mirroring results from Ahn et al. and Said et al., who linked elevated SEBES with increased risk of delayed cerebral ischemia and unfavorable clinical outcomes (3,7).

In addition to mortality, our data highlighted that patients with SEBES scores greater than 2 experienced prolonged mechanical ventilation and longer ICU stays, indicating more severe systemic and neurological compromise. This trend underscores SEBES's role not only as a static prognostic marker but also as a dynamic indicator of disease severity influencing critical care resource utilization. Previous investigations, including those by Duan et al., have emphasized the utility of SEBES in guiding aggressive interventions such as decompressive craniectomy in poor-grade aneurysmal SAH, further supporting its clinical relevance (11).

Age-stratified analyses reinforce the higher prognostic accuracy of SEBES in patients under 60 years old, consistent with Eibach et al.'s findings that younger patients exhibit a stronger association between brain edema severity and outcome (12). This phenomenon may reflect age-dependent differences in cerebral plasticity and resilience, suggesting that SEBES could be particularly valuable in predicting outcomes among younger SAH populations.

Regarding the temporal profile of cerebral edema, our findings align with the limited but growing body of literature indicating edema resolution occurs around one week post-ictus (5,13). Patients with persistently high SEBES scores also exhibited markedly elevated serum sodium levels on days 3 and 7 ($p<0.001$), paralleling previous reports that hypernatremia serves as an early biochemical predictor of delayed cerebral edema and correlates with increased mortality (5,10,14). The mechanisms underlying hypernatremia post-SAH may involve osmotherapy administration, central diabetes insipidus, or disruption of sodium regulation due to hypothalamic injury (5). These findings highlight the importance of integrating biochemical markers with radiological scores to better predict patient trajectories and potentially guide tailored interventions.

From a practical standpoint, the ease of SEBES application using routine CT scans makes it a promising tool for widespread clinical adoption. Early identification of patients with severe brain edema could inform decisions regarding intensive monitoring modalities such as intracranial pressure measurement, cerebral oxygenation monitoring, or early consideration of surgical decompression (11). Additionally, consistent use of SEBES could improve interprofessional communication and standardize care protocols across neurocritical units, addressing a notable gap identified in prior SAH management guidelines (7,8).

This study has several limitations. Its retrospective design and small sample size limit the strength and generalizability of the results. The lack of serial imaging data prevented us from evaluating temporal resolution or progression of cerebral edema or to examine its relationship with delayed infarction and large-scale edema. These issues should be addressed in future prospective studies (13). Another limitation is not to include inflammatory markers and detailed hemodynamic vaiables, may have restricted the scope of prognostic modeling (2,6).

Despite these limitations, our logistic regression analysis confirms that SEBES$>$ 2 is associated with poor outcomes in both traumatic and non-traumatic SAH. To our knowledge, this is among the first studies to extend the application of SEBES to traumatic SAH, supporting its broader prognostic utility. Nonetheless, before widespread routine use, further validation

through large-scale, multicenter prospective trials is warranted to refine cutoff values and adapt the scoring system for diverse SAH populations.

In conclusion, the SEBES scoring system is a valuable radiographic marker that correlates with mortality, neurological deterioration, and ICU burden in SAH patients. A score >2 is consistently associated with worse outcomes, regardless of etiology. These findings support the integration of SEBES into early neurocritical care decision-making. Future prospective multicenter studies with larger cohorts and longitudinal imaging follow-up are warranted to validate these findings and refine SEBES-based prognostic models.

Ethical approval

This study has been approved by the T.C. İzmir Bakırçay University Non-Interventional Clinical Research Ethics Committee (approval date: 03.07.2024, number: 1670). Written informed consent was obtained from the participants.

Author contribution

Study conception and design: AÇ, YA; data collection: SN, AÇ, AEÖ, İD; analysis and interpretation of results: YA, NŞ; draft manuscript preparation: YA, AÇ. The author(s) reviewed the results and approved the final version of the article.

Source of funding

The authors declare the study received no funding.

Conflict of interest

The authors declare that there is no conflict of interest.

References

1. Zhang A, Zhang Z, Zhang WB, et al. Development of a nomogram for predicting clinical outcome in patients with angiogram-negative subarachnoid hemorrhage. CNS Neurosci Ther. 2021;27:1339-47. [Crossref]
2. Savarraj J, Parsha K, Hergenroeder G, et al. Early brain injury associated with systemic inflammation after subarachnoid hemorrhage. Neurocrit Care. 2018;28:203-11. [Crossref]
3. Ahn SH, Savarraj JP, Pervez M, et al. The Subarachnoid hemorrhage early brain edema score predicts delayed cerebral ischemia and clinical outcomes. Neurosurgery. 2018;83:137-45. [Crossref]
4. Rass V, Helbok R. Early brain injury after poor-grade subarachnoid hemorrhage. Curr Neurol Neurosci Rep. 2019;19:78. [Crossref]
5. Rass V, Ianosi BA, Wegmann A, et al. Delayed resolution of cerebral edema is associated with poor outcome after nontraumatic subarachnoid hemorrhage. Stroke. 2019;50:828-36. [Crossref]
6. Ahn SH, Burkett A, Paz A, et al. Systemic inflammatory markers of persistent cerebral edema after aneurysmal subarachnoid hemorrhage. J Neuroinflammation. 2022;19:199. [Crossref]
7. Said M, Gümüs M, Herten A, et al. Subarachnoid Hemorrhage Early Brain Edema Score (SEBES) as a radiographic marker of clinically relevant intracranial hypertension and unfavorable outcome after subarachnoid hemorrhage. Eur J Neurol. 2021;28:4051-9. [Crossref]
8. Said M, Odensass S, Gümüs M, et al. Comparing radiographic scores for prediction of complications and outcome of aneurysmal subarachnoid hemorrhage: which performs best? Eur J Neurol. 2023;30:659-70. [Crossref]
9. Fang YJ, Mei SH, Lu JN, et al. New risk score of the early period after spontaneous subarachnoid hemorrhage: for the prediction of delayed cerebral ischemia. CNS Neurosci Ther. 2019;25:1173-81. [Crossref]
10. Lantigua H, Ortega-Gutierrez S, Schmidt JM, et al. Subarachnoid hemorrhage: who dies, and why? Crit Care. 2015;19:309. [Crossref]
11. Duan YH, He J, Liu XF, et al. Role of the subarachnoid hemorrhage early brain edema score in the management of decompressive craniectomy for poor-grade aneurysmal subarachnoid hemorrhage. World Neurosurg. 2022;166:e245-52. [Crossref]
12. Eibach M, Won SY, Bruder M, et al. Age dependency and modification of the Subarachnoid Hemorrhage Early Brain Edema Score. J Neurosurg. 2020;134:946-52. [Crossref]
13. Torné R, Hoyos J, Llull L, et al. Edema resolution and clinical assessment in poor-grade subarachnoid hemorrhage: useful indicators to predict delayed cerebral infarctions? J Clin Med. 2021;10:321. [Crossref]
14. Qureshi AI, Suri MF, Sung GY, et al. Prognostic significance of hypernatremia and hyponatremia among patients with aneurysmal subarachnoid hemorrhage. Neurosurgery. 2002;50:749-56. [Crossref]

Turk J Intensive Care 2026;24(1):49-62
DOI: 10.63729/TJIC.2025.679

ORIGINAL RESEARCH

Clinical efficacy of a protocol-based hemoadsorption therapy in patients with septic shock

Fethi Gül[1], Esra Tekin[2], Esra Çankaya[2], Mehmet Süleyman Sabaz[2], Işıl İnan Çiloğlu[3], Burçin Doruk Oktay[2], Antoine Guillaume Schneider[4]

[1]Division of Intensive Care, Department of Anesthesiology and Reanimation, Faculty of Medicine, Marmara University, İstanbul, Türkiye
[2]Division of Intensive Care, Department of Anesthesiology and Reanimation, Marmara University Pendik Training and Research Hospital, İstanbul, Türkiye
[3]Department of Anesthesiology and Reanimation, Faculty of Medicine, Marmara University, İstanbul, Türkiye
[4]Division of Intensive Care, Lausanne University Hospital, Lausanne, Switzerland

ABSTRACT

Introduction: Hemoadsorption (HA) removes circulating inflammatory mediators and is used as an adjunct in septic shock. We assessed whether a protocol-based HA330 strategy improved early organ dysfunctions and outcomes.

Materials and Methods: We performed an observational study of adults with septic shock admitted to a 59-bed mixed ICU (January 2023–June 2024). We compared outcomes of patients who were treated with HA, to those who received standard of care alone.

Results: During the study period, 52 of 127 septic shock patients received hemoadsorption therapy (HA group), while 75 received standard care (control group). On ICU admission age, sex, comorbidity, APACHE II, and SOFA scores were similar. By day 3, SOFA score decreased with HA (8 [5–11] to 7 [5–9]; $p<0.05$) but was unchanged in controls. Vasoactive inotropic score declined in both groups, more prominently with HA. Mechanical ventilation requirement and ICU length of stay were comparable. AKI decreased from 71.2% to 46.2% in the HA but increased from 44.0% to 50.7% in the control group. Hospital stay was longer with HA (29,5 [18-47,75] vs 19 [12-30], $p=0.009$), whereas 28-day mortality was lower (30.8% vs 49.8%, $p<0.05$).

Conclusions: Protocol-based early HA at high vasopressor requirements was associated with improved organ dysfunctions and reduced 28-day mortality in septic shock patients.

Keywords: hemoadsorption, septic shock, vasoactive inotropic score, acute kidney injury, intensive care unit, mortality

Introduction

As per the Sepsis-3 definition, sepsis is a life-threatening organ dysfunction caused by dysregulated host response to infection (1). Sepsis represents a significant portion of all admissions in intensive care units (ICU) throughout the world. Septic shock, the most severe form of sepsis, is characterized by a need for vasopressors and elevated lactate levels and is associated with very high ICU mortality (1-5). Worldwide, sepsis is estimated to cause approximately 20 million deaths annually and account for 31.5% of all deaths (6). Sepsis associates an uncontrolled inflammatory response, cytokine storm, endothelial dysfunction, coagulopathy, and impairment in microcirculation (3). Standard management includes source identification, rapid broad-spectrum antimicrobial therapy, appropriate fluid resuscitation, and organ support. However, despite these therapies, the observed mortality remains very high. Hence, adjunct treatment strategies are required (7).

In recent years, hemoadsorption based therapies have been proposed as an adjunct treatment to the

✉ Fethi Gül • gulfethi@gmail.com

Received: 25.10.2025 **Accepted:** 26.12.2025 **Published:** 28.12.2025

standard of care for sepsis or sepsis-like syndrome (8). The rationale is to remove harmful substances, such as excess cytokines, bacterial endotoxins and toxins, selectively or non-selectively from the circulation. The goal is to improve hemodynamics, reduce the need for vasopressor, preserve organ function, and ultimately decrease mortality (3,9). However, the evidence supporting the utilization of hemoadsorption in sepsis remains scarce and controversial. While some studies have reported a faster reduction in vasopressor dose (10,11), a decrease in inflammatory markers, and clinical improvement with HA treatment, some have not (12-14). Therefore, international guidelines currently do not recommend the routine use of hemoadsorption but encourage further investigations in selected patient groups (7).

Studies systematically examining the effect of hemoadsorption therapy on hemodynamic response, vasopressor requirement, lactate clearance, SOFA score, and organ functions are limited in number and have heterogeneous treatment protocols. Therefore, adequately designed clinical studies are needed to clarify the true clinical efficacy of hemoadsorption therapy, the patient groups likely to benefit from it, and the factors determining response to treatment.

In Türkiye, reimbursement for hemoadsorption (HA) by healthcare insurance was introduced in 2014. It was included in our institutions' sepsis management protocol in 2021. However, due to budget restrictions, it was only available during certain periods of time. We sought to compare outcomes of patients with sepsis who received HA therapy (admitted during periods where the device was available) and controls (when it was not available at our center).

Materials and Methods

This observational cohort study was conducted in a 59-bed mixed ICU. Our center is a closed-unit ICU where extracorporeal therapies (extracorporeal membrane oxygenation (ECMO), hemodialysis, hemoadsorption, plasmapheresis) can be provided 24/7 by intensive care specialists, intensive care subspecialty residents, and anesthesiology and reanimation residents.

Study population: All adult (≥18 years) patients who met Sepsis-3 diagnostic criteria for septic shock and were admitted to our ICU for a duration of more than 24 hours were considered for inclusion in the study (1). We excluded pregnant or lactating women, patients with advanced malignancies and those with missing data. Patients who received hemoadsorption with the HA330 cartridge (HA group) were matched with septic patients who had similar APACHE II, SOFA, and age measurements at ICU admission but did not receive HA therapy (control group).

Standard of care

In our ICU, standard of care for sepsis corresponds to the Surviving Sepsis Campaign (SSC) international guidelines (7). Briefly, this includes, early recognition, identification and control of the source, obtaining appropriate cultures, initiation of broad-spectrum antibiotic therapy, fluid resuscitation with 30 mL/kg of crystalloid fluid and initiation of vasopressor (first choice norepinephrine) if mean arterial pressure (MAP) remained <65 mmHg despite fluid resuscitation. When norepinephrine dose exceeded 0.25 μg/kg/min or hemodynamic instability persisted despite increasing vasopressor requirements, hydrocortisone (200 mg/day) was added, and a second vasopressor agent started.

Hemoadsorption protocol

According to our protocol, hemoadsorption is considered in patients with sepsis, when despite all measures described above, the norepinephrine dose exceeds 0.20-0.25 μg/kg/min. This threshold is considered as indicative of refractory septic shock and of a high inflammatory response. When CRRT is applied, hemoadsorption therapy consists of the insertion of an HA 330 (Jafron Biomedical Co., Ltd., Zhuhai, China) cartridge within the CRRT device.When no CRRT is provided, similar cartridges are used but in hemoperfusion mode within a dedicated device. Once

initiated, hemoadsorption therapy is administered once daily for an aimed duration of 3 days. Consistent with reports in which hemoperfusion sessions were extended up to 8 hours in selected settings (15) we used a treatment duration of approximately 6–8 hours, with flow rates ranging between 150 and 250 mL/min.

Data Collection: Eligible patients were identified and data retrieved from their electronic medical records as well as from daily ICU observation charts. Patients' age, gender, body mass index, comorbid diseases, and admission diagnoses were recorded as well as clinical parameters and laboratory results obtained during ICU admission. We assessed acute kidney injury (AKI) presence and stage according to kidney disease: improving global outcomes (KDIGO). Glasgow coma scale (GCS), acute physiology and chronic health evaluation II (APACHE II), and sequential organ failure assessment score (SOFA) were calculated upon ICU admission. Initial AKI and vasoactive inotropic score (VIS) were calculated at the time septic shock was diagnosed, and then recalculated daily for the first three days. In addition, we recorded administered treatments (vasoactive drugs, antibiotics), interventions (mechanical ventilation, hemodialysis, hemoadsorption, plasmapheresis, ECMO) and complications. Finally, 28-day mortality was recorded.

Outcomes: Our primary outcome was 28-day mortality. Our secondary outcomes included ICU and hospital length of stay (LOS), duration of mechanical ventilation, changes in SOFA score, organ dysfunctions, as well as vasopressor and inotrope requirements.

Sample Size: Based on prior evidence, to detect a 23.6% reduction in ICU mortality associated with the intervention with 80% statistical power, a two-sided 95% confidence interval, and a 1:1 allocation ratio, a minimum of 48 patients per group was required (16).

Ethical Issues: The study was approved by Marmara University Medical Faculty Research and Ethics Committee (approval no: 09.2024.811). The research was conducted in conformity with the Declaration of Helsinki and Good Clinical Practice guidelines. As this study had a retrospective design and was based on the analysis of routinely collected, anonymized clinical data, informed consent from individual patients could not be obtained and the need for informed consent was therefore waived in accordance with current ethical guidelines.

Data evaluation and statistical analysis

Statistical analyses were performed using SPSS Statistics, version 22.0 (IBM Corp., Armonk, NY, USA). The Shapiro–Wilk test was used to assess the normality of distribution for continuous variables. Categorical variables are presented as counts and percentages. Continuous variables with a normal distribution are expressed as mean ± standard deviation, whereas non-normally distributed variables are expressed as median and interquartile range (IQR). Between-group comparisons of continuous variables were performed using the independent-samples t test for normally distributed data and the Mann–Whitney U test for non-normally distributed data. Within-group comparisons of continuous variables were conducted using the Wilcoxon signed-rank test. For the within-group analysis of more than two numerical variables, repeated-measures ANOVA was used; when the assumptions of this test were not met, the Friedman test was applied. Categorical variables were compared using the chi-square test or McNemar test, as appropriate; when the assumptions for the chi-square test were not met, Fisher's exact test was applied. A two-sided p-value < 0.05 was considered statistically significant

Results

Patients: During the study period, 2533 patients were admitted to our unit. Of those, as shown in Figure 1, we excluded 1399 who had did not have sepsis, 32 who were <18 yo and 272 who stayed less than 24

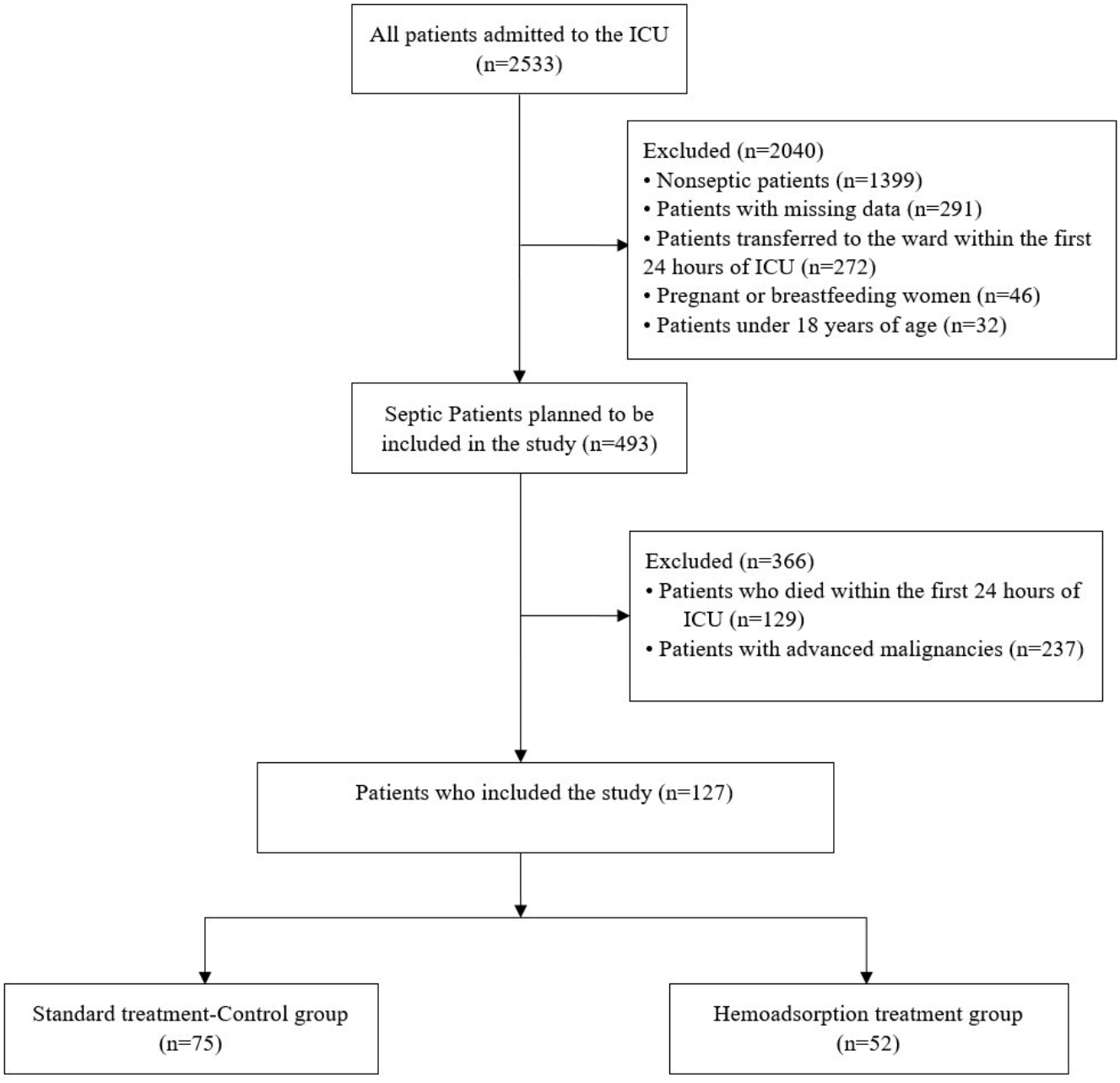

Figure 1. Flow diagram of patients selection

ICU, Intensive care unit.

hours in ICU, 46 who were pregnant or breastfeeding and 291 who missing data. In addition, another 366 were excluded from the analysis as they died within the first 24 hours (129) or had advanced malignancies (237). Hence, 127 were eligible to enter the study. Of these, 52 received hemoadsorption (HA group), and 75 did not (control group).

The two groups and their baseline characteristics are described in Table 1. Overall, there were no significant differences at baseline between the two groups sex, body mass index, Charlson comorbidity index. There were imbalances in the source of sepsis. Indeed, pulmonary infections were more frequent in the control group (58.7% vs. 23.1%, $p<0.001$), whereas

Table 1. Demographic characteristics, ICU disease severity scores and VIS score

Parameters	Hemoadsorption group (52; 40,9%) Median (IQR)	Control group (75; 59,1%) Median (IQR)	P value
Age, mean±SD	51,73±18,97	57,88±20,80	0,075
Gender, n(%)			0,534
Male	32 (61,5)	42 (56,0)	
Female	20 (38,5)	33 (44,0)	
Body mass index, mean±SD (kg/m^2)	28,18±6,62	27,45±6,47	0,352
Height	168 (160-175)	169 (160-175)	0.308
Weight	80 (68,5-88.0)	78 (66-83)	0.272
Charlson comorbidty index	3 (1-4)	2 (4-6)	0,156
ICU Scores			
APACHE II	22 (18-26)	20 (15-25)	0,102
GCS first day	7 (3-11)	7 (3-11)	0,678
GCS 2. day	8 (3-11)	7 (3-11)	0.739
GCS 3. day	9 (3-15)	8 (4-13)	0.698
SOFA first day	8 (5-11)	8 (5-11)	0,973
SOFA 2. day	8 (6-9)	9 (7-11)	0.073
SOFA 3. day	7 (5-9)	8 (6-11)	0.046
VIS first day	18.5 (5.5-33.5)	12 (5-24)	0.171
VIS 2. day	6 (0-30)	10 (4-20)	0.550
VIS 3. day	3 (0-24)	6.5 (0-18)	0.442
Noradrenaline first day (mg/day)	11,88 (5.26-28.60)	10.28 (4.60-19.04)	0.116
Noradrenaline 2. day (mg/day)	11.36 (2.0-28.76)	8.60 (3.98-16.72)	0.452
Noradrenaline 3. day (mg/day)	7.84 (3.32-24.56)	8.44 (3.80-14.57)	0.551
Adrenaline first day (mg/day)	9.40 (2.30-16.25)	6.65 (3.0-12.0)	0.507
Adrenaline 2. day (mg/day)	7.53 (1.61-19.31)	5.35 (1.29-13.99)	0.526
Adrenaline 3. day (mg/day)	6.77 (1.05-25.61)	3.05 (0.75-32.50)	0.604
Adrenaline, n (%)	25 (48.1)	31 (41.3)	0.452
Terlipressin, n (%)	9 (17.3)	14 (18.7)	0.845
Methylen blue, n (%)	2 (3.8)	2 (2.7)	0.543
Steroid, n (%)	25 (48.1)	34 (45.3)	0.760

ICU: intensive care unit; APACHE: acute physiology and chronic health evaluation; GCS: Glasgow coma scale; SOFA: sequential organ failure assessment; VIS: vasoactive-inotropic score; SD: standard deviation; IQR: inter quartile range.

bloodstream infections were more common in the HA group (26.9% vs. 8.0%, p<0.05). Gram-negative organisms tended to be more frequent in the HA group, and gram-positive organisms in the control group (Table 2).

Primary outcome: 28-day mortality

Compared with patients in the control group, patients in the HA group had a lower 28-day mortality (30.8 versus 49.3%, p = 0.037) (Table 3).

Secondary outcomes

Clinical outcomes

Compared with the control group, patients in the HA group had similar ICU LOS but longer hospital LOS (21 vs 13, p=0.079 and 29.5 vs 19, p=0.009, respectively). The duration of mechanical ventilation was determined to be 13 (5.5-31.5) days in the HA group and 10 (7-19) days in the control group (p>0.05) (Table 4).

Table 2. Infection parameters

Enfection Parameters	Hemoadsorption Group (52; 40,9%) Median (IQR)	Control Group (75; 59,1%) Median (IQR)	P value
Procalcitonin first day	2.86 (0.80-11.91)	1.29 (0.25-5.0)	0.098
Procalcitonin 2. day	7.38 (2.65-24.86)	1.85 (0.29-6.16)	**<0.001**
Procalcitonin 3. day	6.40 (2.98-25.54)	2.0 (0.28-7.76)	**<0.001**
CRP first day	138 (49-237)	128 (59-213)	0.928
CRP 2. day	145 (89-272)	143 (71-225)	0.653
CRP 3. day	122 (69-203)	125 (72-200)	0.955
Enfection sources, n (%)			
Lung	12 (23.1)	44 (58.7)	<0.001
Blood circulation	14 (26.9)	6 (8.0)	0.004
Urinary system	3 (5.8)	3 (2.7)	0.399
Central catheter	3 (5.8)	2 (2.7)	0.399
Central nervous system	0 (0)	2 (2.7)	0.513
Intraabdominal	6 (11.5)	4 (5.3)	0.173
Surgical site	2 (3.8)	1 (1.3)	0.315
Culture negative	12 (23.1)	14 (18.7)	0.545
Pozitive culture, n (%)			
Gram negative			
Acinetobacter baumannii	11 (21.2)	27 (36.0)	0.072
Klebsiella Pneumonia	10 (19.2)	15 (20.0)	0.915
Pseudomonas Aeruginosa	9 (17.3)	9 (12.0)	0.399
Other Gram negative	18 (34.6)	7 (9.3)	**<0.001**
Gram positive			
Staph Aureus	2 (3.8)	10 (13.3)	0.064
Streptococus pneumoniae	2 (3.8)	3 (4.0)	0.669
Other Gram positive	2 (3.8)	2 (2.7)	0.543
Fungal			
Candida albicans	5 (9.6)	0 (0)	**0.010**
Candida auris	4 (7.7)	1 (1.3)	0.090
Other fungal	1 (1.9)	2 (2.7)	0.635

CRP: C-reactive protein, IQR: inter quartile range.

Organ dysfunctions

As shown in Figure 2, SOFA scores were similar between the two groups on days 1 and 2, but lower on day 3 in the HA group (7 [5-9] versus 8 [6-11], ($p<0.05$).

Within 72 hours of ICU admission, there was no difference between the two groups in terms of VIS Score, noradrenaline or adrenaline doses or the proportions of patients receiving adrenaline, methylene blue, terlipressin, and steroids (Table 1). Similarly, there was no difference in terms of MAP or heart rate (Table 5).

The proportion of patients requiring mechanical ventilation was similar (94.2% vs 93.3%), in the two groups. There was no difference between the two groups in terms of FiO_2, PEEP, pressure support values, PaO_2/FiO_2 ratios. Arterial blood gas analyses showed no between-group differences in pH, lactate,

Table 3. Acute kidney injury, CRRT rates, length of stay, and 28-day mortality

Parameters	Hemoadsorption Group (52; 40,9%) n (%)	Control Group (75; 59,1%) n (%)	P value
AKI first day	37 (71,2)[a]	33 (44.0)	**0,002**
AKI 2. day	31 (59.6)[b]	35 (46.7)	0.151
AKI 3. day	29 (56.9)[c]	36 (48.6)	0.366
AKI last day	24 (46,2)	38 (50.7)	0,617
AKI stage first day			**0.010**
Non-AKI	15 (28.8)	42 (56.0)	
AKI stage 1	15 (28.8)	8 (10.7)	
AKI stage 2	7 (13.5)	8 (10.7)	
AKI stage 3	15 (28.8)	17 (22.7)	
AKI stage 2. day			0.538
Non-AKI	21 (40.4)	40 (53.3)	
AKI stage 1	8 (15.4)	10 (13.3)	
AKI stage 2	8 (15.4)	8 (10.7)	
AKI stage 3	15 (28.8)	17 (22.7)	
AKI stage 3. day			0.631
Non-AKI	22 (43.1)	38 (51.4)	
AKI stage 1	12 (23.5)	13 (17.6)	
AKI stage 2	4 (7.8)	5 (6.8)	
AKI stage 3	13 (25.5)	18 (24.3)	
AKI lastday			0.948
Non-AKI	28 (53.8)	37 (49.3)	
AKI stage 1	6 (11.5)	11 (14.7)	
AKI stage 2	4 (7.7)	6 (8.0)	
AKI stage 3	14 (26.9)	21 (28.0)	
CRRT	37 (71,2)	20 (26,7)	**<0.001**
CRRT total days, median (IQR)	10 (3-24)	5 (2-6)	**0.016**
Length of stay			
ICU LOS, day median(IQR)	21 (10-36)	13 (8-23)	0,079
Hospital LOS, day median(IQR)	29,5 (18-47,75)	19 (12-30)	**0,009**
Mortality			
28 day mortality	16 (30,8)	37 (49,3)	**0,037**

AKI: acute kidney injury; LOS: Length of stay, CRRT: Continuous renal replacement therapy, IQR: inter quartile range.
[a]: 1. day versus lastday (p<0.05), [b]: 2. day versus lastday (p<0.05), [c]: 3. day versus lastday (p<0.05)

or other parameters (p>0.05). In the within-group analysis, a significant decrease in lactate level was observed in the HA group on day 3 (1.5 [1.1–2.2]) compared with day 1 (1.9 [1.3–3.9]) and day 2 (2.2 [1.2–4.1]), whereas no significant change in lactate was detected in the control group (Figure 2).

There was no difference in terms of GCS scores.

Acute kidney injury (AKI) was significantly more common in the HA group on day 1 (71.2% vs. 44.0%, p<0.05). However, the proportion was similar in the two groups on days 2 and 3 as well as on ICU discharge (46.2% vs. 50.7%, p>0.05) (Table 3). In the within-group analysis, AKI rates remained stable across day 1, day 2, day 3, and the last ICU day in the control group, whereas in the HA group the AKI

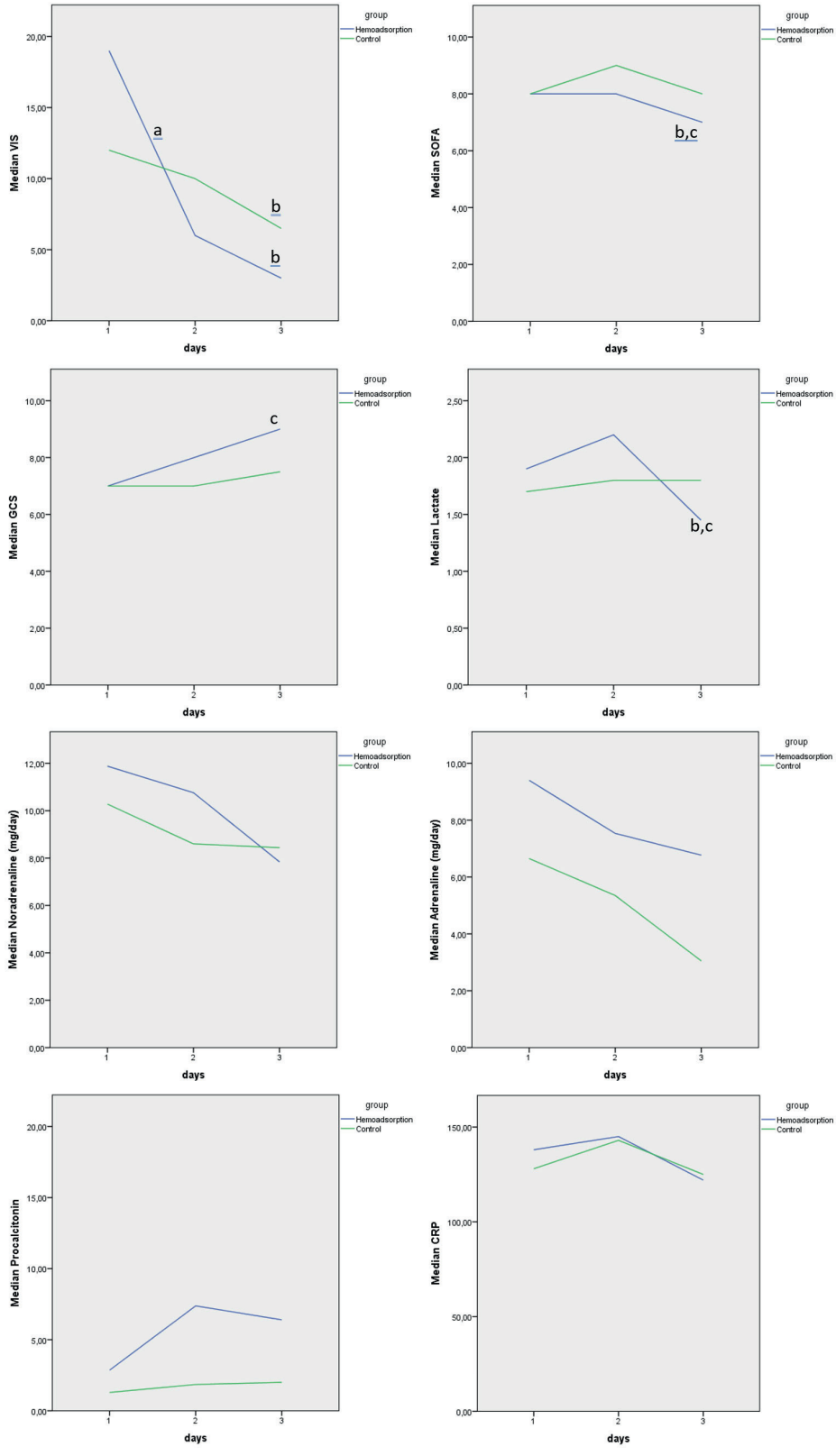

Figure 2. VIS, SOFA, GCS, CRP, Pocalcitonin, lactate and vasopressors trend graphs

[a]: 1. day versus 2.day ($p<0.05$), [b]: 1. day versus 3.day ($p<0.05$), [c]: 2. day versus 3.day ($p<0.05$)

Table 4. Mechanical ventilation and blood gas parameters

Parameters	Hemoadsorption Group (52; 40,9%) Median (IQR)	Control Group (75; 59,1%) Median (IQR)	P value
Mechanical ventilation and blood gas parameters			
Mechanical ventilation, n(%)	49 (94.2)	70 (93.3)	0.838
Mechanical ventilation duration (day)	13 (5.5-31.5)	10 (7-19)	0.462
FiO_2 (%) first day	40 (30-50)	40 (30-60)	0.397
FiO_2 (%) 2. day	35 (30-50)	40 (30-50)	0.605
FiO_2 (%) 3. day	35 (30-50)	35 (30-50)	0.770
PEEP first day	6 (5-8)	6 (6-8)	0.902
PEEP 2. day	6 (5-8)	6 (6-8)	0.921
PEEP 3. day	6 (6-8)	6 (6-8)	0.861
PS first day	15 (13-18)	15 (12-18)	0.708
PS 2. day	15 (13-18)	15 (12-18)	0.477
PS 3. day	14 (12-18)	16 (12-18)	0.871
PaO_2/FiO_2 ratio first day	280 (189-371)	282 (163-376)	0.540
PaO_2/FiO_2 ratio 2. day	287 (211-396)	321 (208-408)	0.667
PaO_2/FiO_2 ratio 3. day	279 (161-407)	290 (179-393)	0.633
Ph first day	7.42 (7.33-7.47)	7.41 (7.34-7.48)	0.569
Ph 2. day	7.43 (7.38-7.46)	7.43 (7.37-7.48)	0.402
Ph 3. day	7.42 (7.35-7.47)	7.45 (7.38-7.49)	0.217
Lactate first day	1.9 (1.3-3.9)	1.7 (1.2-2.8)	0.251
Lactate 2. day	2.2 (1.2-4.1)	1.8 (1.2-2.6)	0.128
Lactate 3. day	1.5 (1.1-2.2)	1.8 (1.2-2.7)	0.115

FiO_2: fraction of inspired oxygen; PEEP: positive end-expiratory pressure; PS: pressure support; PaO_2/FiO_2: partial pressure of oxygen/ fraction of inspired oxygen; IQR: inter quartile range.

rate on the last ICU day was significantly lower than on each of the first three days. No between-group differences in creatinine levels were observed. Fluid balance over the three-day period was similar in both groups (Table 4). CRRT use was significantly higher in the HA group (71.2% vs. 26.7%, $p<0.001$), and CRRT duration was longer in the HA group ($p<0.05$).

Hemoglobin level on day 3 was significantly lower in the HA group (8.2 [7.8–9.6]) compared with the control group (9.0 [8.2–10.1]) ($p<0.05$). Platelet counts were lower in the HA group from day 1 onwards, and this difference was statistically significant on days 2 and 3 (Figure 3). Within groups, platelet counts decreased significantly in both arms, with a more marked decline in the HA group ($p<0.001$).

Procalcitonin levels were significantly higher in the HA group on days 2 and 3 (day 2: 7.38 [2.65–24.86] vs. 1.85 [0.29–6.16]; day 3: 6.40 [2.98–25.54] vs. 2.0 [0.28–7.76]; $p<0.001$ for both). No difference was observed between groups in CRP levels.

Table 5. Hemodynamic monitoring and laboratory parameters

Parameters	Hemoadsorption Group (52; 40,9%) Median (IQR)	Control Group (75; 59,1%) Median (IQR)	P value
MAP min first day	67 (61-71)	65 (61-71)	0.521
MAP min 2. day	70 (60-76)	67 (61-73)	0.413
MAP min 3. day	69 (64-74)	67 (60-75)	0.370
MAP max first day	92 (86-102)	94 (87-104)	0.576
MAP max 2. day	94 (87-104)	91 (82-104)	0.481
MAP max 3. day	99 (90-105)	94 (87-102)	0.077
Heart rate min first day, mean±SD	83±18	79±17	0.247
Heart rate min 2. day, mean±SD	73±24	79±18	0.101
Heart rate min 3. day, mean±SD	75±18	77±20	0.506
Heart rate max firstday, mean±SD	113±22	115±23	0.766
Heart rate max 2. day, mean±SD	111±23	116±23	0.245
Heart rate max 3. day, mean±SD	108±25	110±22	0.567
Hemoglobin first day	9,6 (8.3-11.2)	9.6 (8.5-10.7)	0.944
Hemoglobin 2. day	8.4 (7.9-9.9)	9.0 (8.0-10.2)	0.311
Hemoglobin 3. day	8.2 (7.8-9.6)	9.0 (8.2-10.1)	**0.023**
Platelet firstday	170 (85-246)	204 (115-293)	0.226
Platelet 2. day	92 (55-185)	182 (108-254)	**0.001**
Platelet 3. day	95 (54-144)	154 (102-231)	**<0.001**
Leukocyte first day	11.5 (7.9-17.3)	12.1 (8.4-18.0)	0.799
Leukocyte 2. day	13.1 (8.8-17.0)	11.2 (7.3-16.3)	0.207
Leukocyte 3. day	11.3 (8.1-16.4)	9.9 (6.9-14.6)	0.173
Lymphocyte first day	1.1 (0.7-1.7)	1.1 (0.7-1.9)	0.858
Lymphocyte 2. day	0.8 (0.6-1.2)	1.2 (0.6-1.7)	0.095
Lymphocyte 3. day	1.0 (0.6-1.3)	1.1 (0.5-1.5)	0.572
Bilirubin firstday	1.0 (0.7-1.3)	1.1 (0.6-1.5)	0.774
Bilirubin 2. day	1.1 (0.8-2.1)	1.0 (0.6-1.2)	0.103
Bilirubin 3. day	1.1 (0.8-1.8)	1.0 (0.6-1.6)	0.116
Creatinine first day	1.22 (0.69-2.04)	0.93 (0.64-1.79)	0.189
Creatinine 2. day	1.40 (0.68-2.18)	0.93 (0.60-1.71)	0.149
Creatinine 3. day	1.19 (0.61-3.48)	1.02 (0.57-1.63)	0.179
Input firstday	4091 (3065-5064)	3790 (2697-5171)	0.667
Input 2. day	3959 (3161-5327)	3707 (2850-4720)	0.268
Input 3. day	3742 (2930-4228)	3368 (2553-4297)	0.411
p value (Input within-group analysis)	0.074	0.014[b,c]	
Output firstday	1530 (1007-2626)	2090 (1265-2880)	0.169
Output 2. day	2070 (1080-3070)	2140 (1600-3070)	0.497
Output 3. day	2640 (2110-3640)	2491 (1692-3335)	0.292
p value (Output within-group analysis)	0.021[b]	0.015[a,b]	
Balance first day	2162 (516-3699)	1588 (486-3516)	0.479
Balance 2. day	1817 (525-3212)	1200 (360-2372)	0.110
Balance 3. day	730 (11-2075)	778 (-150-1813)	0.927
p value (Balance within-group analysis)	0.002[b,c]	0.006[a,b,c]	

MAP: mean arterial pressure; SD: standard deviation; IQR: inter quartile range.
[a]: 1. day versus 2.day (p<0.05), [b]: 1. day versus 3.day (p<0.05), [c]: 2. day versus 3.day (p<0.05)

Discussion

We conducted a matched control study to evaluate the effect of hemoadsorption in patients with septic shock requiring more than 0.2 mcg/kg/min of noradrenaline. We found that, despite a higher infection burden and a greater frequency of AKI in patients receiving HA, the intervention was associated with a lower 28-day mortality rate compared with patients receiving conventional therapy. The length of hospital stay was longer in the HA group, which may be explained by the lower mortality in this group compared with the control group. The intervention was associated with a lower SOFA score on day 3. There was no other difference in terms of physiological parameters except for a mild decrease in hemoglobin and a significant decrease in platelet count.

The lower mortality observed in the HA group is particularly noteworthy given the conflicting results in the literature (14). Although randomized controlled trials have reported no significant effect of hemoadsorption on mortality (13,14), observational studies in septic shock patients with a high inflammatory burden have described improvements in survival (10,11,17,18). This variability may be related to differences in patient selection, sepsis severity, and timing of treatment initiation. In our cohort, the observation that treated patients had a lower mortality rate despite a more severe baseline profile suggests that the timing of hemoadsorption may play a critical role in clinical outcomes. Specifically, initiating treatment at the refractory shock stage, defined as a norepinephrine dose >0.20-0.25 μg/kg/min may partly explain the mortality difference observed in our study.

VIS has been validated as an independent predictor of mortality in adult patients with septic shock; higher mean and peak VIS values in the first 48 hours are strongly associated with non-survival (19). With regard to hemodynamic response, the absence of a significant difference between groups in VIS, norepinephrine, and adrenaline doses over the first three days is an expected finding and aligns with previous reports indicating that hemoadsorption may not lead to a dramatic reduction in vasopressor requirements within the first 24–72 hours (8,13).

Hemoadsorption was associated with a decrease in SOFA scores by day 3. This is consistent with reports of improved organ function by reducing inflammatory load with hemoadsorption (3,9). In addition, the reduction in vasopressor requirement together with the decrease in inflammatory burden may have improved vascular tone and tissue perfusion, thereby supporting organ recovery. The significant decrease in lactate levels in the HA group, as an indicator of improved microcirculation and perfusion, further reinforces this interpretation.

A larger proportion of patients from the HA group had AKI on day 1 and ultimately required CRRT. However, this difference disappeared over the 3 days follow-up suggesting a beneficial effect of hemoadsorption on renal dysfunction. This finding is consistent with studies indicating that hemoadsorption may help preserve renal perfusion by removing endotoxins and proinflammatory cytokines (3,9). Lower ICU or 30-day mortality were also observed in cohorts of patients with septic shock and AKI requiring CRRT when hemoadsorption was administered. (20) Such improvements in organ function, including AKI and liver dysfunction, may translate into better long-term survival (13), although this remains to be demonstrated (21,22).

The higher procalcitonin levels in the HA group on days 2 and 3 is unexpected. It might potentially be explained by a different type of infection foci. Indeed, bloodstream infections were more frequent in the HA group, whereas pulmonary infections were more common in the control group.

Interpretation

Altogether, our findings indicate that hemoadsorption may be beneficial when applied to the appropriate patient population at an appropriate time point in the

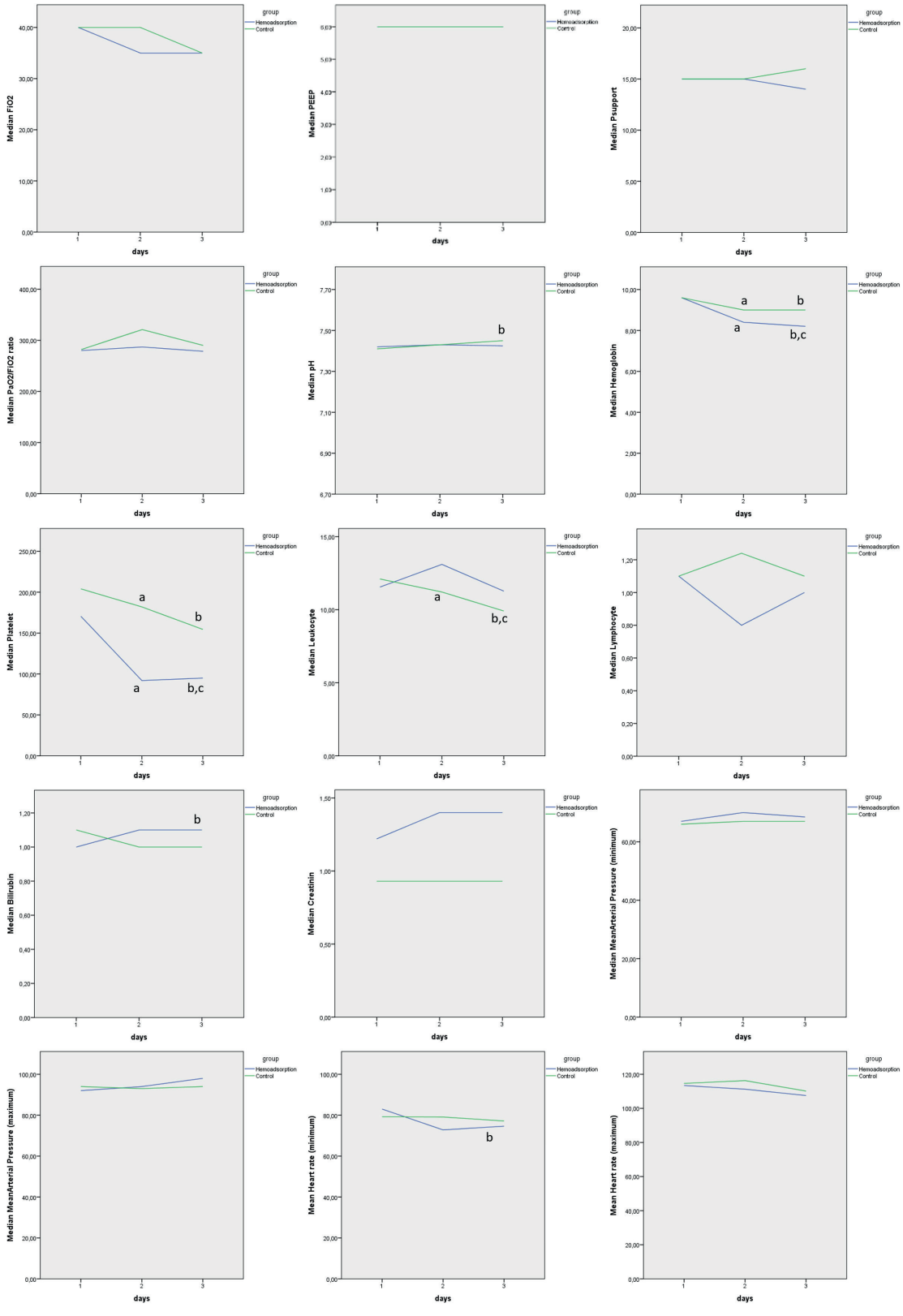

Figure 3. Mechanical ventilation, vital signs and laboratory parameters

[a]: 1. day versus 2.day (p<0.05), [b]: 1. day versus 3.day (p<0.05), [c]: 2. day versus 3.day (p<0.05)

disease course. The potential of hemoadsorption to improve survival appears particularly relevant in cases with a high infection load, refractory shock, and rapidly evolving organ dysfunction.

The observed longer length of hospital stay in the HA group, may be explained by the lower mortality in this group compared with the control group.

Strengths and limitations

One of the main strengths of this study is the evaluation of hemoadsorption therapy using a large, detailed dataset of critically ill patients with septic shock. A thorough analysis of hemodynamic, laboratory, and organ function parameters was performed. In addition, strict adherence to the Surviving Sepsis Campaign guidelines in both groups enabled a reliable evaluation of the incremental contribution of hemoadsorption within a standardized treatment framework. Importantly, the use of a protocol-based HA strategy in our unit strengthens the internal validity and interpretability of the findings.

However, the study also has limitations to be acknowledged. First, its retrospective design precludes definitive conclusions about causality and does not fully eliminate the risk of selection bias. However, we have performed careful matching to identify a control group with similar baseline characteristics. Second, the single-center setting may limit the generalizability of the findings, as patient characteristics and treatment protocols may reflect local practice patterns. Thirdly, residual confounding may be present, as suggested by the higher incidence of AKI on day 1 and higher procalcitonin levels in the HA group. However, this should bias our results against the intervention, overall strengthening our main result. Finally, the lack of long-term follow-up data, such as renal function, readmission rates, or health-related quality of life, limits our ability to evaluate the late effects of hemoadsorption therapy.

Conclusion

Early protocol based hemoadsorption was associated with an improved 28 days mortality, a decrease SOFA score in critically ill patients with septic shock. These results should be confirmed in prospective, randomized controlled trials.

Ethical approval

The study was approved by the Marmara University Medical Faculty Research and Ethics Committee (09.2024.811). Informed consent was not obtained due to retrospective nature of the study

Author contribution

Study conception and design: FG, MSS, BDO, AGS; data collection: FG, ET, EÇ, MSS, İİÇ; analysis and interpretation of results: FG, MSS, AGS; draft manuscript preparation: FG, MSS, AGS. The author(s) reviewed the results and approved the final version of the article.

Source of funding

The authors declare the study received no funding.

Conflict of interest

The authors declare that there is no conflict of interest.

References

1. Singer M, Deutschman CS, Seymour CW, et al. The third international consensus definitions for sepsis and septic shock (Sepsis-3). JAMA. 2016;315:801-10. [Crossref]
2. Gül F, Arslantaş MK, Cinel İ, Kumar A. Changing definitions of sepsis. Turk J Anaesthesiol Reanim. 2017;45:129-38. [Crossref]
3. Jarczak D, Kluge S, Nierhaus A. Sepsis-pathophysiology and therapeutic concepts. Front Med (Lausanne). 2021;8:628302. [Crossref]

4. Vincent JL, Marshall JC, Namendys-Silva SA, et al. Assessment of the worldwide burden of critical illness: the intensive care over nations (ICON) audit. Lancet Respir Med. 2014;2:380-6. [Crossref]

5. Vincent JL, Sakr Y, Sprung CL, et al. Sepsis in European intensive care units: results of the SOAP study. Crit Care Med. 2006;34:344-53. [Crossref]

6. GBD 2021 Global Sepsis Collaborators. Global, regional, and national sepsis incidence and mortality, 1990-2021: a systematic analysis. Lancet Glob Health. 2025;13:e2013-26. [Crossref]

7. Evans L, Rhodes A, Alhazzani W, et al. Surviving sepsis campaign: international guidelines for management of sepsis and septic shock 2021. Intensive Care Med. 2021;47:1181-247. [Crossref]

8. Bottari G, Ranieri VM, Ince C, et al. Use of extracorporeal blood purification therapies in sepsis: the current paradigm, available evidence, and future perspectives. Crit Care. 2024;28:432. [Crossref]

9. Malard B, Lambert C, Kellum JA. In vitro comparison of the adsorption of inflammatory mediators by blood purification devices. Intensive Care Med Exp. 2018;6:12. [Crossref]

10. Kogelmann K, Jarczak D, Scheller M, Drüner M. Hemoadsorption by CytoSorb in septic patients: a case series. Crit Care. 2017;21:74. [Crossref]

11. Schultz P, Schwier E, Eickmeyer C, Henzler D, Köhler T. High-dose CytoSorb hemoadsorption is associated with improved survival in patients with septic shock: A retrospective cohort study. J Crit Care. 2021;64:184-92. [Crossref]

12. Abdullayev R, Gul F, Bilgili B, Seven S, Cinel I. Cytokine adsorption in critically ill COVID-19 patients, a case-control study. J Intensive Care Med. 2022;37:1223-8. [Crossref]

13. Schädler D, Pausch C, Heise D, et al. The effect of a novel extracorporeal cytokine hemoadsorption device on IL-6 elimination in septic patients: a randomized controlled trial. PLoS One. 2017;12:e0187015. [Crossref]

14. Becker S, Lang H, Vollmer Barbosa C, Tian Z, Melk A, Schmidt BMW. Efficacy of CytoSorb®: a systematic review and meta-analysis. Crit Care. 2023;27:215. [Crossref]

15. Abbasi S, Naderi Z, Amra B, et al. Hemoperfusion in patients with severe COVID-19 respiratory failure, lifesaving or not? J Res Med Sci. 2021;26:34. [Crossref]

16. Premužić V, Babel J, Gardijan D, et al. Extracorporeal blood purification is associated with improvement in biochemical and clinical variables in the critically-ill COVID-19 patients. Ther Apher Dial. 2022;26:316-29. [Crossref]

17. Brouwer WP, Duran S, Kuijper M, Ince C. Hemoadsorption with CytoSorb shows a decreased observed versus expected 28-day all-cause mortality in ICU patients with septic shock: a propensity-score-weighted retrospective study. Crit Care. 2019;23:317. [Crossref]

18. Rugg C, Klose R, Hornung R, et al. Hemoadsorption with CytoSorb in septic shock reduces catecholamine requirements and in-hospital mortality: a single-center retrospective 'genetic' matched analysis. Biomedicines. 2020;8:539. [Crossref]

19. Kara İ, Sargın M, Bayraktar YŞ, Eyiol H, Duman İ, Çelik JB. The use of vasoactive-inotropic score in adult patients with septic shock in intensive care. J Crit Intensive Care. 2019;10:23-30. [Crossref]

20. Epstein D, Badarni K, Bar-Lavie Y. Impact of haemoadsorption therapy on short term mortality and vasopressor dependency in severe septic shock with acute kidney injury: a retrospective cohort study. Antibiotics (Basel). 2024;13:1233. [Crossref]

21. Hellman T, Uusalo P, Järvisalo MJ. Renal replacement techniques in septic shock. Int J Mol Sci. 2021;22:10238. [Crossref]

22. Şenol EA, Karakoç E, Göçerler Z, Aydın OÖ, Yelken B. The efficacy of continuous renal replacement therapy and hemoabsorption treatments in COVID-19 patients in the intensive care unit: a retrospective evaluation. Turk J Intensive Care 2023;21:181-9. [Crossref]

Turk J Intensive Care 2026;24(1):63-76
DOI: 10.63729/TJIC.2026.688

ORIGINAL RESEARCH

Renal resistive index and biomarkers of cell cycle arrest in the early diagnosis of sepsis-induced acute kidney injury in rats

Sinan Oğuzhan Ulukaya[1], Alper Yosunkaya[2], Eyüp Fatih Cihan[3], Funda Gök[2], Fahriye Kılınç[4], Süleyman Bakdık[5], Cemile Topçu[6]

[1]Division of Algology, Faculty of Medicine, Eskişehir Osmangazi University, Eskişehir, Türkiye
[2]Division of Critical Care Medicine, Department of Critical Care Medicine, School of Medicine, Necmettin Erbakan University, Konya, Türkiye
[3]Department of Anesthesiology and Reanimation, Bursa Yüksek İhtisas Training and Research Hospital, University of Health Sciences, Bursa, Türkiye
[4]Department of Pathology, School of Medicine, Necmettin Erbakan University, Konya, Türkiye
[5]Department of Radiology, School of Medicine, Necmettin Erbakan University, Konya, Türkiye
[6]Department of Biochemistry, School of Medicine, Necmettin Erbakan University, Konya, Türkiye

ABSTRACT

Objective: This study evaluates the diagnostic performance of renal resistive index (RRI) and urinary cell cycle arrest biomarkers for early detection of sepsis-induced acute kidney injury (AKI) in a rat model using cecal ligation and puncture (CLP).

Materials and Methods: Sixty female Wistar Albino rats were allocated into six groups (n=10): five CLP groups based on measurement timing (3, 6, 12, 24, and 48 hours post-procedure) and one sham group. Following CLP, RRI measurements were performed, and blood, urine, and tissue samples were collected before sacrifice. Urinary tissue inhibitor of metalloproteinase-2 (TIMP-2) and insulin-like growth factor binding protein-7 (IGFBP-7) were quantified via enzyme-linked immunosorbent assay (ELISA). Serum creatinine and lactate levels were measured, and histopathological kidney examination was conducted.

Results: RRI increased significantly at six hours (0.44±0.04), peaking at 24 hours (0.73±0.02) post-CLP. The [TIMP-2×IGFBP-7] combination elevated significantly at three hours ($P<0.05$) versus sham, reaching maximum levels at 48 hours. Strong positive correlations existed between histopathological injury severity and IGFBP-7 ($p=0.764$), TIMP-2 ($p=0.779$), [TIMP-2×IGFBP-7] ($p=0.785$), and RRI ($p=0.837$) (all $P<0.0001$). For predicting grade ≥3 tubular injury (>25% damage), cell cycle arrest biomarkers outperformed serum creatinine and lactate. RRI >0.45 demonstrated optimal diagnostic accuracy (sensitivity 89%, specificity 87%).

Conclusions: In this CLP-induced polymicrobial sepsis model, both RRI and urinary cell cycle arrest biomarkers predicted early AKI within similar timeframes, with RRI >0.45 showing superior predictive value.

Keywords: sepsis, acute kidney injury, cell cycle arrest biomarkers, renal resistive index, animal model

Introduction

Sepsis is life-threatening clinical syndrome characterized by organ dysfunction that is caused by the host's exaggerated immune response to an infection (1). Acute kidney injury (AKI), one of the most common organ dysfunctions caused by sepsis, occurs in approximately 40–50% of septic patients, resulting in a 6–8-fold increase in mortality (2).

Sepsis induced-AKI (SI-AKI) differs from other etiologies in terms of its pathophysiological basis (2,3,4). The changes in kidney function occurring in the early periods of SI-AKI can be regarded as clinical and biochemical reflections of adaptive responses that arise as a survival response (2). For this reason, renal damage in the early periods of SI-AKI is functional rather than structural (2). The early detection of such damage and taking the necessary precautions may

✉ Sinan Oğuzhan Ulukaya • sinanulukaya@outlook.com

Received: 24.12.2025 **Accepted:** 27.01.2026 **Published:** 26.03.2026

reverse this damage before structural alterations can occur. Increased serum creatinine, which is in common use today in the diagnosis and classification of AKI, is affected by various extrarenal factors such as body weight, race, gender, body fluid volume, several medications, muscle metabolism and protein intake, and serves as a weak biomarker, sometimes causing a delay of 48–72 hours in the identification of an impairment in kidney function (5). Various biomarkers released from the kidney into the blood and urine after a kidney injury may define AKI in an early period before an increase in serum creatinine is observed. Although more than 20 biomarkers have been described to date for the early diagnosis of AKI, none can be defined as the optimum approach (6,7).

The tissue inhibitor of metalloproteinase-2 (TIMP-2) and the insulin-like growth factor binding protein-7 (IGFBP-7) are promising stress biomarkers in the early detection of AKI that have been introduced in recent years, and may appear 24–48 hours earlier than an increase in serum creatinine, with values that can be measured in the urine (8). Previous studies involving intensive care unit patients have reported that a combined analysis of [TIMP-2]-[IGFBP-7] is superior in performance than serum creatinine, urinary and plasma neutrophil gelatinase-associated lipocalin (NGAL), cystatin-C and kidney injury molecule-1 (KIM-1) (6,8,9). Recent studies have validated the measurement of urinary cell-cycle arrest biomarkers (CCAB), particularly for the early diagnosis of postoperative AKI, and there are ongoing studies aimed at making definitive recommendations regarding the use of these molecules in SI-AKI.

The use of Doppler ultrasound (USG) as a screening tool in intensive care units has rapidly become a widespread practice. The lack of additional costs at each use, being non-invasive, the absence of ionizing radiation exposure, and being a dynamic and reproducible method are important factors underlying the increasingly widespread use of ultrasound in intensive care units. Color Doppler USG can non-invasively visualize the effects of vasoconstriction, hypoxia, stress response and hemodynamic changes on the kidney (10,11). Changes in the blood flow in the intrarenal arch and interlobar arteries can be evaluated, while the renal resistive index (RRI) – a sonographic index reflecting the resistance to flow – can be measured by renal Doppler USG. RRI identifies resistance in the kidney vessel, in other words, renal vasoconstriction, which is an important physiopathological change that occurs in the early periods of AKI in patients with sepsis (12). RRI would seem to be a promising parameter in predicting the development and reversal of AKI in critically ill patients, although there have been few studies to date assessing the performance of RRI in predicting SI-AKI (13,14).

The present study compares the performances of RRI and urinary CCAB in the early detection of AKI resulting from sepsis in a rat model of polymicrobial sepsis induced by the cecal ligation and puncture (CLP) method.

Materials and Method

Experimental study

The animals in this study were kept in accordance with the Guide for the Care and Use of Laboratory Animals of the National Institute of Health. The protocol for the model was reviewed and approved by the Necmettin Erbakan University KONÜDAM Experimental Medicine Application and Research Center Directorate Local Ethics Committee on Animal Experiments. Ethics committee meeting dated 18.05.2018 and protocol numbered 2018-18.

Acquired for the study were 60 female Wistar Albino rates aged five months or above, weighing 300–375 gr. The rats were placed in cages in an environment at 22±1°C and 45–55% humidity, with free access to food and water, and were kept on 12 hours dark and 12 hours light cycle. The rats were divided into five groups of 10 rats based on the time between the CLP procedure and the time of measurement (3, 6, 12, 24, and 48 hours), and an additional sham

group. All interventional and imaging procedures were performed under Isoflurane while preserving spontaneous respiration, as described earlier (15,16). The CLP method was used to create the sepsis model. For fluid resuscitation, an intravenous cannula was inserted for the administration of fluids at a rate of 10 ml/kg in the first hour, followed by a rate of 5 ml/kg/hr throughout the experiment. No antibiotherapy was administered to avoid interference in the results due to drug-induced kidney injury. A balanced fluid was used for resuscitation.

CLP Sepsis Model: All rats were placed in the supine position on a heated operating table, with the body temperature measured by a rectal probe. The abdomen was shaved while paying attention to avoid skin damage. The area was wiped with a povidone iodine solution twice using an aseptic technique. The abdomen was opened with a 2-cm midline incision, and the cecum was located and explored. The antimesenteric surface of the cecum (comprising 25%) was ligated distal to the ileocecal valve using 3/0 silk sutures and punctured twice with an 18G needle. The cecum was released into the peritoneal cavity after observing fecal discharge, and the abdomen was closed with 3/0 silk sutures in layers using a simple suturing technique.

RRI was measured and blood, urine and tissue samples were collected 3 hours after the CLP procedure in Group 1, at 6 hours in Group 2, at 12 hours in Group 3, at 24 hours in Group 4, and at 48 hours Group 5, and the rats were sacrificed. An intravenous cannula was inserted, and fluid resuscitation was performed in the rats in the sham-operated group, while spontaneous respiration was maintained under isoflurane anesthesia, while no CLP procedure was performed. RRI was measured by Doppler ultrasound at the beginning and end of the procedure. A midline laparotomy incision was made to collect blood, urine and tissue samples, with a 22-Gauge needle used to aspirate urine from the bladder. The left kidneys of the rats in all groups were recovered and placed in pathology specimen containers filled with 4% formaldehyde for histopathological examination. Finally, the procedure was ended after collecting intracardiac blood samples. The rats were sacrificed by cervical dislocation.

The urine samples collected from the bladder were stored at -80°C for the measurement of TIMP-2 and IGFBP-7 using the (ELISA) enzyme-linked immunosorbent assay method. The blood samples were transferred to blood collection tubes for the measurement of serum creatinine, blood gases and lactate levels, and the samples were analyzed immediately.

Ultrasonographic examination

A linear transducer (12 MHz, GE, Logiq e, USA) was used for the sonographic examination, with the "vascular imaging" option preselected. While the experimental animal was in the supine position, the probe was inserted in the transverse plane through the midline to acquire images of the aorta. The platform was then shifted together with the animal to reach the level of the renal artery. The color Doppler mode was used to acquire images of the renal artery and renal vein. The (PW) pulsed-wave mode was used to evaluate blood flow in the renal artery. The indicator line in the PW mode was brought to the renal artery in the flow direction. Typically, three to five arterial signals were acquired from the renal artery. The appearance of the waveform was optimized using the lowest pulse repetition frequency and the highest possible gain. The images of the waveforms indicating the velocity of the flow in the artery at peak systole and diastole were acquired, and RRI was calculated using the following formula:

$$RRI = (PeakSystolicVelocity - EndDiastolicVelocity) / PeakSystolicVelocity$$

All sonographic examinations were performed by the same investigator, who had previous experience in the procedure.

Examination of urine serum and tissue samples

Serum lactate levels were measured as part of the blood gases analysis using an ABL800 FLEX© (Radiometer Medical ApS, 2700 Brønshøj, Denmark) analyzer. Urinary IGFBP-7 and TIMP-2 levels were measured using ELISA technique (SinoGeneClon Biotech Co., Ltd. HangZhou, China). The combination of the two molecules [IGFBP-7*TIMP-2] was evaluated using the following formula, which is reported to be more valuable than individual measurements of IGFBP-7 and TIMP-2 in predicting acute kidney injury(9,17,18):

$$[\mathrm{IGFBP}-7*\mathrm{TIMP}-2]=[(\mathrm{IGFBP}-7\times\mathrm{TIMP}-2)\div 1000]$$

The rat kidneys fixed in 10% neutral buffered formalin solution for histopathological examination were subjected to standard tissue-processing steps in an automated device and embedded in paraffin blocks. Four μm-thick sections, on average, were cut from each block using a microtome and mounted on three slides, one of which was stained with Hematoxylin and Eosin (H&E), one with Periodic acid Schiff (PAS) for morphological assessment and one using the terminal deoxynucleotidyl transferase-mediated dUTP nick-end labeling technique (TUNEL), using ApopTag® Peroxidase In Situ Apoptosis Detection Kit for the assessment of apoptosis. The tissue sections prepared for examination were assessed by an experienced pathologist under a light microscope attached to a camera (Olympus BX53F; Tokyo, JAPAN) in a blind manner. Tubular necrosis and dilatation, vacuolar degeneration, the loss of the brush border and the cast development, as well as the ratio of findings in the percentage of tubules, were assessed to determine the tubular damage score. Using the Tubular Damage Scoring system, the damage grade is expressed at five levels: no damage=0, 1–10% = 1, 11–25% = 2, 26–50% = 3, 51–75% = 4, >75% = 5 (19,20). For the assessment of apoptosis, the number of TUNEL-positive nuclei in a total of 10 HPF was detected on the slides prepared using the TUNEL method.

Statistical analysis

The data was assessed using SPSS Statistics (Version 19.0. Armonk, NY:IBM Corp.), and tested for normality of distribution, with the results. Expressed as mean ± standard deviation (SD). A Kruskal Wallis test was used for multiple comparisons; a Mann-Whitney U test with Bonferroni correction was used for paired group comparisons; and the relationships between variables were analyzed using Pearson's correlation coefficient. The cut-off point for the area under the curve in a ROC curve analysis was considered as 0.5. The level of significance was set to $p< 0.05$ in all statistical tests.

Results

RRI was evaluated using a renal Doppler USG, 3, 6, 12, 24 and 48 hours after the CLP procedure. RRI started increasing 3 hours (0.38 ± 0.07) after the CLP procedure when compared to the sham group (0.36 ± 0.03), while the increase in RRI started to become significant at 6 hours (0.44 ± 0.04) and peaked at 24 hours (0.73 ± 0.02) after the CLP procedure. Although the increase in RRI tended to decrease at 48 (0.66 ± 0.15) when compared with the mean value at 24 hours (0.73 ± 0.02) after the CLP procedure, the difference was not statistically significant ($p>0.05$) (Figure 1). The RRI measurements in the sham group and at different time points after the CLP procedure are presented in Figure 2.

IGFBP-7 significantly increased at 3 hours (Group1) after the CLP procedure when compared to the sham group ($P<0.05$), and TIMP-2 significantly increased at 6 hours (Group 2) after the CLP procedure when compared to the sham group ($P<0.05$). A further comparison of the rats in the sham group revealed that both IGFBP-7 and TIMP-2 molecules were significantly increased in the other groups ($P<0.05$), with the highest levels of the two molecules observed 48 hours after the CLP procedure (Table 1). The combined analysis of the two molecules *[(IGFBP-*

7×TIMP-2)÷1000] showed a significant increase at 3 hours after the CLP procedure when compared to the sham group (P<0.05); and while the values in the test groups remained significantly higher than in the sham group (P<0.05), the highest values were observed at 48 hours after the CLP procedure (Table 1). A statistical analysis of serum creatinine and lactate levels is presented in Table 1.

The tissue samples were subjected to a histopathological examination and examined for the presence of tubular necrosis, loss of brush-border, cast formation, vacuolization, and tubular dilatation, in an evaluation of tubular damage. The loss of brush-border, tubular dilatation and vacuolization were the prominent findings in a histopathological examination following the CLP procedure (Figure 3-6). The Tubular Damage Score was used to grade the pathological damage (Table 2) and was significantly higher in Group 1 (at 3 hours after the CLP procedure) than in the sham group, with the highest damage score observed in Group 5 (Table 3). The percentage of apoptosis was similar across the groups when compared to the sham group (P>0.05), and there was no significant difference between the groups (P<0.05) (Table 3 and Figure 7).

In an analysis of the correlation between the degree of histopathological damage in the kidneys occurring after the CLP procedure and the levels of urinary

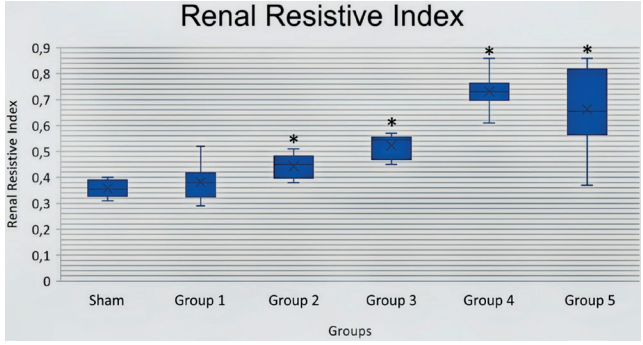

Figure 1. Changes in Renal Resistive Index (RRI) across the groups

Sham: CLP procedure not performed; Group 1: Measurement 3 hours after the CLP procedure; Group 2: Measurement 6 hours after the CLP procedure; Group 3: Measurement 12 hours after the CLP procedure; Group 4: Measurement 24 hours after the CLP procedure; Group 5: Measurement 48 hours after the CLP procedure; CLP, cecal ligation and puncture. *P<0.05, compared to the sham.

CCAB, a strong positive correlation was found between the degree of histopathological injury and IGFBP-7 (Spearman's p=0.764, P<0.0001), TIMP-2 (Spearman's p=0.779, P<0.0001) and [IGFBP-7*TIMP-2] (Spearman's p=0.785, P<0.0001). Furthermore, there was a moderate positive correlation between serum creatinine levels and the degree of histopathological damage (Spearman's p=0.412, P<0.01). The strongest correlation was noted between the RRI measurements and the degree of histopathological damage at different time points after the CLP procedure (Spearman's p=0.837, P<0.0001).

Table 1. Creatinine, lactate, IGFBP-7, TIMP-2, and [IGFBP-7*TIMP-2] values of the groups (Mean ± SD)

Groups	Creatinine (mg/dl)	Lactate (mmol/lt)	IGFBP-7 (ng/ml)	TIMP-2 (ng/ml)	IGFBP-7*TIMP-2 (ng/ml)^2
Sham	0.36 ± 0.02	1.84 ± 0.33	49.20 ± 6.50	5.80 ± 0.97	0.28 ± 0.03
Group 1	0.48 ± 0.06*	2.41 ± 0.51	98.62 ± 35.38*	8.77 ± 2.93	0.93 ± 0.55*
Group 2	0.40 ± 0.07	2.55 ± 0.61	215.03 ± 91.26*†	32.87 ± 20.27*†	7.65 ± 5.18*†
Group 3	0.52 ± 0.10$^{*\#}$	5.17 ± 0.86$^{*\dagger\#}$	219.61 ± 99.66*†	23.13 ± 10.44*†	5.33 ± 3.56*†
Group 4	0.55 ± 0.10$^{*\#}$	5.97 ± 1.18$^{*\dagger\#}$	160.12 ± 48.91*†	24.33 ± 9.38*†	4.08 ± 2.53*†
Group 5	0.48 ± 0.10$^{*\#}$	7.82 ± 1.95$^{*\dagger\#\pi}$	360.01 ± 180.03*†	53.29 ± 29.56*†	23.33 ±19.96*†

Sham: CLP procedure not performed; Group 1: Measurement 3 hours after the CLP procedure; Group 2: Measurement 6 hours after the CLP procedure; Group 3: Measurement 12 hours after the CLP procedure; Group 4: Measurement 24 hours after the CLP procedure; Group 5: Measurement 48 hours after the CLP procedure; CLP, Cecal ligation and puncture; IGFBP-7, Insulin-Like Growth Factor Binding Protein-7; TIMP-2, Tissue Inhibitor of Metalloproteinase-2.
*P<0.05, compared with the sham; †P<0.05, compared with group 1; $^{\#}$P<0.05, compared with group 2; $^{\pi}$P<0.05, compared with group 3. CLP, cecal ligation and puncture.

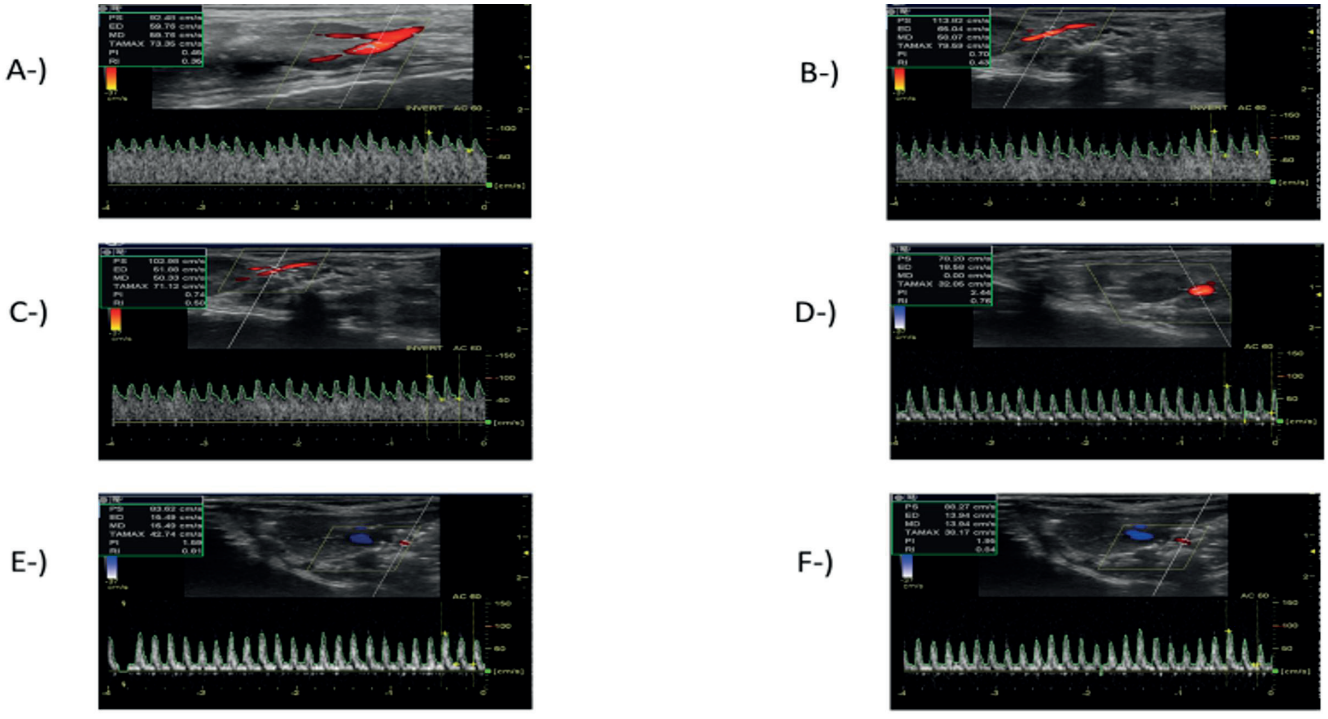

Figure 2. A sample ultrasonographic measurement of RRI in the groups

Renal Resistive Index (RRI) reflects the relationship between the systolic peak velocity in renal blood vessels and the decrease in the loss of end-diastolic flow velocity [RRI= (PSV-EDV) / PSV]. In the present study, RRI increased with increasing tubular damage in the model of sepsis-induced acute kidney injury. A-) Measurement in the sham group; B-) Measurement 3 hours after the CLP procedure (Group 1); C-) Measurement 6 hours after the CLP procedure (Group 2); D-) Measurement 12 hours after the CLP procedure (Group 3); E-) Measurement 24 hours after the CLP procedure (Group 4); F-) Measurement 48 hours after the CLP procedure (Group 5). CLP, cecal ligation and puncture.

There was also a significant correlation between blood lactate levels and histopathological findings in this rat model of sepsis (Spearman's p=0.816, P<0.0001). The correlations between the degree of histopathological damage and CCAB, serum creatinine, lactate and RRI are shown in Figure 8.

An analysis of the correlation between RRI and CCAB also showed a strong positive correlation between RRI and IGFBP-7 (Spearman's p=0.686, P<0.0001), TIMP-2 (Spearman's p=0.732, P<0.0001) and [IGFBP-7*TIMP-2'] (Spearman's p=0.718, P<0.0001) (Figure 9).

RRI, CCAB and serum creatinine were further evaluated in a ROC curve analysis to identify their ability to predict a histopathological tubular damage score of 3 or greater (more than 25% injury) (Figure 10).

Table 2. Tubular damage score (19,20)

Percentage of Damage (%)	Damage Score Grade
0%	0 (No damage)
1-10%	Grade 1
11-25%	Grade 2
26-50%	Grade 3
51-75%	Grade 4
≥ 76%	Grade 5

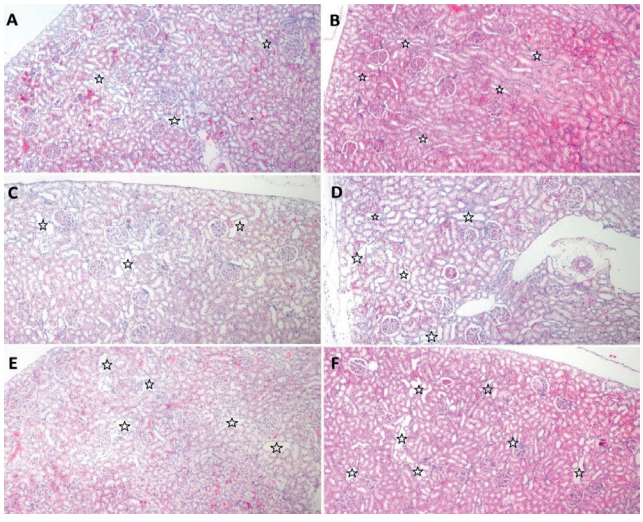

Figure 3. Tubular dilatation and depression in the epithelium of the dilated tubules

Tubular dilatation and depression in the epithelium of the dilated tubules (marked with an asterisk) is observed in a few tubules in the sham group, while the number of involved tubules gradually increases from Group 1 through to Group 5. A: sham group, B: Group 1, 3 hours after the CLP procedure, C: Group 2, 6 hours after the CLP procedure, D: Group 3, 12 hours after the CLP procedure, E: Group 4, 24 hours after the CLP procedure, F: Group 5, 48 hours after the CLP procedure (Hematoxylin and Eosin, A, B, C, D, E, F, 40x).

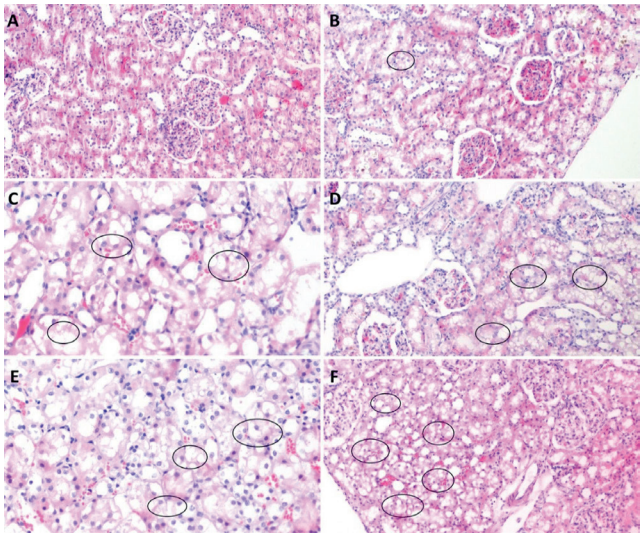

Figure 4. Vacuolization in the tubule epithelium

Vacuolization in the tubule epithelium (round shape) was observed at low rates in the sham group and Group 1, while the number of involved tubules increased from Group 2 and Group 5. A: sham group, B: Group 1, 3 hours after the CLP procedure, C: Group 2, 6 hours after the CLP procedure, D: Group 3, 12 hours after the CLP procedure, E: Group 4, 24 hours after the CLP procedure, F: Group 5, 48 hours after the CLP procedure, (Hematoxylin and Eosin, A, B, C, D, E, F, 200x).

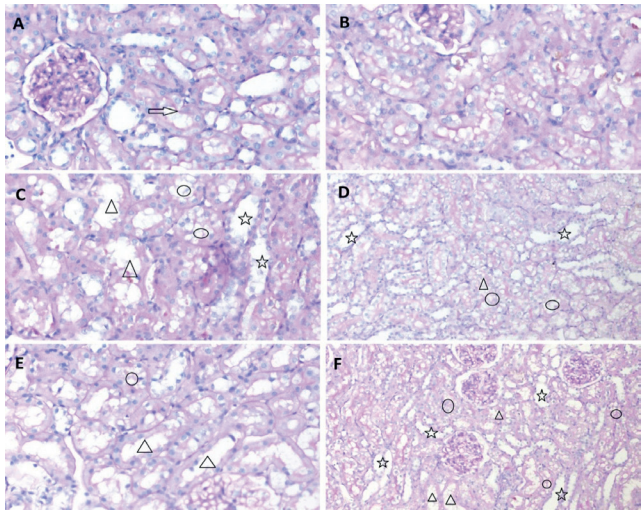

Figure 5. The loss of brush-border, vacuolar changes and dilated tubules are observed across the groups

The brush-border of the tubules in A (arrow) is regular, while the brush-border, in general, is preserved in B and vacuolization is rare. The loss of brush-border (triangles), vacuolar changes (round) and dilated tubules (asterisk) are observed in C,D,E and F A: sham group, B: Group 1, 3 hours after the CLP procedure, C: Group 2, 6 hours after the CLP procedure, D: Group 3, 12 hours after the CLP procedure, E: Group 4, 24 hours after the CLP procedure, F: Group 5, 48 hours after the CLP procedure (PAS; A, B, C, E, 200x; D, F, 100x).

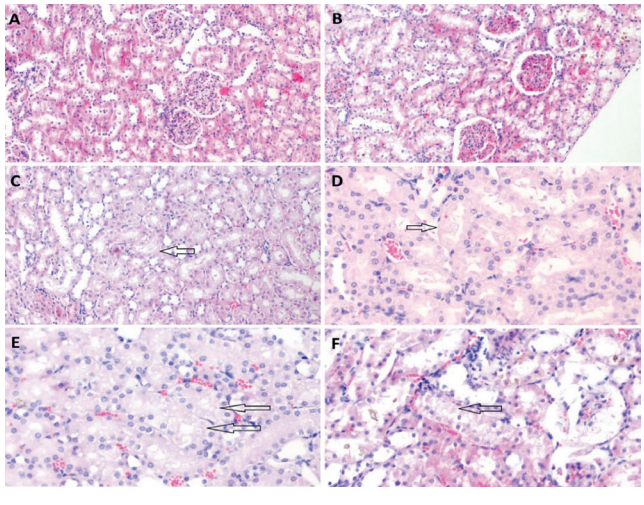

Figure 6. Cellular necrosis is shown in the tubules of the groups

Cellular necrosis (arrow) is observed in the tubules in the sham group and Group 1, while cellular necrosis is rare in the other groups. A: sham group, B: Group 1, 3 hours after the CLP procedure, C: Group 2, 6 hours after the CLP procedure, D: Group 3, 12 hours after the CLP procedure, E: Group 4, 24 hours after the CLP procedure, F: Group 5, 48 hours after the CLP procedure, (Hematoxylin and Eosin, A, B, C, 100x; D, E, F, 200x).

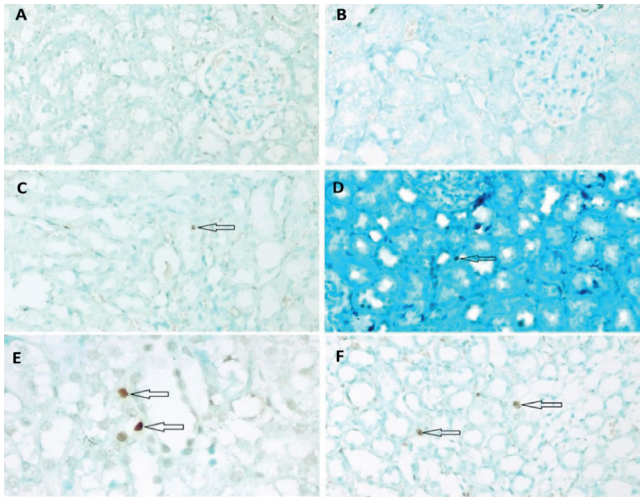

Figure 7. TUNEL-stained sections of the groups

In TUNEL-stained sections, no apoptotic cells are observed in the sham group (A) and Group 1 (B), while 1 or 2 apoptotic tubular epithelial cells (arrow) are observed in the other groups. A: sham group, B: Group 1, 3 hours after the CLP procedure, C: Group 2, 6 hours after the CLP procedure, D: Group 3, 12 hours after the CLP procedure, E: Group 4, 24 hours after the CLP procedure, F: Group 5, 48 hours after the CLP procedure (TUNEL; A, B, C, D, F, 200x; E, 400x).

In the present study, an IGFBP-7 value greater than 131.3 ng/ml (84% sensitivity, 83% specificity), a TIMP-2 value greater than 12.87 ng/ml (86% sensitivity, 84% specificity) and a [IGFBP-7*TIMP-2] greater than 1.91 $(ng/ml)^2$ (87% sensitivity, 86% specificity) predicted renal injury. An RRI greater than 0.45 predicted renal injury with a sensitivity of 89% and a specificity of 87%.

Discussion

In this rat model of sepsis, RRI was measured at 3, 6, 12, 24 and 48 hours after the CLP procedure to identify any impairment in renal circulation in the early period, which is considered an early sign of SI-AKI (11,14). Increases in RRI values were noted starting at 3 hours after the CLP procedure, and this increased to reach statistical significance at 6 hours. As reported by Song et al. in a study of human subjects evaluating the ability of RRI to detect SI-AKI in the early period, the pulsed-wave Doppler spectrum of the AKI group showed a narrow and steep waveform character that resulted in a high RRI value, similar wave forms were noted in the present study, becoming narrow and spiky, and with an increase in RRI that paralleled the degree of kidney injury(21). The present study also identified a strong positive correlation between RRI values and the degree of tubular damage in a histopathological examination. The authors believe the change in RRI to be a result of the greater decrease in diastolic blood flow than in the systolic blood flow, which we attributed to the increase in renal vascular resistance caused by sepsis induced-inflammation and the impairment of microvascular functions.

Table 3. Tubular Damage Score and the number of TUNEL-positive nuclei (apoptosis) in the groups (Mean ± SD)

Groups	Tubular Damage Score	Apoptosis (n)
Sham	0	1.40 ± 0.97
Group 1	1.50 ± 0.71*	1.00 ± 0.67
Group 2	2.06 ± 1.03*	1.10 ± 0.74
Group 3	4 ± 0.81*†	1.20 ± 0.63
Group 4	4.40 ± 0.52*†#	2.10 ± 1.10
Group 5	4.90 ± 0.32*†#π	1.60 ± 1.17

Sham: CLP procedure not performed; Group 1: Measurement 3 hours after the CLP procedure; Group 2: Measurement 6 hours after the CLP procedure; Group 3: Measurement 12 hours after the CLP procedure; Group 4: Measurement 24 hours after the CLP procedure; Group 5: Measurement 48 hours after the CLP procedure; CLP, Cecal Ligation and Puncture; Apoptosis, number of TUNEL-positive nuclei. TUNEL, terminal deoxynucleotidyl transferase-mediated *P<0.05, compared with the sham; †P<0.05, compared with group 1; #P<0.05, compared with group 2; πP<0.05, compared with group 3. CLP, cecal ligation and puncture.

A Color Doppler USG can non-invasively visualize the effects of hemodynamic changes on the kidneys, such as vasoconstriction, hypoxia, stress response and shock (10,11). The monitorization of circulation using only the routinely-used method takes into account only macrocirculation, while RRI measured by Doppler USG reflects the resistance to flow rather than circulation (14). A decrease in renal diastolic pressure resulting from an increase in renal vascular resistance surpasses the decrease in systolic pressure. In the event of an extreme increase in renal vascular resistance, diastolic flow may not be detected, and even retrograde flow can be observed (12). RRI can be calculated by color Doppler USG for the identification of such alterations in renal vascular resistance.

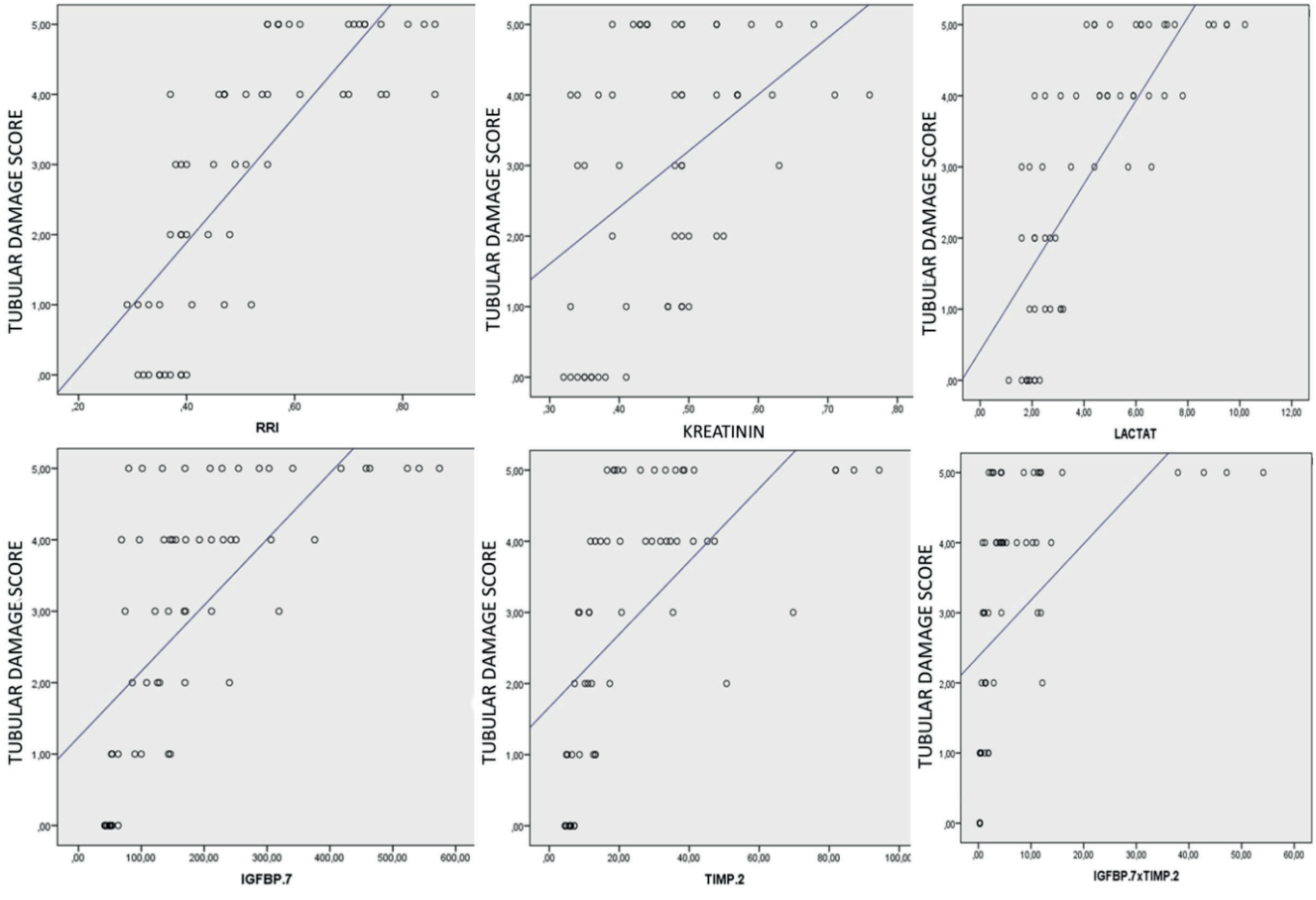

Figure 8. Correlations between the degree of histopathological damage and the biomarkers of cell cycle arrest, serum creatinine, lactate and RRI

RRI, Renal Resistive Index; IGFBP-7, Insulin Like Growth Factor Binding Protein-7; TIMP-2, Tissue Inhibitor of Metalloproteinase-2; IGFBP-7*TIMP-2, [IGFBP-7*TIMP-2/1000].

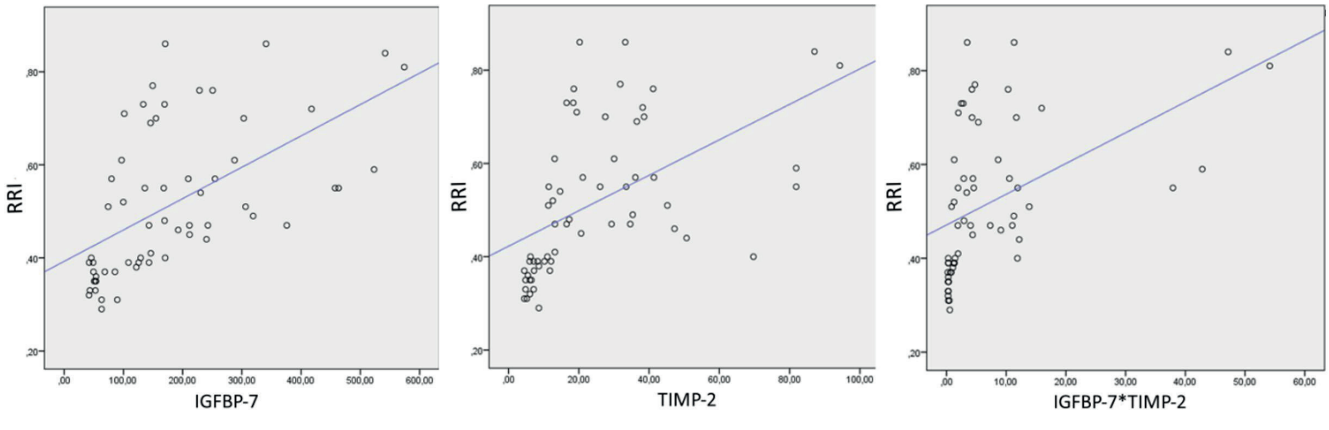

Figure 9. The correlation between RRI and IGFBP-7, TIMP-2 and [IGFBP-7*TIMP-2]

RRI, Renal Resistive Index; IGFBP-7, Insulin Like Growth Factor Binding Protein-7; TIMP-2, Tissue Inhibitor of Metalloproteinase-2; IGFBP-7*TIMP-2, [IGFBP-7*TIMP-2/1000].

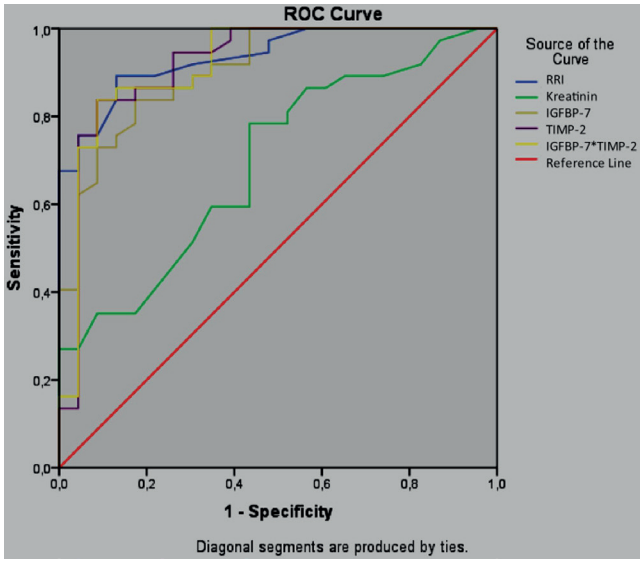

Figure 10. ROC Curve Analysis of RRI, serum creatinine, IGFBP-7, TIMP-2 and [IGFBP-7*TIMP-2]

The relationship between the alterations in kidney function and RRI, and the pulsatility index (PI) measured by color Doppler USG was investigated in a cisplatin-induced renal toxicity model, and reported small animal sonography to be a non-invasive, sensitive and reproducible method requiring a minimum number of laboratory animals, and to be an effective tool in the calculation of RRI in the early detection of drug-induced nephrotoxicity in rat models (22). A study involving rabbits reported a significant increase in RRI 6 hours after the development of AKI, and a cut-off point of 0.7 significantly predicted AKI in an earlier period than serum creatinine. A ROC curve analysis was performed in the present study to test whether RRI can effectively identify kidney injury in the early period in cases with a tubular damage score of 25% or greater. RRI greater than 0.45 predicted kidney damage of 25% of greater, with a sensitivity of 89% and a specificity of 87%. Studies conducted on intensive care unit patients using RRI to predict AKI have failed to identify whether an increase in RRI indicates a risk or true damage in the kidneys due to the inability to perform a histopathological examination, although these studies report RRI to perform better than urine output and serum creatinine measurement in predicting AKI in critically ill patients, regardless of the etiology (23-25). The study by Darmon et al. reported that an RRI greater than 0.795 predicted AKI with a sensitivity of 92% and a specificity of 85% (24).

Our findings regarding the predictive value of RRI for sepsis-associated acute kidney injury demonstrate notable concordance with the clinical study by Huang et al. In the clinical cohort study by Huang and colleagues, RRI exhibited a sensitivity of 93% with a specificity of 35.3% (AUC=0.667, p=0.004) for predicting SI-AKI in human patients (26). In contrast, our experimental sepsis model demonstrated that an RRI threshold greater than 0.45 predicted renal injury with a sensitivity of 89% and specificity of 87%, alongside the strongest correlation with histopathological damage (Spearman's p=0.837, p<0.0001).

In the presence of ischemia or sepsis, renal tubular cells undergo G1 cell cycle arrest, and a G1-phase arrest of the cell cycle prevents cell division until the DNA damage is repaired (27). Cell cycle arrest occurs in the early period immediately after damage. There is a growing body of evidence suggesting that IGFBP-7 and TIMP-2 are closely related to the regulation of the cell cycle by mitochondria, and that cell cycle arrest may be an important cellular defense strategy in the case of sepsis (3,28). Furthermore, both molecules act as "alarm" proteins through their autocrine and paracrine effects on the cells, with the alarm signal being released from the damaged area (29-31). In the case of SI-AKI, where early interventions are of great importance, the detection of this signal may provide as much to the early timing of management strategies as to changes in the outcomes (32-34). In the present study, IGFBP-7 showed a significant increase from 3 hours after the CLP procedure, whereas TIMP-2 increased significantly at 6 hours. Both IGFBP-7 and TIMP-2 were higher at all measurement points when compared to the values in the sham group, with the highest values for the two molecules detected 48 hours after the CLP procedure. A correlation analysis revealed a strong positive correlation between the

degree of tubular damage and CCAB, although a combined analysis of the two molecules ([IGFBP-7] x[TIMP-2]) even showed an even stronger correlation than with individual measurement of the molecules.

In a ROC curve analysis to evaluate the performance of these molecules in predicting kidney injury, a [IGFBP-7]x[TIMP-2] value greater than 1.91 $(ng/ml)^2$ significantly predicted AKI with a sensitivity of 87% and a specificity of 86%. This cut-off point, which is closer to the cut-off point of 2.0 $(ng/ml)^2$ reported in other studies, can detect pathological damage with a sensitivity of 87%. The present study did not analyze the changes in cell cycle arrest molecules during the recovery period, which can be noted as a limitation of the present study (8,9,35,36).

Similar to the findings of the present study, a study of a rat model of SI-AKI using the CLP method reported that IGFBP-7 increased significantly earlier than TIMP-2 (12 hours) and suggested that the combined analysis of the two molecules offers higher sensitivity than serum creatinine in the diagnosis of AKI (37). The same study also reported peak serum urea and creatinine concentrations to be observed at 3 hours, and that high hematocrit levels at this time point caused an increase in serum creatinine due to hemoconcentration. After the initiation of fluid resuscitation at 2 hours, the authors reported a progressive decrease to normal in the serum urea and creatinine concentrations between 6 and 12 hours. The same study reported that a significant increase was noted in serum urea and creatinine concentrations after 24 hours, with the highest serum creatinine being 1.5 times higher (30μmol/L) than the baseline. Similar to the findings in the study by Arulkumaran et al. the authors of the present study consider the decrease in serum creatinine at 6 hours to be attributable to fluid resuscitation in this sepsis model (37). In a correlation analysis, the weakest correlation was observed between tubular damage and serum creatinine. As mentioned earlier in several studies, the present study confirms the findings that CCAB increase at an earlier time point and are more specific biomarkers than serum creatinine (31,37).

Our review of literature revealed no studies evaluating the combined used of RRI and CCAB in the early diagnosis of SI-AKI. Furthermore, there were only two studies, conducted by the same investigators, evaluating the combined used of RRI and CCAB in patients undergoing open heart surgery. The investigators in these studies attempted to determine the predictive value of these new biomarkers in a specific population undergoing open heart surgery and (TAVI) transcatheter aortic valve implantation, who are considered to be at high risk of developing AKI following the procedure (38,39). The investigators reported that both RRI and urinary [TIMP-2]*[IGFBP-7] failed to predict the development of AKI within 24 hours of surgery in the two groups of patients. In a study involving patients undergoing open heart surgery, Zaouter et al. reported that the combined use of RRI and [IGFBP-7]x[TIMP-2] was incapable of recognizing patients within clinically acceptable limits who may develop AKI within 24 hours of surgery, although they reported a slightly increased negative predictive value (38).

Zaitoun et al. demonstrated that RRI ($T1 \geq 0.72$, AUROC=0.905) effectively diagnosed AKI but poorly predicted persistence, with Cystatin C emerging as the superior prognostic marker (AUROC=0.977) (40). In our experimental model, the predictive performance of RRI combined with CCAB for SI-AKI and their correlation with histopathological renal damage were investigated, revealing complementary insights. Notably, RRI demonstrated the strongest correlation with histopathological kidney damage (Spearman's $p=0.837$, $p<0.0001$) in our study, surpassing even the CCAB, $p=0.785$). This suggests that RRI, when measured serially with appropriate timing, captures the hemodynamic and structural renal injury continuum more comprehensively than single-timepoint measurements.

In the analysis of correlation between RRI and CCAB in the present study, both methods showed a strong correlation in the detection of tubular damage. However, an RRI greater than 0.45 showed the highest predictive value in the early detection of AKI, with a sensitivity of 89% and a specificity of 87%. It is stated that the measurement RRI by Doppler USG is easily applicable, but has a steep learning curve (41), and studies have reported RRI measurements to have the potential to be affected by factors such as increased intraabdominal pressure, right ventricular dysfunction, renal venous pressure, renal congestion, tricuspid valve disease and certain mediations in critically ill intensive care unit patients with sepsis (21,42). For this reason, there is a need for large-scale clinical studies to support the current findings related to the early detection of AKI in patients with sepsis.

Tubular dilatation and vacuolization, and the loss of the brush-border, to a lesser extent, were the most prominent alterations associated with AKI in the histopathological examination carried out within our polymicrobial sepsis model, created using the CLP method. In contrast, no apoptosis or necrosis, which are commonly reported as the most striking histopathological findings of SI-AKI in literature, were identified. In the present study, an analysis of the urinary CCAB revealed TIMP-2 to increase earlier, and to predict AKI with a higher sensitivity and specificity than IGFBP-7 (37,43). However, a cut-off value of 1.91 $(ng/ml)^2$ for the combined use of the two molecules showed the highest sensitivity and specificity in the early detection of SI-AKI. Although RRI predicted SI-AKI in the early period at the same time points as CCAB, RRI showed a higher sensitivity and specificity than the other two molecules.

In conclusion, RRI and urinary CCAB predicted AKI in the early period almost at the same time intervals in our rat model of polymicrobial sepsis induced by the CLP method, although an RRI greater than 0.45 had the highest predictive value. There is a need for larger-scale clinical studies to support the findings of this experimental study into the early detection of SI-AKI.

Ethical approval

This study has been approved by the Necmettin Erbakan University KONÜDAM Experimental Medicine Application and Research Center Directorate Local Ethics Committee on Animal Experiments (approval date: 18.05.2018, number: 2018-018). Written informed consent was obtained from the participants.

Author contribution

Study conception and design: SOU, AY; data collection: SOU, EFC; analysis and interpretation of results: SOU, FK, SB, FG, CT; draft manuscript preparation: SOU, AY, EFC. The author(s) reviewed the results and approved the final version of the article.

Source of funding

The authors declare the study received no funding.

Conflict of interest

The authors declare that there is no conflict of interest.

References

1. Evans L, Rhodes A, Alhazzani W, et al. Surviving sepsis campaign: ınternational guidelines for management of sepsis and septic shock 2021. Crit Care Med. 2021;49:e1063-143. [Crossref]
2. Gómez H, Kellum JA. Sepsis-induced acute kidney injury. Curr Opin Crit Care. 2016;22:546-53. [Crossref]
3. Gomez H, Ince C, De Backer D, et al. A unified theory of sepsis-induced acute kidney injury: inflammation, microcirculatory dysfunction, bioenergetics, and the tubular cell adaptation to injury. Shock. 2014;41:3-11. [Crossref]
4. Jameson JL, Fauci AS, Kasper DL, Hauser SL, Longo DL, Loscalzo J. Harrison's principles of internal medicine. 20th ed. New York: McGraw Hill Education; 2018.
5. Coca SG, Yalavarthy R, Concato J, Parikh CR. Biomarkers for the diagnosis and risk stratification of acute kidney injury: a systematic review. Kidney Int. 2008;73:1008-16. [Crossref]

6. Aydoğdu M, Boyacı N, Yüksel S, Gürsel G, Sivri ABÇ. A promising marker in early diagnosis of septic acute kidney injury of critically ill patients: urine insulin like growth factor binding protein-7. Scand J Clin Lab Invest. 2016;76:402-10. [Crossref]
7. Endre ZH, Pickering JW, Walker RJ, et al. Improved performance of urinary biomarkers of acute kidney injury in the critically ill by stratification for injury duration and baseline renal function. Kidney Int. 2011;79:1119-30. [Crossref]
8. Cuartero M, Ballús J, Sabater J, et al. Cell-cycle arrest biomarkers in urine to predict acute kidney injury in septic and non-septic critically ill patients. Ann Intensive Care. 2017;7:92. [Crossref]
9. Kashani K, Al-Khafaji A, Ardiles T, et al. Discovery and validation of cell cycle arrest biomarkers in human acute kidney injury. Crit Care. 2013;17:R25. [Crossref]
10. Bonnin P, Sabaa N, Flamant M, Debbabi H, Tharaux PL. Ultrasound imaging of renal vaso-occlusive events in transgenic sickle mice exposed to hypoxic stress. Ultrasound Med Biol. 2008;34:1076-84. [Crossref]
11. Sullivan JC, Wang B, Boesen EI, D'Angelo G, Pollock JS, Pollock DM. Novel use of ultrasound to examine regional blood flow in the mouse kidney. Am J Physiol Renal Physiol. 2009;297:F228-35. [Crossref]
12. Boddi M, Bonizzoli M, Chiostri M, et al. Renal resistive index and mortality in critical patients with acute kidney injury. Eur J Clin Invest. 2016;46:242-51. [Crossref]
13. Giustiniano E, Meco M, Morenghi E, et al. May renal resistive index be an early predictive tool of postoperative complications in major surgery? Preliminary results. Biomed Res Int. 2014;2014:917985. [Crossref]
14. Rozemeijer S, Haitsma Mulier JLG, Röttgering JG, et al. Renal resistive index: response to shock and its determinants in critically ill patients. Shock. 2019;52:43-51. [Crossref]
15. Dyson A, Rudiger A, Singer M. Temporal changes in tissue cardiorespiratory function during faecal peritonitis. Intensive Care Med. 2011;37:1192-200. [Crossref]
16. Rudiger A, Dyson A, Felsmann K, et al. Early functional and transcriptomic changes in the myocardium predict outcome in a long-term rat model of sepsis. Clin Sci (Lond). 2013;124:391-401. [Crossref]
17. Bihorac A, Chawla LS, Shaw AD, et al. Validation of cell-cycle arrest biomarkers for acute kidney injury using clinical adjudication. Am J Respir Crit Care Med. 2014;189:932-9. [Crossref]
18. Meersch M, Schmidt C, Van Aken H, et al. Urinary TIMP-2 and IGFBP7 as early biomarkers of acute kidney injury and renal recovery following cardiac surgery. PLoS One. 2014;9:e93460. [Crossref]
19. Ko SF, Chen YT, Wallace CG, et al. Inducible pluripotent stem cell-derived mesenchymal stem cell therapy effectively protected kidney from acute ischemia-reperfusion injury. Am J Transl Res. 2018;10:3053-67.
20. Al-Harbi NO, Nadeem A, Ahmad SF, et al. Short chain fatty acid, acetate ameliorates sepsis-induced acute kidney injury by inhibition of NADPH oxidase signaling in T cells. Int Immunopharmacol. 2018;58:24-31. [Crossref]
21. Song J, Wu W, He Y, Lin S, Zhu D, Zhong M. Value of the combination of renal resistance index and central venous pressure in the early prediction of sepsis-induced acute kidney injury. J Crit Care. 2018;45:204-8. [Crossref]
22. Fisch S, Liao R, Hsiao LL, Lu T. Early detection of drug-induced renal hemodynamic dysfunction using sonographic technology in rats. J Vis Exp. 2016;109:52409. [Crossref]
23. Lerolle N, Guérot E, Faisy C, Bornstain C, Diehl JL, Fagon JY. Renal failure in septic shock: predictive value of Doppler-based renal arterial resistive index. Intensive Care Med. 2006;32:1553-9. [Crossref]
24. Darmon M, Schortgen F, Vargas F, et al. Diagnostic accuracy of Doppler renal resistive index for reversibility of acute kidney injury in critically ill patients. Intensive Care Med. 2011;37:68-76. [Crossref]
25. Dewitte A, Coquin J, Meyssignac B, et al. Doppler resistive index to reflect regulation of renal vascular tone during sepsis and acute kidney injury. Crit Care. 2012;16:R165. [Crossref]
26. Huang D, Yang Z, Qiu L, Lin J, Cheng X. The predictive value of renal vascular resistance index and serum biomarkers for sepsis-associated acute kidney injury: a retrospective study. BMC Nephrol. 2025;26:208. [Crossref]
27. Yang QH, Liu DW, Long Y, Liu HZ, Chai WZ, Wang XT. Acute renal failure during sepsis: potential role of cell cycle regulation. J Infect. 2009;58:459-64. [Crossref]
28. Devarajan P. Update on mechanisms of ischemic acute kidney injury. J Am Soc Nephrol. 2006;17:1503-20. [Crossref]
29. Seo DW, Li H, Qu CK, et al. Shp-1 mediates the antiproliferative activity of tissue inhibitor of metalloproteinase-2 in human microvascular endothelial cells. J Biol Chem. 2006;281:3711-21. [Crossref]
30. Price PM, Safirstein RL, Megyesi J. The cell cycle and acute kidney injury. Kidney Int. 2009;76:604-13. [Crossref]
31. Peng ZY, Zhou F, Kellum JA. Cross-species validation of cell cycle arrest markers for acute kidney injury in the rat during sepsis. Intensive Care Med Exp. 2016;4:12. [Crossref]
32. Honore PM, Joannes-Boyau O, Boer W, Janvier G, Gressens B. Acute kidney injury in the ICU: time has come for an early biomarker kit!. Acta Clin Belg. 2007;62(Suppl 2):318-21. [Crossref]

33. Godin M, Murray P, Mehta RL. Clinical approach to the patient with AKI and sepsis. Semin Nephrol. 2015;35:12-22. [Crossref]

34. Kellum JA, Chawla LS, Keener C, et al. The effects of alternative resuscitation strategies on acute kidney injury in patients with septic shock. Am J Respir Crit Care Med. 2016;193:281-7. [Crossref]

35. Koyner JL, Shaw AD, Chawla LS, et al. Tissue Inhibitor Metalloproteinase-2 (TIMP-2)·IGF-Binding Protein-7 (IGFBP7) levels are associated with adverse long-term outcomes in patients with AKI. J Am Soc Nephrol. 2015;26:1747-54. [Crossref]

36. Joannidis M, Forni LG, Haase M, et al. Use of cell cycle arrest biomarkers in conjunction with classical markers of acute kidney injury. Crit Care Med. 2019;47:e820-6. [Crossref]

37. Arulkumaran N, Sixma ML, Jentho E, et al. Sequential analysis of a panel of biomarkers and pathologic findings in a resuscitated rat model of sepsis and recovery. Crit Care Med. 2017;45:e821-30. [Crossref]

38. Zaouter C, Potvin J, Bats ML, Beauvieux MC, Remy A, Ouattara A. A combined approach for the early recognition of acute kidney injury after adult cardiac surgery. Anaesth Crit Care Pain Med. 2018;37:335-41. [Crossref]

39. Zaouter C, Priem F, Leroux L, et al. New markers for early detection of acute kidney injury after transcatheter aortic valve implantation. Anaesth Crit Care Pain Med. 2018;37:319-26. [Crossref]

40. Zaitoun T, Megahed M, Elghoneimy H, Emara DM, Elsayed I, Ahmed I. Renal arterial resistive index versus novel biomarkers for the early prediction of sepsis-associated acute kidney injury. Intern Emerg Med. 2024;19:971-81. [Crossref]

41. Schnell D, Reynaud M, Venot M, et al. Resistive Index or color-Doppler semi-quantitative evaluation of renal perfusion by inexperienced physicians: results of a pilot study. Minerva Anestesiol. 2014;80:1273-81.

42. Beloncle F, Rousseau N, Hamel JF, et al. Determinants of Doppler-based renal resistive index in patients with septic shock: impact of hemodynamic parameters, acute kidney injury and predisposing factors. Ann Intensive Care. 2019;9:51. [Crossref]

43. Langenberg C, Gobe G, Hood S, May CN, Bellomo R. Renal histopathology during experimental septic acute kidney injury and recovery. Crit Care Med. 2014;42:e58-67. [Crossref]

Turk J Intensive Care 2026;24(1):77-82
DOI: 10.63729/TJIC.2026.689

ORIGINAL RESEARCH

The impact of the inspiratory-to-expiratory ratio on mechanical power in ARDS patients

Sinan Aşar[1], Furkan Tontu[2], Özlem Acicbe[3], Zafer Çukurova[4], Gülsüm Oya Hergünsel[4], Nahit Çakar[5]

[1]Department of Anesthesiology and Reanimation, Mardin Training and Research Hospital, Mardin, Türkiye
[2]Department of Anesthesiology and Reanimation, Başakşehir Çam and Sakura City Hospital, University of Health Sciences, İstanbul, Türkiye
[3]Department of Anesthesiology and Reanimation, Intensive Care Unit, Şişli Hamidiye Etfal Training and Research Hospital, University of Health Sciences, İstanbul, Türkiye
[4]Department of Anesthesiology and Reanimation, Bakırköy Dr. Sadi Konuk Training and Research Hospital, University of Health Sciences, İstanbul, Türkiye
[5]Department of Anesthesiology and Reanimation, Intensive Care Unit, Koç University, İstanbul, Türkiye

ABSTRACT

Objective: Mechanical power (MP) is a promising parameter that may guide lung-protective ventilation strategies. The MP equation encompasses all variables involved in the pathogenesis of ventilator-induced lung injury (VILI), as well as the inspiratory-to-expiratory (I:E) ratio. Shortening the inspiratory time—by altering the I:E ratio—increases gas flow and may lead to lung injury. The optimal I:E ratio for preventing VILI remains uncertain. The present study aimed to investigate the effects of different I:E ratios on inspiratory gas flow and MP in patients with acute respiratory distress syndrome (ARDS).

Materials and Methods: This study was conducted on 19 adult patients diagnosed with moderate ARDS who were admitted to the intensive care unit and received mechanical ventilation. Patients were ventilated at a PEEP level of 10 cmH_2O, a tidal volume of 6 mL/kg, and three sequentially applied I:E ratios (1:2, 1:1, and 1.5:1), each maintained for 10 minutes. MP and respiratory parameters across the three I:E groups were compared using repeated-measures ANOVA.

Results: Compared with the I:E ratio of 1:2, ventilation with an I:E ratio of 1:1 resulted in slower inspiratory gas flow, lower inspiratory resistance and peak inspiratory pressure, higher dynamic compliance, and lower MP values. Plateau pressure and driving pressure did not differ significantly. When comparing I:E 1:1 with I:E 1.5:1, a persistent slowing of inspiratory gas flow was observed, but no significant difference in MP was detected.

Conclusion: In patients with ARDS, transitioning the I:E ratio from the conventional 1:2 to 1:1 or 1.5:1 resulted in progressively slower inspiratory gas flow and lower resistive and total mechanical power, suggesting that reducing inspiratory flow may enhance lung-protective ventilation.

Keywords: ARDS, ventilator-induced lung injury, mechanical power, inspiratory-to-expiratory ratio

Introduction

Mechanical ventilation is widely used in the management of respiratory failure and remains one of the cornerstones of intensive care medicine. Ventilator-induced lung injury (VILI) refers to the damage caused by positive-pressure ventilation (1). The development of VILI is influenced by several factors, including tidal volume, transpulmonary pressure, respiratory rate, flow rate, and positive end-expiratory pressure (PEEP) (2-4). These parameters represent the energy applied to the respiratory system, and the total energy delivered per minute is termed mechanical power (MP) (5,6). Mechanical power has been identified as an independent risk factor associated with mortality in critically ill patients (7).

✉ Sinan Aşar • sinan.asaras@gmail.com

Received: 15.01.2024 **Accepted:** 05.02.2026 **Published:** 26.03.2026

The comprehensive formula developed by Gattinoni et al. incorporates all parameters associated with VILI, as well as the inspiratory-to-expiratory (I:E) ratio (6):

$$MPrs = RR \times \{ \Delta V^2 \times [(1/2 \times ELrs) + RR \times (1 + I:E) / (60 \times I:E) \times Raw] + (\Delta V \times PEEP) \} \times 0.098$$

The viscoelastic structure of the lung causes the inspiratory phase of positive-pressure ventilation to require more energy than expiration (8). This energy dissipation corresponds to the area of hysteresis on the pressure–volume (P–V) curve (8). The energy expended within the lung parenchyma is used both for expansion and recoil during breathing and to overcome viscoelastic resistance during rapid inspiration and early expiration (9). This energy is also consumed when direct structural damage occurs at the microelement level (9). Increasing strain rates applied to the viscoelastic polymer structure of the lung elevate the risk of injury (10). Studies have shown that shortening the inspiratory time and altering the I:E ratio to increase gas flow can result in higher strain rates and promote the development of ventilator-induced pulmonary edema (10).

Studies have demonstrated that high driving pressure (DP) and high tidal volume (TV) are the main mediators of ventilator-induced lung injury (VILI) (11-13). In mechanical ventilators, the conventional I:E ratio, in which the inspiratory time is shorter than or equal to the expiratory time, is typically set to 1:2 or 1:1 (9). Although traditional ventilation strategies employing high pressures, high volumes (12 mL/kg), and high gas flow rates have largely been abandoned, the standard I:E ratio of 1:2 remains unchanged. The I:E ratio, similar to respiratory rate and tidal volume, is a key mechanical ventilation parameter that determines gas flow rate. The relationship between the I:E ratio and VILI is thought to depend on gas flow dynamics (14). Slow inspiratory gas flow is considered a critical factor in preventing VILI (9,14).

In intensive care units, different inverse ratio ventilation (IRV) strategies—such as I:E ratios of 1.5:1 and 2:1—are often employed to enhance oxygenation, serving as an essential intervention for patients with ARDS (15). However, the optimal I:E ratio for preventing VILI in this patient population remains uncertain.

This study aimed to determine the impact of varying I:E ratios on inspiratory flow and MP in ARDS patients.

Materials and Methods

Patients

Ethical approval for the study was obtained from the Clinical Research Ethics Committee of the University of Health Sciences, Bakırköy Dr. Sadi Konuk Training and Research Hospital (Decision No: 2019-19-15). Informed consent was obtained from all patients or their legal representatives upon admission to the intensive care unit.

This observational study was conducted during a consecutive three-month period in the Intensive Care Unit of the Department of Anesthesiology and Reanimation at Bakırköy Dr. Sadi Konuk Training and Research Hospital. Nineteen adult patients diagnosed with moderate ARDS according to the Berlin Criteria were included in the study (16).

All patients were ventilated using Maquet Servo-i ventilators (Sweden). According to the Berlin Criteria, the enrolled patients were classified as having moderate ARDS (16). Patient characteristics are presented in Table 1.

Patients were ventilated in volume-controlled mode under deep sedation with propofol and remifentanil, and neuromuscular blockade was achieved using rocuronium. Invasive mechanical ventilation was applied with a PEEP of 10 cmH_2O, a tidal volume of 6 mL/kg, and a respiratory rate of 12 breaths/min. Each patient was ventilated sequentially with three different inspiratory-to-expiratory ratios (1:2, 1:1, and 1.5:1), each maintained for 10 minutes.

All respiratory parameters were recorded every minute using the ImdSoft Metavision/QlinICU Clinical Decision Support Software (Canada), including peak

inspiratory pressure (Ppeak), positive end-expiratory pressure (PEEP), respiratory rate (RR), inspiratory gas flow, inspiratory resistance (Ri), expiratory resistance (Re), end-expiratory velocity (Vee), static compliance (Cstat), and dynamic compliance (Cdyn).

Plateau pressure (Pplat) was automatically measured by the ventilator with a 5% end-inspiratory pause (Tpause). Driving pressure (DP) was calculated using a pre-defined formula on the server (DP = Pplat – PEEP). MP and its components (resistive and elastic) were automatically calculated based on formulas previously defined on the server, as described by Gattinoni et al. (6).

Calculation of total, elastic, and resistive mechanical power:

$$MP\ total = RR \times \{\Delta V^2 \times [\ (1/2 \times ELrs) + RR \times (1 + I:E) / (60 \times I:E) \times Raw\ ] + (\Delta V \times PEEP)\} \times 0.098$$

$$MP\ elastic = RR \times \{\ \Delta V^2 \times [\ (1/2 \times ELrs)\ \}\ \times 0.098$$

$$MP\ resistive = RR \times \{\ \Delta V^2 \times [\ RR \times (1 + I:E) / (60 \times I:E) \times Raw\ ] \times 0.098$$

Statistical methods

Statistical analyses were performed using GraphPad Prism software (version 5.01). Data obtained at different inspiratory-to-expiratory (I:E) ratios (1:2, 1:1, and 1.5:1) were compared using repeated-measures ANOVA. Bonferroni post hoc tests were applied to identify significant pairwise differences between groups, with $p < 0.05$ considered statistically significant.

The primary outcome of the study was defined as the difference in resistive mechanical power between the I:E 1:2 and I:E 1:1 ratios. Based on a preliminary pilot study including five patients, the mean ± SD values for resistive mechanical power were calculated as 0.9 ± 0.3 J/min for I:E 1:2 and 0.65 ± 0.3 J/min for I:E 1:1. According to a power analysis based on these differences, with an alpha error of <0.05 and a power of 80%, the required sample size was estimated to be 18 patients.

The presence of auto-PEEP was assessed by performing an expiratory hold maneuver after each adjustment to measure total PEEP (17). If the end-expiratory flow (Flowee) was close to zero, the absence of intrinsic PEEP was assumed (17). In this study, Flowee values obtained at all I:E ratios were measured close to zero (0.008 ± 0.005; 0.015 ± 0.005; 0.022 ± 0.013), indicating the absence of intrinsic PEEP in the study population.

Results

This study was conducted on 19 patients diagnosed with moderate ARDS. Of these, 7 were female and 12 were male. The characteristics of the patients included in the study are presented in Table 1.

The difference between the mean mechanical power values of I:E 1:2 and I:E 1:1 was calculated as 0.33 J/min (4.3%) and found to be statistically significant ($p < 0.0001$). No statistically significant difference was observed between the mean and standard deviation values of I:E 1:2 vs. I:E 1.5:1 or I:E 1:1 vs. I:E 1.5:1 ($p > 0.05$). There was no statistically significant difference in the mean and standard deviation values of elastic

Table 1. Patient characteristics

Parameter	Mean ± SD
Female, n (%)	7 (%37)
Age, years	65 ± 11
PBW, kg	71 ± 2
BMI, kg/m²	28 ± 1.3
APACHE II score	25 ± 9
Expected mortality, %	59 ± 29
pH	7.43 ± 0.2
PaO_2, mmHg	62 ± 7
SO_2, %	91 ± 2
PCO_2, mmHg	44 ± 16
PaO_2/FiO_2, mmHg	119 ± 14
Duration of IMV, hours	272 ± 118
Length of ICU stay, hours	442 ± 224

APACHE II: Acute Physiology and Chronic Health Evaluation II, ARDS: Acute Respiratory Distress Syndrome, BMI: Body Mass Index, FiO_2: Fraction of Inspired Oxygen, IMV: Invasive Mechanical Ventilation, ICU: Intensive Care Unit, PaO_2: Arterial Oxygen Partial Pressure, PBW: Predicted Body Weight, PCO_2: Arterial Carbon Dioxide Partial Pressure, SO_2: Arterial Oxygen Saturation.

mechanical power among the three I:E ratios (1:2, 1:1, and 1.5:1) ($p > 0.05$). The difference between the mean resistive mechanical power values of I:E 1:2 vs. I:E 1:1 and I:E 1:2 vs. I:E 1.5:1 was calculated as 0.3 J/min (4.0%) and was statistically significant ($p < 0.0001$). No statistically significant difference was detected between the mean and standard deviation values of resistive mechanical power for I:E 1:1 vs. I:E 1.5:1 ($p > 0.05$) (see Table 2).

The differences between the mean and standard deviation values of Ppeak, WOBv, and Ri for I:E 1:2 vs. I:E 1:1 and I:E 1:2 vs. I:E 1.5:1 were statistically significant ($p < 0.05$). However, no statistically significant differences were observed for these parameters between I:E 1:1 and I:E 1.5:1 ($p > 0.05$). Statistically significant differences were also found in the mean and standard deviation values of inspiratory gas flow, Vee, and Cdyn across all three I:E ratios ($p < 0.05$), whereas Pplat, DP, and Cstat showed no statistically significant differences ($p > 0.05$) (see Table 2).

Discussion

MP, encompassing all parameters linked to VILI, serves as a key guide in its prevention. In this study, while all parameters in the MP equation developed by Gattinoni et al. were kept constant, the effect of changes in the I:E ratio on total MP and its components was investigated.

The inspiratory gas flow, Ri, and Ppeak values at an I:E ratio of 1:1 were found to be lower compared with those at an I:E ratio of 1:2. Consequently, the I:E 1:1 setting was associated with higher dynamic compliance and lower MP values. When I:E 1:1 was compared with I:E 1.5:1, the inspiratory gas flow remained slower; however, no clinically significant differences were observed in other respiratory parameters. The significant difference in MP between I:E 1:2 and I:E 1:1 was attributed to the reduction in the MPresistive, resulting from slower inspiratory gas flow and decreased Ri. Changing the I:E ratio from 1:2 to 1:1 reduced the amount of MP applied to the

Table 2. Mechanical power and its components at different I:E ratios (Mean ± SD)

	I:E 1:2 vs I:E 1:1	I:E 1:2 vs I:E 1.5:1	I:E 1:1 vs I:E 1.5:1
MP_{tot}, J/min	7.6±1.0 vs 7.3±0.8*	7.6±1.0 vs 7.3±0.9 ^{ns}	7.3±0.8 vs 7.3±0.9 ^{ns}
$MP_{elastic}$, J/min	2.4±0.6 vs 2.4±0.6^{ns}	2.4±0.6 vs 2.5±0.6^{ns}	2.4±0.6 vs 2.5±0.6^{ns}
$MP_{resistive}$,J/min	0.9±0.3 vs 0.6±0.2***	0.9±0.3 vs 0.6±0.3***	0.6±0.2 vs 0.6±0.3^{ns}
WOB_v, J	0.86±0.16 vs 0.70±0.15***	0.86±0.16 vs 0.68±0.14***	0.70±0.15 vs 0.68±0.14^{ns}
P_{peak}, cmH_2O	24.5±2.6 vs 22.9±2.7***	24.5±2.6 vs 23.0±2.8***	22.9±2.7 vs 23.0±2.8^{ns}
P_{plat}, cmH_2O	21±2.5 vs 21.1±2.5^{ns}	21±2.5 vs 21.2±2.5^{ns}	21.1±2.5 vs 21.2±2.5^{ns}
DP, cmH_2O	11.1±2.6 vs 11.2±2.7^{ns}	11.1±2.6 vs 11.2±2.6^{ns}	11.2±2.7 vs 11.2±2.6^{ns}
$Flow_{ins}$, L/s	0.37±0.04 vs 0.20±0.02***	0.37±0.04 vs 0.16±0.02***	0.20±0.02 vs 0.16±0.02***
Ri, cmH_2O. s/L	9.6±3.3 vs 8.5±2.9*	9.6±3.3 vs 8.7±3.6*	8.5±2.9 vs 8.7±3^{ns}
Re, cmH_2O. s/L	17.2±3.8 vs 17.5±3.8^{ns}	17.2±3.8 vs 18.0±4.1*	17.5±3.8 vs 18.0±4.1^{ns}
Vee, L / s	0.008±0.005 vs 0.015±0.005*	0.008±0.005 vs 0.022±0.013***	0.015±0.005 vs 0.022±0.013*
C_{stat}, ml/cmH_2O	34.5±9.6 vs 34.7±9.6^{ns}	34.5±9.6 vs 34.1±9.2^{ns}	34.7±9.6 vs 34.1±9.2^{ns}
C_{dyn}, ml/cmH_2O	35.8±9.4 vs 36.3±9.4**	35.8±9.4 vs 34.4±9.0**	36.3±9.4 vs 34.4±9.0**

MPtot: total mechanical power, MPelastic: Elastic mechanical power, MPresistive: Resistive mechanical power, Cst: Static compliance, Cdyn: Dynamic compliance, Ppeak: Peak inspiratory pressure, Pplat: Plateau pressure, DP: Driving Pressure, $Flow_{ins}$: inspiratory gas flow, Ri: inspiratory resistance, Re: expiratory resistance, Vee= end expiratory velocity.

^{ns}: not significant ($p \geq 0.05$); * $p < 0.05$; ** $p < 0.01$; *** $p < 0.0001$.

conductive components of the respiratory system that deliver gas to the alveoli. Since the elastic component of MP, which represents the energy applied to the alveoli, did not change, this reduction was considered clinically insignificant in terms of VILI risk.

Minimizing gas flow velocity during the inspiratory phase of the respiratory cycle is recommended to reduce the energy that contributes to lung injury (5,9,14). Therefore, the use of high airway pressures, high tidal volumes, or high respiratory frequencies should be avoided (5,9). Excessive energy levels can severely damage the alveolocapillary barrier, while even small amounts may cause localized injury in already weakened lung regions (9). The reduction of ventilated areas—the so-called "baby lung" phenomenon—can lead to the rupture of microstructural elements and increase stress on the remaining lung tissue. Once a certain threshold is exceeded, this may result in an exponential progression of injury. Thus, gas flow plays a critical role under such conditions (9). Adopting a higher I:E ratio, such as 1:1 instead of the conventional 1:2, may promote a slower and more homogeneous inspiratory flow, thereby reducing the MP applied to the lungs.

In an experimental study, the energy accumulated in the airway tissue during slow, constant inspiratory flow was found to be approximately half of that measured in the group ventilated with an exponentially increasing, high inspiratory flow pattern (18). Another study conducted under operating room conditions emphasized that an I:E ratio of 1:1 provides the minimum energy dissipation (19). To optimize mechanical power and prevent ventilator-induced lung injury (VILI), it has been recommended that the I:E ratio be adjusted to 1:1 (20).

An experimental study in mice investigated the effect of prolonging inspiratory time on ventilator-induced lung injury (VILI) (21). In this study, the use of low tidal volume with I:E ratios of 1:1 or 1:2 did not result in the development of VILI. In the high tidal volume group, however, the I:E ratio of 1:2 produced fewer histological signs of lung injury and better compliance values compared with I:E 1:1. In contrast, the group ventilated with high tidal volume and an I:E ratio of 1:1 showed worsened oxygenation and compliance, as well as a significantly increased mortality rate. The authors concluded that prolongation of inspiratory time and an increased I:E ratio exacerbated VILI in mice. However, in that study, the increased VILI and mortality associated with an I:E ratio of 1:1 were observed only when high tidal volumes were applied, which are already a well-known risk factor for VILI.

Limitations

This study has several limitations. First, it was conducted in a single center with a relatively small sample size, which may limit the generalizability of the findings. Second, the study was performed under controlled ventilation settings with fixed tidal volume and PEEP levels; therefore, the results may not be directly applicable to patients under spontaneous or assisted ventilation. Third, the analysis was limited to short-term physiological effects, and no long-term clinical outcomes such as mortality or duration of ventilation were evaluated.

Conclusion

In patients with ARDS, transitioning the I:E ratio from the conventional 1:2 to 1:1 or 1.5:1 resulted in progressively slower inspiratory gas flow and lower resistive and total mechanical power, suggesting that reducing inspiratory flow may enhance lung-protective ventilation.

Ethical approval

This study has been approved by the Bakırköy Dr. Sadi Konuk Training and Research Hospital Clinical Research Ethics Committee (approval date: 30.09.2019, number: 2019-19-15). Written informed consent was obtained from the participants or their legal representatives.

Author contribution

Study conception and design: SA, FT; data collection: SA, FT, ÖA; analysis and interpretation of results: SA, FT, ÖA; draft manuscript preparation: SA, FT, ZÇ, GOH, NÇ. The author(s) reviewed the results and approved the final version of the article.

Source of funding

The authors declare the study received no funding.

Conflict of interest

The authors declare that there is no conflict of interest.

References

1. Slutsky AS, Ranieri VM. Ventilator-induced lung injury. N Engl J Med. 2013;369:2126-36. [Crossref]
2. Kumar A, Pontoppidan H, Falke KJ, Wilson RS, Laver MB. Pulmonary barotrauma during mechanical ventilation. Crit Care Med. 1973;1:181-6. [Crossref]
3. Dreyfuss D, Soler P, Basset G, Saumon G. High inflation pressure pulmonary edema. Respective effects of high airway pressure, high tidal volume, and positive end-expiratory pressure. Am Rev Respir Dis. 1988;137:1159-64. [Crossref]
4. Hotchkiss JR, Blanch L, Murias G, et al. Effects of decreased respiratory frequency on ventilator-induced lung injury. Am J Respir Crit Care Med. 2000;161:463-8. [Crossref]
5. Cressoni M, Gotti M, Chiurazzi C, et al. Mechanical power and development of ventilator-induced lung injury. Anesthesiology. 2016;124:1100-8. [Crossref]
6. Gattinoni L, Tonetti T, Cressoni M, et al. Ventilator-related causes of lung injury: the mechanical power. Intensive Care Med. 2016;42:1567-75. [Crossref]
7. Serpa Neto A, Deliberato RO, Johnson AEW, et al. Mechanical power of ventilation is associated with mortality in critically ill patients: an analysis of patients in two observational cohorts. Intensive Care Med. 2018;44:1914-22. [Crossref]
8. Santini A, Collino F, Votta E, Protti A. Risk factors of ventilator-induced lung injury: mechanical power as surrogate of energy dissipation. J Emerg Crit Care Med. 2019;3:13. [Crossref]
9. Marini JJ. Evolving concepts for safer ventilation. Crit Care. 2019;23:114. [Crossref]
10. Protti A, Maraffi T, Milesi M, et al. Role of strain rate in the pathogenesis of ventilator-induced lung edema. Crit Care Med. 2016;44:e838-45. [Crossref]
11. Amato MB, Meade MO, Slutsky AS, et al. Driving pressure and survival in the acute respiratory distress syndrome. N Engl J Med. 2015;372:747-55. [Crossref]
12. Guérin C, Papazian L, Reignier J, et al. Effect of driving pressure on mortality in ARDS patients during lung protective mechanical ventilation in two randomized controlled trials. Crit Care. 2016;20:384. [Crossref]
13. Bellani G. How respiratory mechanics are associated with outcome. Paper presented at: International Symposium on Intensive Care and Emergency Medicine (e-ISICEM); 2020 Sep 20.
14. Schumann S, Goebel U, Haberstroh J, et al. Determination of respiratory system mechanics during inspiration and expiration by FLow-controlled EXpiration (FLEX): a pilot study in anesthetized pigs. Minerva Anestesiol. 2014;80:19-28.
15. Bein T, Grasso S, Moerer O, et al. The standard of care of patients with ARDS: ventilatory settings and rescue therapies for refractory hypoxemia. Intensive Care Med. 2016;42:699-711. [Crossref]
16. Ferguson ND, Fan E, Camporota L, et al. The Berlin definition of ARDS: an expanded rationale, justification, and supplementary material. Intensive Care Med. 2012;38:1573-82. [Crossref]
17. Ashworth L, Norisue Y, Koster M, Anderson J, Takada J, Ebisu H. Clinical management of pressure control ventilation: an algorithmic method of patient ventilatory management to address “forgotten but important variables”. J Crit Care. 2018;43:169-82. [Crossref]
18. Barnes T, van Asseldonk D, Enk D. Minimisation of dissipated energy in the airways during mechanical ventilation by using constant inspiratory and expiratory flows - Flow-controlled ventilation (FCV). Med Hypotheses. 2018;121:167-76. [Crossref]
19. Barnes T, Enk D. Ventilation for low dissipated energy achieved using flow control during both inspiration and expiration. Trends in Anaesthesia and Critical Care. 2019;24:5-12. [Crossref]
20. Marini JJ. How I optimize power to avoid VILI. Crit Care. 2019;23:326. [Crossref]
21. Müller-Redetzky HC, Felten M, Hellwig K, et al. Increasing the inspiratory time and I:E ratio during mechanical ventilation aggravates ventilator-induced lung injury in mice. Crit Care. 2015;19:23. [Crossref]

Turk J Intensive Care 2026;24(1):83-88
DOI: 10.63729/TJIC.2026.690

CASE REPORT

Refractory lactic acidosis and hypoglycemia: a very rare presentation in critically ill leukemic patient possibly associated with adult-onset glycogen storage disease type Ib

Abdullah Said[1], Sayed Gaber[2], Ghada Ahmed[3]

[1]Department of Oncology Critical Care, National Cancer Institute of Egypt, Cairo University Hospitals, Cairo, Egypt
[2]Department of Critical Care Medicine of Kasr Alainy, Cairo University Hospitals, Cairo, Egypt
[3]Department of Internal Medicine (Rheumatology Branch) of Kasr Alainy, Cairo University Hospitals, Cairo, Egypt

ABSTRACT

Lactic acidosis is a serious and frequently encountered condition in oncological critical care. Although it is commonly associated with generalized or localized tissue hypoperfusion, metabolic and drug-related causes should also be considered. Early recognition and appropriate management are essential for improving outcomes in critically ill patients. We report a case of refractory lactic acidosis associated with unexplained hypoglycemia, hypertriglyceridemia, and hyperuricemia. Common causes of type A lactic acidosis, including hypoperfusion, anemia, hypoxia, and seizures, were excluded. Other potential causes of type B and D lactic acidosis, such as liver disease and medication effects, were also ruled out. The patient had no known history of metabolic disease during childhood; however, the clinical presentation and laboratory findings were highly suggestive of glycogen storage disease type Ib (GSD-Ib).

GSD-Ib is a rare autosomal recessive metabolic disorder caused by mutations in the glucose-6-phosphate translocase (G6PT) gene located on chromosome 11q23. The resulting defect impairs both glycogenolysis and gluconeogenesis, leading to metabolic abnormalities including hypoglycemia, hyperlactatemia, hyperuricemia, and hypertriglyceridemia. GSD-Ib Patients commonly develop neutropenia, which predisposes them to recurrent infections and often requires treatment with granulocyte colony-stimulating factor (G-CSF). Long-term G-CSF therapy has been associated with an increased risk of myeloid malignancies, particularly acute myeloid leukemia (AML).

Glycogen storage diseases are genetic disorders that are typically diagnosed in childhood, making diagnosis in adulthood extremely rare. In this case, a late genetic mutation was suspected to have resulted in adult-onset GSD-Ib and malignancy. This rare presentation suggests a possible link between GSD-Ib and AML. Therefore, surveillance for glycogen storage disease in patients with AML, and vice versa, may be warranted. This association should be considered in critically ill AML patients presenting with refractory lactic acidosis after exclusion of other etiologies.

Keywords: AML, Acute myeloid leukemia, Lactic acidosis, Hypoglycemia, Cancer, Glycogen storage disease, Hypertriglyceridemia

Introduction

Lactic acidosis is a significant concern in oncological critical care, as it can result from generalized or local hypo perfusion, or other underlying causes. Prompt identification and management of lactic acidosis are crucial for improving outcomes in critically ill patients. We present a case of refractory lactic acidosis associated with unexplained hypoglycemia, hypertriglyceridemia, and hyperuricemia. After excluding hypo perfusion, anemia, hypoxia, seizures, or any other causes of Type A lactic acidosis, as well as liver diseases, medications, or other factors contributing to Type B or D lactic acidosis (1), we considered that the patient's clinical presentation and investigations best align with adult-onset Glycogen Storage Disease Type Ib.

Glycogen Storage Disease Type Ib (GSD-Ib) is one of over 12 inherited metabolic disorders that affect

✉ Abdullah Said • dr.abdullah.el.sa3ed@gmail.com

Received: 13.04.2025 **Accepted:** 31.07.2025 **Published:** 26.03.2026

glycogen metabolism. It is an autosomal recessive condition caused by mutations in the glucose-6-phosphate translocase (G6PT) gene located on chromosome 11q23 (2). G6PT deficiency disrupts both glycogenolysis and gluconeogenesis. Patients with GSD-Ib typically experience hepatomegaly, growth retardation, hypoglycemia, hyperlactatemia, hyperuricemia, and hyperlipidemia in early infancy. In addition, they develop neutropenia, which increases their risk of severe infections (3).

To manage these complications, long-term treatment with granulocyte colony-stimulating factor (G-CSF) is often used. However, this treatment can increase the risk of acute myeloid leukemia (AML) or myelodysplastic syndromes (MDS) in patients with inherited bone marrow failure conditions such as severe congenital neutropenia (4). The development of these myeloid malignancies is often linked to cytogenetic abnormalities involving chromosome 7, and G-CSF is known to promote the proliferation of monosomy 7 cells in vitro.

Although glycogen storage diseases are typically diagnosed in childhood due to their genetic basis, our patient was diagnosed in adulthood with a mutation that led to Glycogen Storage Disease Type Ib and malignancy. There have been several reports in recent years of patients with GSD-Ib developing AML after prolonged treatment with G-CSF. However, it is rare for this association to be observed in adult patients with leukemia and adult-onset GSD-Ib.

Given the potential strong association, surveillance for both Glycogen Storage Disease and acute myeloid leukemia in such patients is essential. This association should be considered in cases of refractory lactic acidosis in critically ill patients with acute myeloid leukemia, particularly after excluding other etiologies of lactic acidosis.

Case Presentation

A 52 years old male patient who is not known with any cardiovascular, endocrinal, renal, hepatic disorders, familial hyperlipidemia, congenital anomalies or abnormal milestones, noticed a lump over his chest wall, superficial ultrasound was done and revealed a hypoechoic mass with surrounding edema.

A biopsy was taken revealed fibrous tissue infiltrated by a tumor formed of small round cells with extensive crushing possessing hyperchromatic nuclei. The immature cells are positive for CD43, KCA, TdT and negative for MPO, CD117, CD 56, CD 20, CD30 and CD3 by immunohistochemical stains confirming a diagnosis of myeloid sarcoma.

Initial bone marrow biopsy revealed hypercellularity with dysplastic features and a blast count of 20%, which was confirmed by flow cytometry with 30% CD34-positive cells. A second bone marrow biopsy showed 21% blasts and persistent dysplastic features. Cytogenetic analysis revealed monosomy 7 in 33 of 34 metaphases and a translocation t(3;8)(q26;q24).

A diagnosis with chest wall myeloid sarcoma which is a subtybe of Acute Myeloid Leukemia is then confirmed. The patient received 3+7 protocol of chemotherapy “Daunorubicin and Cytarabine”. After 3 months the patient came to the ER department at Egyptian National Cancer Institute and was presenting with persistent vomiting and fatigue.

Thorough medical & drug history taking and full body examination were done revealing a history of persistent vomiting for the last month, abnormal lipid profile with extremely high serum levels of triglycerides exceeding 3000 mg/dl. This lab test was done at the last day of Ramadan 2024 “a month for MUSLIMS intended fasting to cultivate self-discipline, spiritual growth, and empathy for the less fortunate” which preceded the patient admission at our institute critical care unit by 1 month. It`s worthy to be mentioned, that the patient even didn`t receive any kind of treatment for hypertriglyceridemia.

The patient was admitted our critical care unit. He was fully conscious, oriented to time, place and persons. His calf muscles were lax, intact peripheral pulsations, clear chest by auscultation and no abdominal pain or

tenderness. His hemodynamics on admission were as follow; HR 90 beats/min, RR 20 breaths/min, BP 120/80 mmHg, Temp 37°C, RBS 70 mg/dL.

Full labs were done on admission; CBC showed pancytopenia: WBC 1900/μl, hemoglobin 6.7 g/dl, and platelet count 86 × 10^3/μl, with a differential count of 61% lymphocytes, 5% monocytes, 4% mature neutrophilic granulocytes, and 30% blasts.

Also hyperlactatemia (19mmol/l), high anion gap metabolic acidosis with anion gap 26, hyperuricemia (11mg/dl), hypertriglyceridemia (850mg/dl), while the renal function tests, liver function tests, sepsis markers, and electrolytes were average apart from mild hypokalemia (Serum potassium = 3.3mmol/L).

CT Abdomen with contrast was done and ruled out pancreatitis, but bilateral almost symmetrical nephromegaly were very evident (Figure 1).

The patient received crystalloids and insulin infusion to lower serum triglycerides' level as insulin enhances lipoprotein lipase which is the crucial enzyme for the hydrolysis of triglycerides. Dextrose 25% infusion was added to support serum normoglycemia.

An approach for lactic acidosis was followed and the hyper lactatemia wasn't neither explained by type A or type B nor type D lactic acidosis causes as the patient was not shocked, or hypoxic, or severely anemic, or taking any medications, or hepatic or suffering from any kind of local hypo perfusion. Also, the patient has no history of any bariatric or intestinal surgeries. Warburg effect of leukemic cells which is rare could not explain hypoglycemia, hyperuricemia and hypertriglyceridemia, leaving a question mark about the etiology of his presentation with severe lactic acidemia without any identifiable reason.

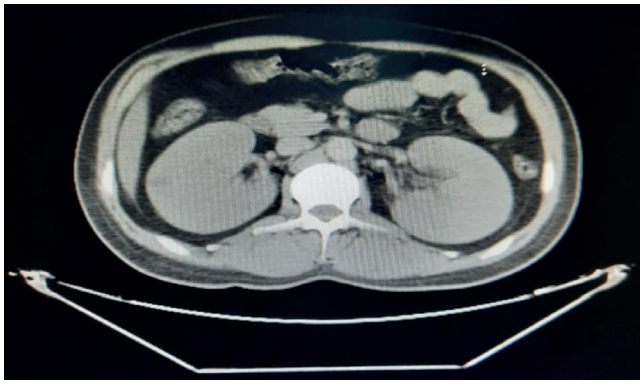

Figure 1. Contrast CT abdomen showing bilateral symmetrical nephromegaly

On the 3rd day of ICU stay with continuous crystalloids and insulin/dextrose 25% infusion, the serum lactate level dropped to 12mmol/l, improved metabolic acidosis with anion gap 18, serum triglycerides` serum level declined to 370mg/dl and then, Insulin infusion was stopped and instead, statin and fenofibrate were added.

The patient`s serum glucose level, for couple of days, was inappropriately steady low not exceeding 60mg/dl in spite of withholding insulin infusion, receiving 200cc of dextrose 25% infusion hourly and adding sources of simple carbs to his meals but it didn't make any difference in his serum glucose levels leaving another question mark about his condition.

Serum C-Peptide level, Thyroid Profile, Cortisol level were normal excluding an insulinoma, hypothyroidism and hypoadrenalism respectively.

Classic Clinical Presentation of Hypertriglyceridemia, Hypoglycemia, Hyperlactatemia, Hyperuricemia, Nephromegaly and Neutropenia raised a suspicion of Glycogen Storage Disease Type Ib. Due to financial issues, we could not confirm diagnosis with genetic sequencing.

Steroids were not added to his treatment plan due to their known effect on uric acid and triglycerides serum levels. The patient was encouraged to avoid fasting at all being the precipitating factor in worsening condition in such a disease. Uncooked starch and other starchy food stuff were added to his nutrition plan, then improvement of serum glucose levels were noted.

Dextrose 25% infusion was discontinued and the patient was discharged to home with slight metabolic acidosis with Anion Gap 14, Lactate 8mmol/l, RBS 70mg/dl, Uric acid 7mg/dl, Triglycerides 250mg/dl.

The patient was then informed with the special nutrition instructions specific for Glycogen Storage Disease Type I and keeping on statins, allopurinol and omega 3, however the patient wasn't complaint.

1 month later the patient came to the ER department presenting with Severe Dyspnea, Stridor, Drowsiness, Severe Hypoglycemia (20mg/dl), Severe Anion Gap Metabolic acidosis with Anion Gap 30, Profound Neutropenia, Thrombocytopenia and Sepsis.

The patient was resuscitated with boluses of dextrose 25% solution, intubated and mechanically ventilated, Urgent CT neck was done showing vocal cord mass thought to be a vocal cord chloroma (myeloid sarcoma of the larynx) as an extramedullary manifestation of leukemia spreading to soft tissues.

The patient condition was worsened due to development of a septic shock, granulocyte-colony stimulating factor & empirical antibiotics and antifungal were added to combat with sepsis. Neutropenia and dysfunction of neutrophils can be linked to the accumulation of 1,5-anhydroglucitol-6-phosphate (1,5-AG6P). This compound, a potent hexokinase inhibitor, forms slowly in cells from 1,5-anhydroglucitol (1,5-AG), a glucose analog found in the blood. In healthy neutrophils, accumulation of 1,5-AG6P is normally prevented by hydrolysis via G6PC3 after being transported into the endoplasmic reticulum (ER) by G6PT which is deficient in a such condition.

SGLT2 inhibitors, has been reported in previous studies with effectiveness in significant reduction of blood 1,5-AG6P levels, improving neutrophil counts and function.

However, despite the potential benefits of this treatment, it was not included in our patient's treatment plan due to concerns about hemodynamic instability. Tragically, the patient developed refractory shock and, despite efforts to manage the condition, he did not survive.

Discussion

Glycogen storage disease type I (GSD I), also known as Von Gierke disease, is an inherited disorder caused by deficiencies of specific enzymes in the glycogen metabolism pathway. It comprises 2 major subtypes, GSD Ia and GSD Ib. The incidence of GSD I in the overall population is 1/100,000 with GSD Ia and Ib prevalent in 80% and 20% respectively in a previous study by Nirzar S. Parikh, 2023 (5).

In GSD Ia, there is a deficiency of enzyme glucose-6-phosphatase (G6Pase) which cleaves glycogen to glucose.

In GSD 1b, there is a normal G6Pase enzyme activity but with a deficiency of the transporter enzyme, glucose-6-phosphate translocase (G6PT), GSD Ib results from mutations in the *SLC37A4* gene on chromosome 11q23.3.

The lack of either glucose-6-phosphatase (G6Pase) catalytic activity or glucose-6-phosphate transporter SLC37A4 (G6PT) activity in the liver impairs the normal conversion of glucose-6-phosphate to glucose through glycogenolysis and gluconeogenesis (5).

This impairment leads to severe hypoglycemia and a range of symptoms characteristic of Glycogen Storage Disease Type I (GSD I). The deficiency in G6Pase disrupts the final step of glucose production from glycogen, while the deficiency in G6PT prevents the transport of glucose-6-phosphate into the endoplasmic reticulum where it can be converted to glucose (5).

Both deficiencies result in the accumulation of glucose-6-phosphate, which contributes to hypoglycemia and over production of triglycerides, uric acid and lactic acid (5).

High serum triglycerides level may lead to Acute Pancreatitis which is an emergency and could be excluded by a abdomen CT with contrast (6).

Serum triglycerides levels more than 1000mg/dl should be managed by plasmapheresis, Insulin/Dextrose infusion is highly beneficial for serum triglycerides level below 1000mg/dl to boost lipoprotein lipase activity enhancing cellular uptake of triglycerides, while Statins are sufficient for serum triglyceride levels below 500mg/dl. However treating the etiology is a must (7).

Glycogen accumulation in liver and kidneys may lead to hepatic adenomas and nephromegaly up to renal failure.

Fasting is prohibited for those patients, because it activates glycogenolysis and gluconeogenesis pathways for boosting up serum glucose levels, but with G6Pase or G6PT deficiency ,the patient will experience hypoglycemia, hypertriglyceridemia, hyperuricemia, hyperlactatemia and may be lethal high anion gap metabolic acidosis (8).

Although GSD Ia, GSD 1b are similar in their clinical presentations, but they differ in being neutropenia and thrombocytopenia are characteristic findings in GSD Ib.

A recent research by Veiga-da-Cunha et al. (2019) identified that the inability to eliminate 1,5-anhydroglucitol-6-phosphate (1,5-AG6P), a potent inhibitor of hexokinases, which is slowly formed in the cells from 1,5-anhydroglucitol (1,5-AG), a glucose analog that is normally present in blood. Healthy neutrophils prevent the accumulation of 1,5-AG6P due to its hydrolysis by G6PC3 following transport into the ER by G6PT. G6PT deficiency in the endoplasmic reticulum (ER) membrane of neutrophils, leads to a lack of glucose and heightened oxidative stress, impaired respiratory burst, reduced chemotaxis, and disrupted calcium flux contributing to neutropenia and neutrophil dysfunction in GSD Ib. Additionally, these neutrophils are more prone to apoptosis, which exacerbates neutropenia (9).

An understanding of this mechanism has led to a treatment aimed at lowering the concentration of 1,5-AG6P and 1,5-AG in blood by treating patients with empagliflozin, an SGLT2 (sodium-glucose cotransporter 2) inhibitor, which inhibits renal glucose reabsorption. The enhanced urinary excretion of glucose inhibits the 1,5-AG transporter, SGLT5, causing a substantial decrease in the concentration of this polyol in blood, an increase in neutrophil counts and function and a remarkable improvement in neutropenia-associated clinical signs and symptoms (10).

To manage these complications in GSD Type 1b infants, long-term treatment with granulocyte colony-stimulating factor (G-CSF) is frequently used. However, this treatment can elevate the risk of acute myeloid leukemia (AML) or myelodysplastic syndromes (MDS) in patients with inherited bone marrow failures such as severe congenital neutropenia. The onset of these myeloid malignancies is often associated with cytogenetic abnormalities involving chromosome 7, and G-CSF is known to stimulate the proliferation of monosomy 7 cells in vitro.

Cases of GSD-Ib in early infancy who developed acute myeloid leukemia after couple of years of continuous G-CSF treatment have been reported in the last years, but it has rarely been reported among adult patients with leukemia to be associated with an Adult-Onset GSD Ib.

Our patient has lived a healthy childhood and adulthood till he have been diagnosed with Myeloid Sarcoma (A subtype of Acute Myeloid Leukemia) and GSD-Ib 3 months after without taking even one dose of GSF.

Glycogen storage diseases are explained by genetic defects so it is very unlikely to be diagnosed in adulthood, however our patient was thought to had a genetic mutation in his adulthood that led to development of myeloid leukemia and GSD Ib.

Conclusion

Acute myeloid leukemia and GSD-Ib are linked and may complicate each other with or without GSF treatment. As regarding to our observations, we are recommending that both Surveillance of Acute Myeloid Leukemia in patients of GSD-Ib and Surveillance of GSD-Ib in Acute Myeloid Leukemia patients seem to be mandatory.

This association must be kept in mind in a case of refractory lactic acidosis in a critically ill acute myeloid leukemia patient after exclusion of different etiologies of lactic acidosis.

Ethical approval

This study has been approved by the Egyptian National Cancer Institute (approval date: 12.2.2025). Written informed consent was obtained from the participants.

Author contribution

Study conception and design: AS; data collection: SG, AS; analysis and interpretation of results: GA; draft manuscript preparation: AS, SG, GA. The author(s) reviewed the results and approved the final version of the article.

Source of funding

The authors declare the study received no funding.

Conflict of interest

The authors declare that there is no conflict of interest.

References

1. Baddam S, Tubben RE. Lactic Acidosis. [Updated 2025 Apr 28]. In: StatPearls. Treasure Island (FL): StatPearls Publishing; 2025. Available at: https://www.ncbi.nlm.nih.gov/books/NBK470202
2. Dissanayake VH, Jayasinghe JD, Thilakaratne V, Jayasekara RW. A novel mutation in SLC37A4 gene in a Sri Lankan boy with glycogen storage disease type Ib associated with very early onset neutropenia. J Mol Genet Med. 2011;5:262-3. [Crossref]
3. Sim SW, Weinstein DA, Lee YM, Jun HS. Glycogen storage disease type Ib: role of glucose-6-phosphate transporter in cell metabolism and function. FEBS Lett. 2020;594:3-18. [Crossref]
4. Calip GS, Moran KM, Sweiss KI, et al. Myelodysplastic syndrome and acute myeloid leukemia after receipt of granulocyte colony-stimulating factors in older patients with non-Hodgkin lymphoma. Cancer. 2019;125:1143-54. [Crossref]
5. Nana M, Anastasopoulou C, Parikh NS, et al. Glycogen Storage Disease Type I. [Updated 2025 Apr 6]. In: StatPearls. Treasure Island (FL): StatPearls Publishing; 2026. Available at: https://www.ncbi.nlm.nih.gov/books/NBK534196
6. Hidalgo NJ, Pando E, Alberti P, et al. Elevated Serum Triglyceride Levels in Acute Pancreatitis: A Parameter to be Measured and Considered Early. World J Surg. 2022;46:1758-67. [Crossref]
7. Poonuru S, Pathak SR, Vats HS, Pathak RD. Rapid reduction of severely elevated serum triglycerides with insulin infusion, gemfibrozil and niacin. Clin Med Res. 2011;9:38-41. [Crossref]
8. Froissart R, Piraud M, Boudjemline AM, et al. Glucose-6-phosphatase deficiency. Orphanet J Rare Dis. 2011;6:27. [Crossref]
9. Veiga-da-Cunha M, Chevalier N, Stephenne X, et al. Failure to eliminate a phosphorylated glucose analog leads to neutropenia in patients with G6PT and G6PC3 deficiency. Proc Natl Acad Sci U S A. 2019;116:1241-50. [Crossref]
10. Maiorana A, Tagliaferri F, Dionisi-Vici C. Current understanding on pathogenesis and effective treatment of glycogen storage disease type Ib with empagliflozin: new insights coming from diabetes for its potential implications in other metabolic disorders. Front Endocrinol (Lausanne). 2023;14:1145111. [Crossref]

Turk J Intensive Care 2026;24(1):89-94
DOI: 10.63729/TJIC.2026.691

CASE REPORT

A case of thoracic aortic thrombosis in a patient with COVID-19 pneumonia

Kutlay Aydın[1], Murat Emre Tokur[2]

[1]Intensive Care Unit, Department of Anesthesiology and Reanimation, Aydın State Hospital, Aydın, Türkiye
[2]Intensive Care Unit, Department of Chest Disease, School of Medicine, Ege University, İzmir, Türkiye

ABSTRACT

Patients infected with the 2019 novel coronavirus (COVID-19) predominantly present with respiratory symptoms. In severe cases, COVID-19 creates a prothrombotic state that significantly increases the risk of thromboembolic events. These complications are primarily in the form of venous thromboembolism, with a cumulative incidence of up to 49% among hospitalized patients. In contrast, arterial thromboembolic events such as ischemic stroke and myocardial infarction have been rarely reported in the literature. In this case report, we present a case of aortic thrombosis complicated by peripheral embolism and/or thrombosis as an example of arterial thromboembolism.

Keywords: aortic thrombosis, peripheral embolism, COVID-19 associated thrombosis, arterial thromboembolism

Introduction

In December 2019, the novel coronavirus (COVID-19) was discovered and identified in the viral pneumonia cases in Wuhan, Hubei Province, China (1).

Among the several coronaviruses, two are associated with severe clinical symptoms: severe acute respiratory syndrome (SARS) coronavirus (SARS-CoV), and Middle East respiratory syndrome (MERS) coronavirus (MERS-CoV) (2). The clinical manifestation and severity of COVID-19 are similar to those of SARS-CoV. At least 20.5% of cases had one underlying disease, including hypertension, diabetes mellitus, coronary heart disease, chronic obstructive pulmonary disease, cerebrovascular disease, and chronic liver disease. Common indicator abnormalities include decreased white blood cell count (41.0%), increased C-reactive protein (75.2%) and lactate dehydrogenase (LDH) levels (23.6%), and decreased lymphocyte count (26.1%) (3).

Fever was present in 43.8% of the patients on admission, but developed in 88.7% during hospitalization. The second most common symptom was cough (67.8%); nausea or vomiting (5.0%) and diarrhea (3.8%) were uncommon (4).

By October 2024, over 776 million confirmed cases and over 7 million deaths have been reported globally (5).

Up to 14% of infected patients develop interstitial pneumonia, which may progress to acute respiratory distress syndrome needing intensive Care Unit (ICU) care. Evidence indicates severe COVID-19 is linked to a pro-hemostatic state affecting thromboembolism risk.

✉ Kutlay Aydın • kutlayaydin@hotmail.com

Received: 10.04.2025 **Accepted:** 15.08.2025 **Published:** 26.03.2026

This study was presented in Antalya at the 21st National Intensive Care Congress in 2022.

A pooled analysis showed that rising D-dimer levels predict adverse outcomes, indicating coagulopathy, with higher D-dimer in severe cases than milder ones (6).

A study found a higher risk of pulmonary embolism in COVID-19 ARDS patients than other ARDS causes, even with thromboprophylaxis. Venous thromboembolism (VTE) occurrence was about 20%, reaching 49% during hospitalization. A COVID-19 thrombosis guide recommends a baseline CT chest and sequential D-dimer monitoring. Few arterial thromboembolism cases, like stroke or myocardial infarction, were reported (6).

This article presents a case of aortic thrombosis complicated by peripheral embolism and/or thrombosis.

Case Presentation

A 66-year-old male patient with a 5-year history of hypertension presented to our hospital's COVID-19 outpatient clinic on August 5, 2020, with complaints of fever, cough, and shortness of breath. The patient tested positive for COVID-19 via a PCR test from a nasopharyngeal swab and was admitted to the hospital with a diagnosis of COVID-19 pneumonia for monitoring.

On the second day of hospitalization, due to worsening respiratory difficulty and oxygen saturation (Sat O2) remaining below 90% despite the administration of oxygen via nasal cannula at 10 L/min, the patient was transferred to ICU. Upon ICU admission, the patient received 14 L/min nasal oxygen, and the Glasgow Coma Scale (GCS) was E4M6V5. Vital signs were: respiratory rate 42/min, blood pressure 145/82 mmHg, pulse rate 98/min, and temperature 37.4°C.

Laboratory findings revealed the following:

- Blood glucose: 153 mg/dL (70–110 mg/dL)
- Urea: 16.82 mg/dL (7–20 mg/dL)
- Creatinine: 0.87 mg/dL (0.51–0.95 mg/dL)
- CRP: 198.4 mg/L (0–5 mg/L)
- LDH: 498 U/L (0–247 U/L)
- Procalcitonin: 0.55 ng/mL (0–0.1 ng/mL)
- D-dimer: 910 ng/mL (190–500 ng/mL)
- Ferritin: 1151.6 ng/mL (10–291 ng/mL)

Arterial blood gas analysis revealed:

- pH: 7.518 (7.35–7.45)
- pCO2: 20.7 mmHg (35–45 mmHg)
- pO2: 53.3 mmHg (83–108 mmHg)
- HCO3: 16.7 mmol/L (22–26 mmol/L)
- SpO2: 82.6% (95–99%)
- Lactate: 2 mmol/L (0.5–1.6 mmol/L)

Complete blood count results were:

- WBC: 7.67 × 10 ^ 9/L (4.23–9.07 × 10 ^ 9/L)
- Hgb: 126 g/L (137–175 g/L)
- Hct: 36.2% (40.1–51%)
- Platelets: 297 × 10 ^ 9/L (160–340 × 10 ^ 9/L)
- Neutrophils: 6.70 × 10 ^ 9/L (1.78–5.38 × 10 ^ 9/L)
- Lymphocytes: 0.62 × 10 ^ 9/L (1.32–3.57 × 10 ^ 9/L)

Coagulation parameters revealed:

- PT: 14.5 s (9–15 s)
- INR: 1.14 (0.8–1.2)
- APTT: 27.8 s (22–38 s)
- Fibrinogen: 645.14 mg/dL (60–150 mg/dL)

The patient was treated with Favipiravir 200 mg 2 × 3 tablets, Gemifloxacin 320 mg 1 × 1 tablet, Dexamethasone 6 mg once daily, Enoxaparin 40 mg twice daily, Pantoprazole 40 mg twice daily, and Isolyte at 20 cc/h. The patient was monitored with 14 L/min nasal oxygen, 4×2 hours of noninvasive ventilation, and intermittent prone positioning. On the 5th day of ICU admission, the patient received the first dose of Tocilizumab 400 mg, followed by a second dose 48 hours later.

On the 8th day, the patient was intubated and connected to mechanical ventilation due to respiratory failure and was monitored with FiO2 at 90%. On the 9th day, antibiotic treatment was adjusted based on

the consultation of infectious diseases, including Meropenem 1 g 3×1, Linezolid 600 mg 2×1, and Tigecycline 50 mg 2×1. Due to reduced urine output, hemodialysis was initiated on the 10th day, while enteral feeding was maintained. Subsequently, urine output improved.

On the 13th day, the left foot was noted to be cold and ischemic, with the posterior tibial pulse not palpable. Similarly, the left hand was cold, and the radial pulse was absent. Arterial thrombosis was suspected, and Doppler ultrasonography confirmed thrombosis in the posterior tibial artery. A contrast-enhanced CT angiogram (Figure 1-3) revealed arterial thrombosis extending downward from the descending aorta, a splenic subcapsular ischemic appearance, arterial thrombosis narrowing the lumen in the left iliac and femoral arteries, and posterior tibial artery occlusion in the left leg. The patient was managed medically without surgical intervention, pentoxifylline 1500 mg/24 h infusion, dipyridamole 75 mg 1x1 tablet was started, and enoxaparin was increased to 60 mg twice daily.

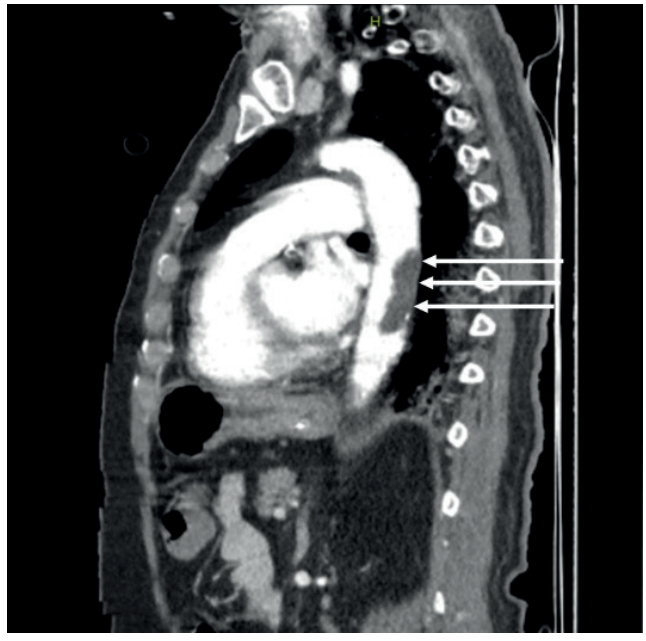

Figure 1. The appearance of a thrombus causing 70% narrowing in the thoracic aorta at the level of the left ventricle on a sagittal section of a computed tomography scan

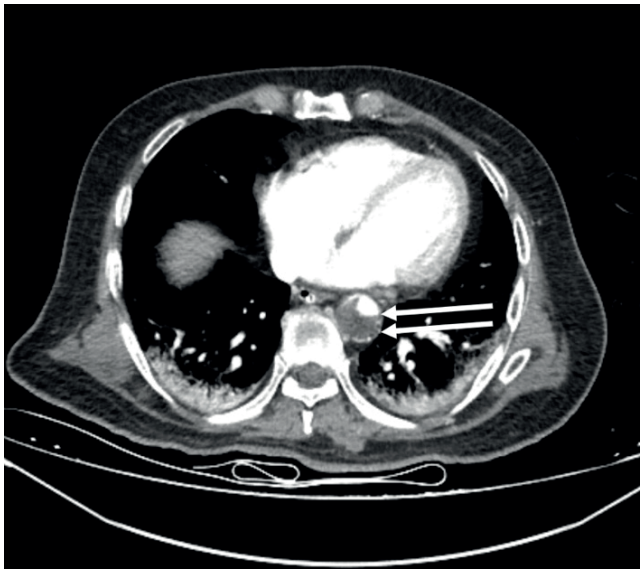

Figure 2. The appearance of a thrombus causing 70% narrowing in the thoracic aorta at the level of the left ventricle on an axial section of a computed tomography scan

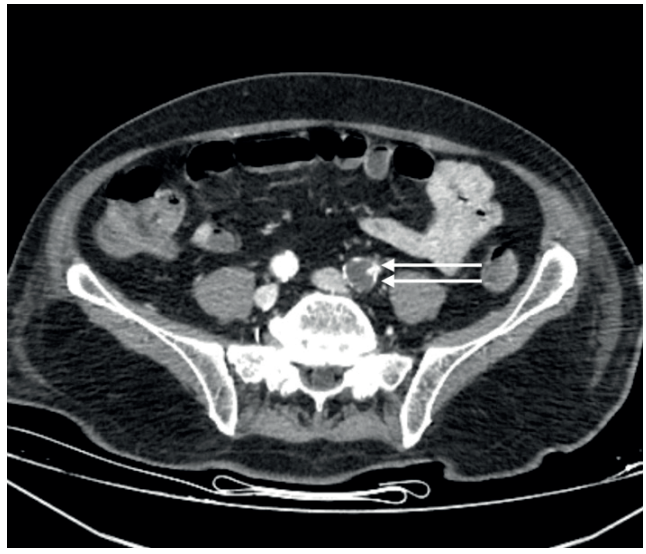

Figure 3. The appearance of a thrombus causing narrowing in the left femoral artery on an axial section of a computed tomography scan

On the 20th day, fresh blood was observed in the lower GI tract, and due to hemoglobin levels dropping below 70 g/dL, 2 units of erythrocyte suspension were transfused. Gastroenterology recommended monitoring for GI bleeding. Anticoagulant therapy was reduced to a prophylactic dose. Orthopedic consultation reported absent pulses in the left lower extremities and recommended amputation when a demarcation line developed.

On the 21st day, the patient was extubated and monitored with 5 L/min nasal oxygen; GCS was E4M6V4. On the 23rd day, the case was re-discussed in the council. The following decisions were made:

1. No thrombectomy or similar interventional procedure for the left foot
2. Continue enoxaparin 2×0.6 ml as anticoagulant therapy
3. Delay contrast-enhanced CT for thrombus control due to high creatinine; perform non-contrast CT instead
4. Non-contrast brain CT and neurology consultation for altered consciousness
5. Wait for the demarcation line before possible amputation of the left foot

On the 27th day, hemoglobin levels dropped again, necessitating the transfusion of 1 unit of erythrocyte suspension. On the 30th day, the patient's general condition deteriorated, requiring intubation and mechanical ventilation. The patient suffered cardiac arrest and passed away the same day.

Discussion

Some studies from China reported that 40% of hospitalized patients with COVID-19 were at high risk of VTE. Myocardial injury in COVID-19 is associated with severe disease. DIC is common in COVID-19. Regular laboratory monitoring of platelet count, PT, D-dimer, and fibrinogen in patients with COVID-19 is important to diagnose worsening coagulopathy (7).

Malas et al., in a review of 8,271 COVID-19 patients, found ICU VTE incidence at 21%, with rates up to 31%. ICU VTE rates are higher than typical for infections. The deep venous thrombosis (DVT) was 28%, the pulmonary embolism (PE) 19%, and the arterial thromboembolism (ATE) 5%. Thromboembolism raised mortality odds by 74% (8).

COVID-19 mainly affects the respiratory system but can involve other systems, notably the vascular system, which contributes significantly to morbidity and mortality. This increased thromboembolism risk arises from systemic inflammation, endothelial injury caused by the virus attaching to angiotensin-2 receptors, and viral replication, leading to prothrombotic endothelial dysfunction. To address this, the International Society of Thrombosis and Hemostasis (ISTH) interim guidance recommends considering prophylactic low molecular weight heparin (LMWH) for all hospitalized COVID-19 patients without contraindications. Similarly, the American Society of Hematology advises pharmacologic thromboprophylaxis with LMWH or fondaparinux for all hospitalized COVID-19 patients (8).

We recommend implementing standardized thromboprophylaxis for all COVID-19 patients without contraindications. Some authors advocate for higher anticoagulation targets in severely ill patients when standard dose thromboprophylaxis fails to prevent life-threatening thromboembolic complications (8).

Bellosta et al., in their study, reported that the number of patients with Acute Limb Ischemia (ALI) significantly increased in 2020 compared to the same period in 2019, and the high rate of clinical and technical failure was consistent with the presence of a hypercoagulable state triggered by COVID-19 infection (9).

Özen et al., in their study, evaluated 40 COVID-19 patients with ALI, and they mentioned that high levels of D-dimer may have predictive value for the occurrence of arterial thromboembolic events, and in some selected comorbid patients, medical follow-up may be superior to surgery (10).

Yıldız et al. in their study presented a 67-year-old male with upper limb and mesenteric ischemia and mentioned that clinicians should be alert that aortic thrombus may also be a source of embolism in COVID-19 patients, and thoracoabdominal CT angiography should be considered in routine evaluation (11). Bilge et al. in their case report, mentioned that peripheral nerve block may be a better method than general anesthesia and it has important advantages in terms of respiratory and hemodynamic (12).

Hang et al., in their study of 183 enrolled COVID-19 pneumonia patients, showed that the non-survivors had significantly higher D-dimer and fibrin degradation product (FDP) levels and longer ProThrombin than survivors on admission. DIC appeared in most of the deaths. At the late stages of COVID-19 pneumonia, levels of fibrin-related markers (D-dimer and FDP) were moderately or markedly elevated in all deaths, which suggested a common coagulation activation and secondary hyperfibrinolysis condition in these patients (13).

Conclusion

COVID-19 creates a pro-thrombotic environment, and thromboembolism is commonly observed. These complications are more often in the form of VTE. Arterial thrombosis or embolism is less common. The aortic thrombosis case we present is an example of a rare arterial thrombosis case. Thromboembolic complications can also occur in patients receiving prophylaxis with LMWH or unfractionated heparin. Therefore, unless contraindicated, higher doses than those normally used should be preferred. In select cases, adding antiplatelet therapy to anticoagulation may be considered, although further evidence is needed.

Ethical approval

Written informed consent was obtained from the participant.

Author contribution

Study conception and design: KA, MET; data collection: KA, MET; analysis and interpretation of results: KA, MET; draft manuscript preparation: KA, MET. The author(s) reviewed the results and approved the final version of the article.

Source of funding

The authors declare the study received no funding.

Conflict of interest

The authors declare that there is no conflict of interest.

References

1. Jin YH, Cai L, Cheng ZS, et al. A rapid advice guideline for the diagnosis and treatment of 2019 novel coronavirus (2019-nCoV) infected pneumonia (standard version). Mil Med Res. 2020;7:4. [Crossref]
2. Lu R, Zhao X, Li J, et al. Genomic characterisation and epidemiology of 2019 novel coronavirus: implications for virus origins and receptor binding. Lancet. 2020;395:565-74. [Crossref]
3. Zheng F, Tang W, Li H, Huang YX, Xie YL, Zhou ZG. Clinical characteristics of 161 cases of corona virus disease 2019 (COVID-19) in Changsha. Eur Rev Med Pharmacol Sci. 2020;24:3404-10. [Crossref]
4. Guan WJ, Ni ZY, Hu Y, et al. Clinical characteristics of Coronavirus Disease 2019 in China. N Engl J Med. 2020;382:1708-20. [Crossref]
5. World Health Organization (WHO). COVID-19 epidemiological update - 6 November 2024. Available at: https://www.who.int/publications/m/item/covid-19-epidemiological-update-edition-173
6. Al-Ani F, Chehade S, Lazo-Langner A. Thrombosis risk associated with COVID-19 infection. A scoping review. Thromb Res. 2020;192:152-60. [Crossref]
7. Bikdeli B, Madhavan MV, Jimenez D, et al. COVID-19 and thrombotic or thromboembolic disease: implications for prevention, antithrombotic therapy, and follow-up: JACC state-of-the-art review. J Am Coll Cardiol. 2020;75:2950-73. [Crossref]

8. Malas MB, Naazie IN, Elsayed N, Mathlouthi A, Marmor R, Clary B. Thromboembolism risk of COVID-19 is high and associated with a higher risk of mortality: a systematic review and meta-analysis. EClinicalMedicine. 2020;29:100639. [Crossref]

9. Bellosta R, Luzzani L, Natalini G, et al. Acute limb ischemia in patients with COVID-19 pneumonia. J Vasc Surg. 2020;72:1864-72. [Crossref]

10. Özen A, Yiğit G, Yıldırım A, Gül EB, Yılmaz M, İşcan HZ. Our clinical experience in the management of COVID-19-related arterial thrombosis with acute limb ischemia. Cardiovasc Surg Int. 2024;11:33-41. [Crossref]

11. Yıldız İ, Hamideyin Ş, Duman Z, Güngördü F, Korkmaz M. A rare case of multiple thrombosis associated with COVID-19 pneumonia. Turk Kardiyol Dern Ars. 2022;50:466-9. [Crossref]

12. Bilge A, Karasoy İ, Neziroğlu E, Güner Y. Upper extremity arterial thromboembolism in a patient with severe COVID-19 pneumonia: a case report. Jt Dis Relat Surg. 2021;32:551-5. [Crossref]

13. Tang N, Li D, Wang X, Sun Z. Abnormal coagulation parameters are associated with poor prognosis in patients with novel coronavirus pneumonia. J Thromb Haemost. 2020;18:844-7. [Crossref]